UNIVERSITÀ DEGLI STUDI DI PADOVA

Scuola di Dottorato di Ricerca in Scienze Mediche, Cliniche e Sperimentali

Indirizzo: Scienze Cardiovascolari

Ciclo: XXIII

TESI DI DOTTORATO

Molecular imaging of the heart by Mass Spectrometry

Direttore della Scuola: Ch.mo Prof. Gaetano Thiene

Coordinatore d'indirizzo: Ch.mo Prof. Gaetano Thiene

Supervisore: Ch.ma Prof.ssa Annalisa Angelini

Dottoranda: Dott.ssa Lara Fornai

Summary

BACKGROUND

Cardiovascular diseases are the world's number one death cause, accounting for 17.1 million deaths a year. There is still much unknown about cardiovascular diseases and their physiological underlying mechanism. Understanding the nature of complex biological processes occurring in both healthy and diseased heart tissue requires identifying the compounds involved and determining where they are located.

METHODS

We have investigated a complementary mass spectrometry imaging (MSI) approach using matrix-assisted laser desorption/ionization (MALDI) and secondary ion mass spectrometry (SIMS) on the major areas of rat heart: the pericardium, the myocardium, the endocardium, and the great vessels to study the native distribution and identity of atomics, lipids, peptides and proteins in rat heart sections. 40 layers of horizontal tissue slices were acquired and reconstructed into a 3 D dataset.

RESULTS

Surface rastering of heart tissue sections generated multiple secondary ions in a mass range up to 1500 m/z. In the negative spectra we identified cholesterol related ions that show high intensity in both atrias, the aorta, the pulmonary artery and the outline both ventricles. The m/z 105 (choline) signal localizes in both atrias, aorta, pulmonary artery, in the atrioventricular valves and semilunar valves but is not present in ventricles surface. DAG species with probable identifications as Oleic, Linoleic [OL]+ at m/z 602 and [OO]+ (Oleic, Oleic) at m/z 604, can be detected. The images of 3D reconstruction show a highly complementary localization between Na+, K+, ion at m/z 145 and ion at m/z 667. Na+ is localized to tissue regions corresponding to atrias, while K+ is strongly localized to tissue regions corresponding to ventricles surface.The ion at m/z 667 localized very precisely within the aortic wall and the ion at m/z 145 is primarily located to the atria regions.

CONCLUSIONS

To promote further research with cardiovascular disease, we report the identification of characteristic molecules that map the spatial organization in a rat heart's structure. A series of images obtained from successive sections of animal heart could, in principle, be used to produce a molecular atlas. Such tissue atlases (based optical images) are widely used for anatomical and physiological reference. The specific aim of this project is to optimize the data obtained from Heart SIMS a analysis and the 3-D reconstructive techniques developed to aid in investigating and visualizing differential molecular localizations in heart rat structures. The results reported here represent the first 3D molecular reconstruction of rat heart by SIMS imaging.

RIASSUNTO

Introduzione
Le malattie cardiovascolari rappresentano nel mondo la prima causa di morte, contando 17.1 milioni di morti ogni anno. Attualmente i meccanismi fisiopatologici alla base delle patologie sono in larga parte ancora sconosciuti. Capire la natura dei complessi processi biologici in atto sia nel miocardio cardiaco sano che malato richiede l'identificazione e la localizzazione degli stessi elementi molecolari coinvolti.

Metodo
Utilizzando tecniche complementari di spettrometria di massa d'immagine (SMI) quali la spettrometria di massa a ioni secondari (Secondary Ion Mass Spectrometry, SIMS) e la spettrometria di massa a desorbimento /ionizzazione laser assistita da matrice (Matrix-assisted laser desorption/ionization, MALDI) abbiamo analizzato le principali componenti del cuore del ratto: il pericardio, il miocardio, l'endocardio, le valvole e i grandi vasi al fine di studiare ed identificare l'originale distribuzione di atomi, lipidi, peptici e proteine nel tessuto cardiaco normale. Quaranta sezioni di tessuto cardiaco sono state acquisite e ricostruite ottenendo un database tridimensionale.

Risultati
L'analisi della superficie delle sezione di tessuto cardiaco ha generato molteplici ioni secondari con un intervallo di massa che raggiunge i 1500 m/z. Utilizzando la modalita' negativa abbiamo identificato il colesterolo e gli ioni relativi ad esso che mostrato un alta intensita' in entrambi gli atri, l'aorta, l'arteria polmonare e pericardio. La colina corrispondente a 105 m/z di massa molecolare risulta essere localizzata in entrambi gli atri, aorta, arteria polmonare, valvole atrioventricolari e valvole semilunari ma non risulta essere presente sulla superficie ventricolare. Sono state identificate molecole appartenenti al diacilglicerolo come acido Oleico, Linoleico [OL]+ corrispondenti alla massa molecolare di 602 m/z e [OO]+ (Oleico,Oleico) con massa molecolare di 604 m/z. Le immagini ottenute dalla ricostruzione tridimensionale mostrano una specifica localizzazione complementare tra il sodio, il potassio e gli ioni con massa molecolare di 145 m/z e 667 m/z. Il sodio e'maggiormente localizzato nelle regioni cardiache corrispondenti agli atri, mentre il potassio e' maggiormente localizzato nelle regioni corrispondenti alla superficie ventricolari. Lo ione con massa molecolare di 667 m/z e' localizzato con molta precisione all'interno della parete dell'aorta e lo ione con massa molecolare di 145 m/z e' localizzato a livello delle regioni atriali.

Conclusioni
Al fine di promuovere un'ulteriore ricerca in patologia cardiovascolare, riportiamo l'identificazione delle caratteristiche molecole che mappano l'organizzazione spaziale delle strutture cardiache del cuore del ratto. Una serie di immagini ottenute da sezioni successive del cuore potrebbero inizialmente essere utilizzate come un atlante molecolare e similmente, ad un atlante basato sulle immagini ottiche, essere ampiamente utilizzato come referente sia dal punto di vista fisiologico che anatomico. L'aiuto apportato da questo progetto e' l'ottimizzazione dei dati ottenuti dall'analisi SIMS e lo sviluppo della tecnica per la ricostruzione tridimensionale al fine di investigare e visualizzare le differenti molecole localizzate nelle strutture del cuore di ratto. I risultati qui riportati rappresentano la prima ricostruzione tridimensionale ottenuta con immagini SIMS, del cuore di ratto.

LIST OF CONTENTS

1.*Introduction*

Heart diseases resulting in heart failure are among the leading causes of morbidity and mortality and can result from either ischaemic heart diseases or primary heart muscle diseases (*e.g.* dilated cardiomyopathy)[1]. The causes of cardiac dysfunction in most heart diseases are still largely unknown, but are likely to result from underlying alterations in gene and protein expression. Therefore, the functional complexity of an organism far exceeds that indicated by its genome sequence alone [2-5]. Therefore, it is clear that the "omic" approaches to the global study of the products of gene expression, including transcriptomics, proteomics, lipidomics and metabolomics, will play a major role in elucidating the functional role of the many novel genes and their products and in understanding their involvement in biologically relevant phenotypes in health and disease. Proteome databases containing two-dimensional gel electrophoresis 2-D gel images and protein spot identifications have been compiled for canine and rat myocardial tissues [6,7]. To date, there is no comprehensive Image mass spectrometry database for the heart available to researchers. The construction of similar databases will not only aid as a reference for other studies, but will also be important for the identification of pathological changes to the " omic " caused by disease.

Because of the evidence above, there is now a compelling justification for direct and large-scale analysis of ions, lipids, peptides and proteins in a healthy rat heart tissue. The heart is mainly composed by cardiac muscle. The layer of the heart consisting of cardiac muscle is called the myocardium. The inner surface of the myocardium is lined by endocardium, and the outer surface by epicardium. To promote further research with cardiovascular disease we have investigated a complementary mass spectrometry imaging (MSI) approach using Matrix-assisted laser desorption/ionization (MALDI) and secondary ion mass spectrometry (SIMS) on the major areas of rat heart and we report the identification of characteristic molecules that map the spatial organization in a rat heart's structure: the epicardium, the myocardium, the endocardium, and the great vessels. Further we realized the first 3D reconstruction of the rat heart based on molecular information by SIMS. One such discovery tool, Mass Spectrometry (MS), has become increasingly

integral to the study of complex biological systems [8]. MS is an analytical technique that is used to determine the mass of chemical compounds. Because the mass of a chemical compound is dependant on its elemental composition, it is an important measure for its identity [9]. One of the principal motivation for application of MSI in biomolecular heart research is the ability of imaging mass spectrometry to analyze the distribution of hundreds of unknown compounds in a single measurement while the cellular and molecular integrity is maintained [10,11]. Both SIMS and MALDI have been used in this work to increase the mass range of imaged compounds. Ion images for a large number of both identified and unknown compounds provide information on the native composition and distribution of biologically relevant compounds in the heart. The animal model is the first important step in promoting the translation of scientific discoveries into human applications. Rats exhibit physiological characteristics similar to those of humans and have for over a century been a key experimental model in biomedicine. Rat models have been used to advance many areas of medical research, including cardiovascular disease [12]. MALDI can typically analyze molecules up to 100 KDa with a spatial resolution of ~10-50μm and SIMS has been used for imaging of elemental species in cells at high spatial resolution (~50 nm) [13-16].

Therefore both instruments have powerful advantages in imaging mass spectrometry [17].

1.1. Mass Spectrometry

A mass spectrometer is described as the smallest weighing scale ever used in the world [13]. MS is a unique technique that has an interdisciplinary nature, which freely crosses the borders of physics, chemistry, and biology. MS is a great scientific tool due to its capabilities to determine the mass of large biomolecular complexes, individual biomolecules, small organic molecules, and single atoms and their isotopes. Right from the time of its invention in the first decade of the 20th century, MS has undergone tremendous improvements in terms of its sensitivity, resolution, and mass range. It currently finds applications in all scientific disciplines, such as chemistry, physics, biology, pharmacology, medicine, biochemistry, and bioagro-based industry. Introduction of “soft”

ionization sources such as electrospray ionization (ESI) by Fenn et al. and MALDI by Karas et al. in the 1980s revolutionized mass spectrometry, and offered the capability to analyze large intact biomolecules [18,19]. As such, MS became an irreplaceable tool for the biological sciences. Rather this thesis focuses on one of the latest, rapidly developing innovations in MS, namely image mass spectrometry (MSI). This young technique takes benefit from all methodological and technological developments in general MS over the last decades. Over the last 20 years MSI has transformed from an esoteric, specialist technology studied by few researchers only to a technique that now finds itself at the center stage of mainstream MS. Over the last years the technology has matured to find applications in many different areas, with instrument developments taken up by all MS instrument manufacturers resulting in a rapid rise of the number of research groups active in this area.

1.2. Mass Spectrometric Imaging

MSI allows the rapid detection, localization, and identification of many molecules from the most complex, biological sample surfaces. It emerged as a response to the demand for spatial information about biomolecules detected by conventional MS. The MSI instrumentation, methods, and protocols have been developed to study the spatial distribution of endogenous compounds such as lipids or proteins and exogenous compounds such as polymers or pharmaceutical compounds on complex surfaces. It is a *label free* technique that can deliver detailed understanding of biological processes on different length scales, from subcellular to multicellular level and from organs to whole biological systems. Although MSI takes advantage of all modern developments in MS, the concept already existed before the development period reviewed here. In particular, in the field of physics, SIMS was used extensively to study semiconductor surfaces and the like. It was not until the introduction of Matrix-assisted laser desorption/ionization mass spectrometric imaging (MALDI-MSI) in 1997 by Caprioli et al. that the current rapid developments of methodologies, instrumentation, and software used for imaging of biological samples started [20]. Now, peptide and

protein profiling directly from biological tissue samples is almost routine already, while the first images of whole tissue sections were shown only in 2001, illustrating the speed of application development [21]. SIMS has also seen limited application for imaging biological samples. The development of liquid metal ion guns (LMIG) as a primary ion source for SIMS experiments in the 1990s revolutionized SIMS imaging. It realized a much wider scope of applications of high spatial resolution MSI of biological surfaces [22].

These two desorption and ionization methods, MALDI and SIMS, lay at the heart of modern MSI developments.

1.3. MSI Basic Principles and Ionization Techniques

Imaging mass spectrometry is essentially a four step process. It involves sample preparation, desorption and ionization, mass analysis, and image registration. All four elements need to be carefully controlled and monitored to generate meaningful images. Sample preparation is a key to any analytical technique. After introduction of the samples into an MSI instrument, the biomolecules first are desorbed and ionized from the surface. This is achieved through exposure of the surface to a laser beam (LDI/MALDI) and a primary ion beam (SIMS). The ionized molecules are subsequently mass separated inside the mass analyzer. The whole surface of the sample is examined during a MSI experiment to collect mass spectral information about the molecular composition and distribution of the analyzed molecules at every point. The resulting molecular ion distributions are presented in the form of ion images. In the life sciences there is a growing demand for a technique or tool capable of visualizing macromolecular distributions directly from biological samples. So far, MSI is the only technique that generates high resolution biomacromolecular images directly from tissue sections and without the need for labels [22].

1.3.1 Time of Flight Secondary Ion mass Spectrometry

Time of Flight Secondary Ion mass Spectrometry (TOF-SIMS) ion microscope affords molecule-specific information without the incorporation of dye, isotopes or labels. Static TOF-SIMS is a surface-sensitive method where the primary ion dose is low, and thus provides molecular information of the sample surface with minor damage. The use of TOF-SIMS permits ion imaging in areas as large as 500 μm. Allow visualization of the morphology, topology, and chemical composition of significant peaks in the spectrum from the biologic samples with molecular weight of some thousand daltons. TOF-SIMS has several advantages. It has the possibility to direct compare signal intensity of different molecules in biological tissue and the ability to analyze sequential layers to form a three-dimensional analysis.

History

SIMS is a relatively new technique for investigation in biological research. The first prototype to SIMS was developed by Castaing and Slodzian in the early 1960 in parallel to the Americans Liebel and Herzog [23]. There are two different operational regimes in SIMS, the dynamic and the static, which provides fundamentally different information. Dynamic SIMS, with a single non-pulsed primary beam is a rather destructive technique. The high numbers of bombarding ions allows depth profiling, reaching several microns with elemental sensitivity. The maximum mass range is typically ~ 250 m/z. The static SIMS appeared when Benninghoven (1970) reduced the primary ion current density on the sample. It was first used to analyze inorganic compounds as oxids layers on metals, or mapping organic contaminats on semiconductors devices [24]. Static SIMS is surface mass spectrometric techniques which gives information about the chemical composition of the upper most monolayer of the bombarded surface with a high mass resolution. The technique creates some destruction of tissues and therefore it is necessary to use a very low dose of primary ions. Less

than 1% of the top surface layer of atoms or molecules receives an ion impact. Many interesting works have been done since the beginning of the 1980. For example 1981, Burns detected ions in the cat choroidea and in 1982, Na+ and In+ were detected in the kidney from rat [25]. The most famous one is the mapping of stable and radioactive isotopes in the thyroid gland by Berry et al in 1986 [26]. TOF-SIMS has also been used for drug detection in cells (anti-tumor drugs in histological sections) to better evaluate successful early cancer treatments. Drug detection is accomplished indirectly by detecting a tag isotope naturally present or introduced by labeling, mainly with halogens,15N and 14C [27].

Imaging and detection of lipids with TOF-SIMS

Detection of lipids with TOF-SIMS was introduced by McMahon in 1995 by the imaging and detection of phosphatidylcholine and sphingomyeline in porcine brain and dog adrenal gland [28]. The same year Seedorf manages to detect cholesterol in blood from patients suffering from Smith-Lemli-Opitz syndrome, which is another example of early TOF-SIMS studies in the biomedical field. The technique is still developing mainly due to the development of new primary clustering sources as buckminister fulleren (C60+), gold (Au+) and bismuth (Bi+) [29]. Its use in biological research is expanding. McQuaw et al have identified sphingomyelin in cholesterol domains in the process of raft formation in cellular membranes. They have detected lateral heterogeneity of dipalmitoyl phosphatidylethanolaminecholesterol in Langmuir-Blodgett film [30]. Using Au3+ cluster ions Sjövall et al demonstrated cholesterol, sulfatides, phosphatidylinositols, and phosphatidylcholine. Later on the Bi3+ cluster ions have been used in the localization of cholesterol, phosphocholine and galactosylceramide in rat cerebellar cortex [31].

Principal of TOF-SIMS in biological samples

The "Time-of-Flight" of an ion is proportional to the square root of its mass, so that all different masses are separated during the flight and can be detected individually. The sample is sputtered by a primary ion beam with energy between 5 and 25 keV. The beam can be pulsed with a puls lengt from ns up to µs. This generates a sort of collision cascade of atoms and molecules of the <3 upper most layer of the sample surface [32]. A cloud of atoms and molecules arises; most of them are neutrals only, some (approx. 1%) are ionized as secondary ions, positively or negatively charged The emitted ionized particles with different masses leave the surface at the same time via the deflection of the electron trajectories due to the Lorentz force which is transmitted into kinetic energy. Ions are separated charged by the TOF extraction optics. Ions are accelerated to a given energy with an electric potential and transferred into a field-free flight path of vacuum of approximately 2m. With a certain amount of kinetic and internal energy "they" are travelling in free and are separated by their mass in the end of the flight path the ionized particle hits a "detector" where the ions are detected and counted. The flight times of all the ions to the detector are electronically measured and related to the ion mass (m/z). Moreover, some of the identical secondary ions will leave the sample surface with different kinetic energy, which results in a decreased resolution due to a band broadening. To compensate for this, the instrument is equipped with a type of "mirror" called the reflectron in the end of the flight path. Ions with same mass-to-charge ratio but higher kinetic energy penetrate deeper into the reflector, delaying their time of arrival to the detector than the slower low-energy ions. This process increases the resolution of the mass spectra [32]. Hence, for each primary ion pulse, a full mass spectrum is obtained. Thus a mass spectrum of all the ions is generated from the flight time spectrum. Every mass spectrum is transformed to one pixel in the image. One 256 x 256 pixel image contains 65.536 distinct mass spectra; each of them contains several hundreds of ion peaks.

Primary ion sources

The secondary ion yield depends to a large extent of the primary ion source. The basic types of ion guns for SIMS are the electron impact gas ion guns, surface ionization and liquid metal ion gun (LMIG). The electron impact gas ion gun operates with noble gases as argon (Ar+), Xenon (Xe+), oxygen (O-, O2+), SF5+ ionized molecules and C60+. These primary ion sources have been used mostly in dynamic SIMS that gives information about in-depth composition of the sample. Oxygen for example has been used in detection of positive ions such as magnesium (Mg+) isotopes in the kidney [33]. The surface ionization source use Cesium (Cs+) as the primary beam. Cs+ produces a higher beam current and enhances the secondary ion yield, and it is mostly used for generating negative secondary ions and as been used to localize isotopes in melanoma cells and tumour-infiltrating macrophages. The LMIG uses liquid metals (at room temperature) as gallium (Ga+), indium (In+), Au+, and Bi+ as primary ion source. LMIG supplies a well focused ion beam. Ga+ for example, offers high brightness and reasonable energy spread and has a lateral resolution of about 1 um. However, images obtained from tissue samples are generally limited to ions like the phosphatidylcholine headgroup of the membrane lipids at m/z 184. The major weakness of using monoatomic primary ion sources, such as Ga+, has been the low ion intensities and the high fragmentation of the high mass secondary ions.

A breakthrough with SIMS analysis resulted from the development of polyatomic cluster primary ion beam systems. Polyatomic ions involve the simultaneously collision of a number of atoms within a space of a few tenths of a nanometer. Because a cluster ion dissociates upon collision with a surface, the penetration depth of the elements of the cluster is reduced as compared to monoatomic primary ion bombardment. This significantly increases the secondary ion yield and molecular specificity in the MS, even though the formation of oxide fragments arises with

polyatomic ions. The Au3+ cluster ion beams for example have the potential to increase the secondary ion yield to 3 orders of magnitude compared to the conventional monoatomic Ga+ [32]. By using Au3+ Touboul detected cholesterol at m/z 385 in mouse brain and later on different fatty acids and TAG in mouse leg [34]. The Bi3+ cluster ions give better intensities and efficiencies of ions and produces less fragmentation of the parent ions and allow a better lateral and mass resolution. The C60+ is another used cluster ion source. The C60+ projectiles produce about a tenfold increase in the measured signal compared with Ga+. However, this thin primary ion source is primarily used for depth-profiling generating 3- dimentional images [35].

Sputtering process for organic ion is not fully understood. The ion impact on the target is of major importance. During high energetic bombardment when the sample is receiving a high amount of energy, a crater can form. This often occurs when heavy ion such as Cu+ or Au+ cluster are used. When crater is formed only half of the sputtered atoms leave the surface, the other half is stocked in form of a crater rim. Moreover, ionization of secondary ions can be formed either as ionization of the entire molecule M, through an ejection of an electron as radicals (M+, M-), by protonation [M+H] +, de-proteonation [M-H]-, or cationisation by Na+, K+ or Ag+. The protonation (and de-protonation) or cationisation strongly depends on the matrix and this is referred as the matrix effect. In principal the emission of secondary ions could be non-ionized in the absence of cations. On the contrary, adding Na+ or K+ salts to the sample the ionization of the analytes will occur. This was also shown in the presence of hydrogen-rich substrate. To enhance the secondary ion yield other techniques can be used. For example, covering the sample by a nm-thick layer of gold or silver, has been shown to provide increased intensities for large analytes in biological tissue, so-called sample metallization (Meta-SIMS) [36].

.

1.3.2. MALDI Imaging Mass Spectrometry

The major in state of art of MALDI is to identify the constituents of these systems and subsequently understand how they function within the framework of the tissue. With regard to clinical proteomics, there is the added dimension of disease, and therefore, the main goal is to characterize the cellular circuitry with a focus on the impact of the disease and/or therapy on these cellular networks. Mass spectrometry has become a center piece technology predominantly in the field of proteomics. Nonetheless a more comprehensive understanding of the constituents of biological systems will be aided by determining the constituent distribution. This anatomical dimension has been added through MSI especially using MALDI-MSI. MALDI is an ion source that is well compatible with the introduction of raw materials and surfaces. Shortly after its introduction, MALDI was used for direct tissue profiling. The first applications were neurobiological studies on dissected organs from the mollusk *Lymnaea stagnalis* [37-44], crustaceans [45], and other molluscs [46,47]. More recently, MALDI was used to generate profiles from tissue sections and ion images using a scanning method to analyze the surface [48]. This led to the first MALDI-MS tissue section imaging micrographs in 1997 [21,49,50]. These studies were followed by 10 years of intense efforts to improve the sensitivity, reproducibility, data processing, tissue preservation, and preparation treatments to fully characterize the proteome leading to a clear improvement of molecular images [51-74]. These developments led to clinical studies using MALDI-MSI technology. Clinical proteomics has many objectives including 1) diagnosis based on signatures as a complement to histopathology, 2) early disease detection, 3) individualized selection of therapeutic combinations that best target the patient's entire disease-specific protein network, 4) real time assessment of therapeutic efficacy and toxicity, 5) rational redirection of therapy based on changes in the diseased

protein network that are associated with drug resistance, and 6) combinatorial therapy in which the signaling pathway itself is viewed as the target rather than any single "node" in the pathway.

After tissue sectioning and transfer onto a conductive and transparent sample plate, the MALDI matrix is deposited, and data are acquired by recording mass spectra according to a raster of points covering the surface to be analyzed. Mass spectra recorded with their coordinates on the tissue are processed, and molecular images of the localization of molecules can be reconstructed.

DIAGNOSIS BASED ON SIGNATURES AS A COMPLEMENT TO HISTOPATHOLOGY

In some cases, diagnosis or tissue characterization cannot be easily achieved through standard histological staining. Further refinements based on molecular signatures and statistical data, which are currently missing, are crucial for improved diagnostics. The development of rapid and reliable screening of human tissues for diagnostics (*e.g.* biopsies or smears) has been improved with modern proteomics. By using MALDI-MSI, a molecular diagnosis could be done on tissue directly in the environment of the tumors. MALDI-MSI could help to detect the tumor boundary or infiltration of adjacent normal tissue that presents a normal histology. It could also help to detect the early stage of pathology that presents no histological modifications and to prevent tumor recurrence at the site of surgical resection. One of the major advances of MSI is the correlation of the MALDI images with histological information. MALDI-MSI software [for a review, see Ref.75] superimposes the MALDI images over a macroscopic or microscopic optical image of the sample taken before MALDI measurement. Although the primary macroscopic optical image is sufficient to recognize the outline of the tissue and define the measurement area, it is not usually possible to observe histological features in the image (in contrast to microscopic images). For a histological interpretation, it is necessary to use stained tissue sections. Two approaches have been used to correlate histology with MALDI-MSI results: performing MALDI-MSI and histological staining on

consecutive sections [76,77] or staining the sample after MALDI measurement [78]. The latter technique has been successfully used by pathologists [17], which suggests that combining MALDI-MSI and classic histological staining provides pathologists with more information to make better diagnoses. The next step is not only to perform a diagnosis based on *m*/*z* signatures but also on molecular data generated from identification of specific biomarkers that have been characterized as pathological signatures. However, another challenge for pathologists is tissue classification,

which is required to catalogue tumors or benign tissues. The major technological improvement that MALDI-MSI provides is the direct identification of novel markers within an *in situ* context from fixed sections/biopsy embedded in paraffin (*e.g.* archived material) [79]. Several studies on cancer and neurodegenerative diseases have demonstrated that MALDI-MSI is a key technology for identifying biomark- ers, assessing their localization, and cross-validation [64, 79-85]. The use of archived, formalin-fixed, paraffin-embedded tissue from hospital pathology departments represents a "gold mine" of existing data [76, 86-88]. The application of MALDI-MS imaging to archived materials could lead to the creation of an international disease marker database that would facilitate the development of early diagnostics for various pathologies as well as for follow-up examination of disease progression. Therefore, the addition of statistical analysis will be very important for the comparison of the different tissue components (*e.g.* tumor *versus* benign or healthy). Each tissue type depends upon the nature of its composition of cells. Thus, biocomputational methods are absolutely necessary to identify individualized molecular patterns to aid in diagnosis and prognosis. The advantage of MALDI-MSI is the ability to obtain a large collection of mass spectra spread out over a tissue section while retaining the absolute spatial location of these measurements for subsequent analysis and imaging. One of the statistical techniques to reduce the complexity of the information in multidimensional data sets in MALDI-MSI is principal component analysis (PCA) [89]. PCA is a multivariate preanalysis tool that allows for the correlation and identification of the major spatial and mass-related trends in the data that guide further downstream analysis [90]. PCA reduces the dimensionality of the data set but does not classify the spectra. This is a transformation

of the original coordinate system defined by peak intensities to a coordinate system that better explains the variance within the data set. This has been recently used in a prostate cancer study [78]. The next required step is the hierarchical clustering of the tissue based on PCA statistical analyses that reflect the most important variance of ions within the tissue [91]. Dendrograms can be constructed, and each branch represents ions present in the same group of cells (*e.g.* epithelial cancer cells *versus* benign cells). Thus, this representation provides access to huge numbers of individual spectra and reduces the complexity of the data set. It can also be correlated with histology as previously used for mouse kidney [17], gastric [92], and ovarian cancer [93]. Immunohistochemistry confirmed the epithelial expression of this fragment with a nuclear localization in benign epithelial cells and a cytoplasmic localization in carcinoma cells. This localization pattern indicates that this antibody can be used to discriminate borderline tumor cases, which are the most difficult to diagnose. Thus, a specific antibody that discriminates between cells transitioning from benign to malignant will be an asset for early diagnosis. Taken together, these studies indicate that direct tissue analysis and specific MALDI-MSI strategies facilitate biomarker identification and validation. In addition, data can be obtained from fundamental studies by analyzing the ontogeny of protein expression during morphogenesis and tumorigenesis, and proteins that could potentially serve as biomarkers for diagnosing diseases can be identified as demonstrated by an MSI study on murine prostate cancer development [94]. Murine prostate during development (1–5 weeks of age), at sexual maturation (6 weeks of age), and in adulthood (at 10, 15, or 40 weeks of age) was compared with prostate tumors from 15-week-old mice genetically engineered to express the large T antigen gene under the control of the prostate-specific probasin promoter (LPBTag mice). This approach identified proteins that were differentially expressed at specific time points during prostate development. The expression of probasin and spermine-binding protein, which are associated with prostate maturation, decreased during prostate tumor formation. This study was the first use of MALDI-MSI to follow ontogeny to tumorigenesis [94].

There is no doubt of the usefulness of MALDI-MSI in biomarker development for early diagnosis. However, MALDI-MSI is still not being routinely used in a clinical setting and has not yet been adjusted to conform to clinical proteomics procedures. Only a limited number of international groups have used this technology effectively in clinical settings; however, the number of clinical studies applying MSI has dramatically increased in the last years [9,48,78,54,95-100].

INDIVIDUALIZED SELECTION OF THERAPEUTIC COMBINATIONS THAT BEST TARGET THE PATIENT'S ENTIRE DISEASE-SPECIFIC PROTEIN NETWORK

MALDI-MSI is highly advantageous for *in situ* drug tracking. In fact, it enables the detection of both endogenous and exogenous compounds present in tissues with molecular specificity and preserves their spatial orientation. This unique combination coupled with excellent sensitivity and rapid analysis presents potential advantages for a wide range of applications in diverse biological fields. As described previously, recent advances have demonstrated that the technique can be applied to cancer research, neuroscience, and pharmaceutical development [101]. MALDI-MSI can be used in clinical studies to provide a molecular *ex vivo* view of resected organs.

This allows for the label-free tracking of both endogenous and exogenous compounds with spatial resolution and molecular specificity [99-111]. Several examples support the idea that MALDI-MSI technology will become a key tool in drug development [101-107] including novel drug design through the ability to analyze metabolic pathways directly in tissues (*e.g.* through *in situ* multiplex metabolite analysis), as well as in the elucidation of secondary effects and unexpected feedback loops [78]. Currently MSI of biomolecules and chemical compounds in cell-based assays and highly complex tissue sections is used in parallel with classic mass spectrometry ionization techniques to identify chemical compounds interfering with enzymatic function, receptor-ligand binding, or molecules modulating a proteinprotein interaction. There is evidence supporting MSI as a key

technique that can be used in combination with other therapeutic technologies. Recently the efficacy of combining radiation (XRT) with a dual epidermal growth factor receptor (EGFR)/vascular endothelial growth factor receptor inhibitor, AEE788, in prostate cancer models with different levels of EGFR expression was analyzed using Doppler sonography, tumor blood vessel destruction (visualized by immunohistochemistry), and MSI [110].

Tumor xenografts established from DU145 or PC-3 prostate cancer cell lines inoculated into the hind limbs of athymic nude mice were assigned to four treatment groups: 1) control, 2) AEE788, 3) XRT, and 4) AEE788 and XRT. AEE788 had a radiosensitization effect in human umbilical vein endothelial cells and increased their susceptibility to apoptosis. Therefore, concurrent AEE788/XRT treatment compared with either treatment alone led to a significant delay in tumor growth in animals bearing DU145 tumors. Conversely there was no effect on the growth of PC-3 tumors with combination therapy. In DU145 tumors, there was a significant decrease in tumor blood flow with combination therapy as assessed by using Doppler sonography and tumor blood vessel destruction.

MSI demonstrated that AEE788 is bioavailable and heterogeneously distributed in DU145 tumors receiving therapy, supporting the efficacy of the combination of AEE788 and XRT *in vitro* and *in vivo* in DU145-based models. In contrast, in PC-3-based models, the tumors were adequately treated with XRT alone without any added benefit from combination therapy. These findings correlated with differences in EGFR expression. Overall this study demonstrated the effects of therapeutics on both tumor cell proliferation and vascular destruction using complementary technologies, including MALDI-MSI in a clinical proteomics protocol [110].

REAL TIME ASSESSMENT OF THERAPEUTIC EFFICACY AND TOXICITY

MSI technology will also help significantly advance the analysis of novel therapeutics and may provide deeper insight into therapeutic and toxicological processes, revealing the mechanism of efficacy or side effects at the molecular level [113] A study by Atkinson *et al*. using AQ4N

(banoxatrone) (1,4-bis-5,8-dihydroxyanthracene-9,10-dione) as a prodrug demonstrated that MSI can be used for both drug and clinical development é [114]. In hypoxic cells, AQ4N is reduced to AQ4 (cytotoxic form), which is a topoisomerase II inhibitor. By inhibiting topoisomerase II within these hypoxic areas, AQ4N sensitizes tumors to existing chemo- and radiotherapy treatments. The distribution of AQ4N and AQ4 in treated H460 human tumor xenografts has been examined by MALDI-MSI, and images of the distribution of AQ4N and AQ4 show little overlap. The distribution of ATP in the tumor xenografts was studied as an endogenous marker of hypoxia because concentrations of ATP are known to decrease with hypoxia. The ATP distribution was similar to that of AQ4N, suggesting that in regions with abundant ATP expression (*i.e.* normoxic tissue) there was no evidence of conversion of AQ4N to AQ4. This indicates that the cytotoxic metabolite AQ4 is confined to hypoxic regions of the tumor [114].

2. Methodological Description and Current Improvements

2.1. Biological Sample Preparation

In this section we present the key practical aspect of MSI, the preparation of biological samples. Several crucial preparation steps such as sample handling, washing, matrix application, and on-tissue digestion will be discussed. This will be followed by an in-depth description of mass spectrometric instruments and software used for imaging. In this section, we will also explore and explain the difference between profiling and imaging modes of MSI.

2.1.1. Biological Sample Handling

The MSI sample handling protocols must maintain the integrity and spatial organization of the molecules in biological samples. Collection and treatment procedures need to be sufficiently fast to prevent rapid tissue degradation. The samples for MSI come from a variety of biological sources.

They can originate from the resection of an organ or tissue, a whole animal body dosed with a pharmaceutical compound, individual cells, or clusters of cells isolated by laser capture microdissection (LCM) or contact blotting of a tissue on a target membrane. The sample degradation process starts immediately after the blood/oxygen flow to an organ has ceased, even prior to tissue removal (see Sample Degradation). This implies that samples must be properly and timely collected, processed, and stored before MSI analysis.

Types of Samples.

All kinds of biological samples can be subjected to MSI, ranging from single cells, [115] to bacterial colonies,[116] to animal embryos, to tissues from different plants [117] or animal organs, to rodent whole body sections [118]. Different fresh, snap-frozen, alcohol preserved, or formaldehyde-fixed and paraffin-embedded (FFPE) [119] samples were used for MSI. To date, the most imaged tissue type is a rodent brain. This is due to its small size and characteristic internal structure and the ease with which it can be sectioned. Additionally, the symmetrical nature of the brain provides a very good internal control of the imaging process. Other types of animal organs were also subjected to MSI analysis. The sample list shows the imagination of the researchers involved. It consists of a large variety of biological tissue types, from the more difficult to section, air filled lungs, heart, kidney, tumor samples of different origin (glioma, breast cancer, prostate cancer, ovarian cancer, lung tumor), human biopsies and resected tissue from surgery, to cells from cell culture or LCM [9].

Sample Storage.

The most common first step used in MSI protocols is tissue storage utilizing snap-freezing of the material and storage at -80 ◌C. Tissue biopsies, organs, or whole organisms, e.g. zebra fish, should be frozen immediately after collection in order to preserve the sample's morphology and minimize

protein degradation through endogenous enzymatic proteolysis, oxidation of biomolecules, or changes in the metabolome of the cells. However, the freezing process can lead to sample cracking and fragmentation, as different parts of the tissue cool down at different rates and ice crystals may form. To avoid sample damage, the tissue may be loosely wrapped in aluminium foil and frozen in liquid nitrogen, ethanol, or isopropanol at temperatures below -70 ◌̊C by gently lowering the tissue into the liquid over a period of 30-60 s. This preserves the shape of the tissue and also protects the biological tissue components from degradation [120]. It is also important to avoid tissue deformation during storage, which usually occurs due to wrapping of the tissue in plastic film or storing it in a tube. Whole tissues may remain frozen in a freezer at -80 ◌̊C for at least a year with no significant degradation. After one year of storage, even at -80 ◌̊C, it is difficult to obtain good peptide/protein spectra from tissues. This phenomenon of tissue aging is especially important for samples collected and stored over a long time period in medical centralized tissue repositories. It is very important to optimize and standardize the protocols for medical applications of MSI. Especially when it is not always possible to analyze freshly prepared samples [120]. A number of innovative protocols for MSI of fresh and aged biomedical samples have been recently developed. The second most common form of tissue preservation found in medical tissue banks are formaldehyde-fixed and paraffin embedded (FFPE) tissue blocks. They are usually kept at real time (RT) , which leads to of nucleic acids, metabolites, and many bio molecules other than proteins cross-linked by formaldehyde. The cross-linking, in turn, hampers easy desorption and ionization. These samples require special protocols ensuring removal of MS incompatible paraffin, digestion of cross linked proteins, and correct identification of imaged molecules [77] .

Sample Degradation.

In MSI the quality of biological samples is of great importance. Unfortunately, many molecules present in functional tissue undergo rapid degradation just after tissue dissection or even during agonal states of animals. Several factors, including pre- and post-mortem factors, can affect tissue

quality. Premortem factors include prolonged agonal states, perfusions, use of drugs, infections, tumors, hypoxia, and seizures. Post-mortem factors that influence tissue quality include post-mortem interval (PMI), which is the period from death to freezing of the tissue for long-term storage at -80 °C, storage temperature, and duration of the storage as well as tissue processing and handling. Molecular degradation studies show that endogenous proteolytic degradation resulting from the natural activity of enzymes including calpains, cathepsins, and those of the proteasome complex is already extensive at 3 min post-mortem [121]. It has also been demonstrated that the levels of several post-translational modifications (PTMs) in brain tissue are significantly changed within minutes postmortem.Post-mortem degradation of glycerophospholipids (GPLs) was observed within 15 min by MSI in a series of mouse brains extracted at different times, presumably because of stimulation of phospholipases A (PLAs) under ischemic (restricted blood supply) conditions. Most studies concentrated on protein degradation have been conducted on animal (mouse, rat) brains, due to their availability. In these studies, either specific proteins were targeted, such as phosphorylated signal proteins, pre- and postsynaptic proteins, G-proteins, synaptophysin, microtubule-associated proteins, and calpain, or samples were analyzed in a more holistic proteomics approach.

The study of endogenous degradation processes in human prefrontal cortex tissue showed that most human brain proteins are quite stable with respect to post-mortem factors, such as PMI and storage temperature. Nevertheless, the storage temperature seemed to significantly influence certain protein levels. Raising the storage temperature from 4 °C to RT increased the number of degraded proteins from 17 degraded proteins at 4 °C to 54 degraded proteins at RT. This is indicative of the effect of temperature on naturally occurring post-mortem protein degradation. The majority of the identified proteins belonged to the functional classes of structural or metabolic proteins, which appear to degrade very easily during post-mortem delay [122].

To prevent/minimize the molecular degradation process, some strategies such as *in* V*i*V*o* fixation through focused microwave irradiation have been applied in MSI. However, the application of the

focused microwave instrument is limited to smaller samples such as organs from small rodents and optimized for the brain tissue samples. Some other specific protocols need to be developed to meet the requirements of certain samples. For example, some tissues collected for MSI can contain drugs that are lightsensitive. To prevent the photodegradation of these components before analysis, the section should be kept in the dark [121].

2.1.2. Tissue Preparation

Fixation. The majority of samples used for MSI are fresh, snap-frozen, chemically unmodified tissue sections. Unfortunately, it is not always possible to obtain fresh tissue for imaging experiments because many, especially medical samples, are routinely formaldehyde or alcohol fixed just after dissection and before any analysis. Due to protein crosslinking introduced by formalin fixation, the MSI analysis of FFPE tissues is difficult. The development of protocols useful for imaging and a recovery of polypeptides from FFPE samples allowed access to the different tissue banks, which store the samples in the form of paraffin block [123]. A successful example of the application of such a protocol employing on-tissue proteolytic digestion for biomedical imaging of FFPE brain sections. The protocols must include a paraffin removal step followed by tissue digestion. The sample's analysis and data interpretation must consider the oxidation and degradation processes as well as effects of fixation and removal of paraffin on molecular structures. All these aspects must be taken into account when old samples, large sample sets, or patient cohorts are going to be compared. This also implies that the profiling results of a 100-year-old FFPE tissue biopsy obtained from a patient with amyloidosis, presented by Seeley et al. in 2008, have to be dealt with great caution [124]. This puts contraints on the analysis of large existing sample collections using MSI, as in many cases the history of these samples is not well-known. If it is unknown how long the sample was kept at RT and under ambient conditions, it is impossible to compare the MSI results from such samples with the MSI results from comparable modern samples, which typically display well-defined states of the proteome. Alternative fixation methods rely on heat stabilization

of tissues, which causes favorable protein denaturation (see Sample Degradation) or the preservation of samples in an alcohol bath. A new method of tissue fixation using RCL2/CS100, which is a non-cross-linking, nontoxic, and non-volatile organic fixative suitable for shotgun proteomic analyses and tissue imaging, was published by Mange et al. in 2009 [125].

Embedding.

The embedding of the tissue in a supporting material allows easy handling and precise microtoming of sections. For histological applications, tissues cut on cryostat microtomes are usually embedded in the optimal cutting temperature (OCT) polymer. However, materials such as OCT, agar, sucrose, 2% (wt/vol) carboxymethylcellulose (CMC), and other polymer-based embedding media typically used for histological applications ionize easily during MS analysis and act as significant ion suppressors. A large number of FFPE biological samples has been collected and stored in many tissue banks worldwide. Paraffin present in the samples suppresses ionization and must be removed before tissue analysis using a xylene wash. An MSI protocol employing dewaxing and hydration steps of such samples has been published by Lemaire et al. in 2007 [77].

Sectioning.

For IMS the tissue sections are usually 5-20 μm thick. Thinner sections tear easily, while thicker sections, although easier to manipulate, may not be electrically conductive and take longer to dry, which can cause cracking and warping of the sections. Thus, tissues are usually sliced to a thickness of the diameter of a mammalian cell (10-20 μm), so that the majority of the cells in the slice are cut open, exposing the intracellular contents for analysis [121]. However, the thinner tissue sections, cut at 2-5 μm, have been recommended for the analysis of molecules in the larger molecular weight range of 3-21 kDa. Tissue blocks are mounted to the cryo-microtome's cutting stage and sliced with a stainless steel microtome blade. The disposable blades used for sectioning are often packaged with a very thin film of oil between each blade, which potentially can be a source of sample

contamination. To avoid contamination from this oil, it is recommended to rinse the blades with methanol and acetone prior to tissue sectioning. The sample stage temperature is typically maintained between -5 and -25 ̊C, depending on the tissue type. Tissues with high fat content, e.g. brain, require lower temperatures to achieve high quality sections. For example, samples such as breast tissue or visceral fat tissue can coagulate during sectioning at warmer cryo-microtome temperatures [121].

Tissue Attachment.

In order to perform MSI analysis, the tissue sections must be attached to an electrically conductive steal plate or glass slide. Conductive substrates are used to properly define the electric extraction field that will accelerate the ions produced from the surface. In the past, tissue sections were thaw-mounted on flat metallic target plates such as aluminum, stainless steel, and gold-coated plates, with the last offering a fairly nice contrast for visualization of major histological features from the sections. However, opaque target plates were not suitable for microscopic visualization of the section. These plates have been replaced by conductive ITO-coated glass slides, coated with a 130 Å film of indium-tin oxide for electrical conductivity. The transparent glass slides provide the possibility of microscopic observation of the MALDI samples. There are two approaches for tissue attachment to these substrates: the use of an adhesive double-sided conductive tape or thaw-mounting. The tape binds the section to the target while thaw mounting attaches the tissue by warming the reverse of the target to produce a localized warm patch. The first method requires special care to avoid trapping air bubbles, which can affect the image acquisition. The latter method reduces the risk of sample contamination and tissue loss during the washing step. However, the thaw mounting method can cause significant variation in mass profiles due to rapid degradation of molecules during the tissue attachment process.Thaw mounting may not be good enough for additional procedures involving polar solvents (see Washing of Tissue). Transfer of the tissue slice to a target plate or glass slide can be accomplished in several ways. One of the methods

recommends cooling the plate by placing it in the cryomicrotome chamber at -15 ◌̊C before sectioning [121]. The tissue section is picked up using forceps for thicker sections or an artist's brush for thinner sections and transferred onto the cold plate. The plate and tissue section are then quickly warmed together. This method prevents loss of water-soluble proteins, since all ice crystals remain on the tissue section surface and not on the cryo-microtome cutting stage. The second method uses a plate held at RT that is placed over the frozen section. In this case, the ice crystals remain on the cutting surface. Sections transferred with this method may give poorer mass spectra, especially in the case of imaging water-soluble molecules. Properly performed thawing does not cause any significant delocalization of the proteins, which is proved by traditional biochemical assays such as immunohistochemistry and autoradiography [121]. Regardless of the tissue transfer and attachment method used, the section must be transferred to the plate with great care without introducing any scratches, tears, or rolled-up edges. The mounted section should be immediately dried in a vacuum desiccator for 30 min to avoid moisture condensation that could cause delocalization of proteins. Results of MSI often are compared to the histopathological information of the imaged tissue. During sectioning of the sample, an adjacent tissue section is collected on a regular microscopic slide for histological staining in order to correlate morphological information with the mass spectrometric images. In order to visualize tissue histology prior to MSI, protocols utilize optically transparent glass slides, coated with a thin conductive layer (ITO-coated glass slides) together with MSI friendly tissue staining protocols (e.g., methylene blue, cresyl violet). This enables the microscopic evaluation of a tissue section by a pathologist followed by the molecular imaging of the same section by MSI. Another approach involves removal of the matrix from the tissue section followed by hematoxylin and eosin (H&E) staining of the same sample on an ITO slide in order to visualize the morphology of the tissue [126]. In this case, the visualization of microscopic structures may not be easy and depends strongly on the quality of the sample surface after completion of the MSI experiment. Samples used for SIMS or examined with the MALDI approach usually can be successfully stained and subjected to microscopic examination.

Washing of Tissue.

Washing is required to remove unwanted molecules and salts from the surface of the tissue. Salts are released from ruptured cells or interstitial fluids during sectioning and suppress ionization through direct ionization or adduct formation with the proteins and peptides. The standard washing steps usually employ a brief 70% ethanol wash to remove salts and debris followed by a 90-100% ethanol wash to dehydrate and temporarily fix the tissue. The ethanol wash does not cause any significant delocalization of proteins due to its fixative properties [126]. A wash with an organic solvent such as chloroform or xylene is recommended for many tissues that have a high lipid content. Lipid removal simplifies mass spectra in the medium mass range (500-1000 *m*/*z*), thus allowing the identification of low mass peptides that are usually masked by the high abundance of lipid peaks. Washing protocols using organic solvents are acclaimed not to cause any delocalization or extraction of peptides or proteins but also not to reduce salt adducts.

The washing method must be optimized for the specific MSI application, since different classes of molecules require different treatment. For example, peptide analysis may require an additional step of tissue treatment which includes 30 s of washing in 90% ethanol, 9% glacial acetic acid, and 1% deionized water. Tissue samples washed in ethanol can be stored in a closed container at RT for up to 6 h without noticeable degradation observed in the MALDI spectra [121]. Some molecules can be detected only if washing has not been performed. In order to visualize all possible molecules, a combination of different tactics can be tested. The washing method is an important aspect in sample preparation. Usually either the slide, with a tissue sample mounted on it, is immersed in the washing solution or the solution is applied on top of the tissue by pipet [126]. Immersion of the slide in the washing solution brings a risk of tissue loss, especially if the section was not properly mounted on the slide.

On-Tissue Digestion.

The current practical upper limit of MALDI analyzers is 30 kDa (the theoretical limit is much larger for singly charged species), which limits the detection to approximately half of all proteins present in tissue. With approximately 2000 proteins expressed in a typical mammalian cell, 1000 additional proteins could potentially be imaged if MALDI analyzers were able to detect an unlimited mass range. On-tissue digestion is often performed in order to bring more proteins into the MS range. This requires the local application of a proteolytic enzyme on the surface of the tissue section. Optimal enzyme activity requires the sample to remain moist at temperatures ranging from RT to 37 °C for an incubation period of 1 h up to several hours (e.g. overnight) depending on the research target and protocol used. Excess liquid applied in conjunction with the enzyme can lead to analyte diffusion during the incubation process. In order to prevent diffusion of peptides, two methods of enzyme application were optimized: spraycoating or spotting. During spray-coating the entire surface of the sample is covered with the solution of the enzyme. In this case, the spatial resolution is limited by a combination of diffusion and the diameter of the laser spot. The spotting of the enzyme prevents analyte diffusion and can be used if no extremely high spatial resolution is required. In this case, small solution volumes, e.g. 100 pL, are deposited on an area of 100 μm diameter on the surface of the tissue. The digestion process and diffusion of analytes occurs exclusively within the spotted area. The size and distribution of enzyme spots limits the spatial resolution of the MS image. The protocol for on-tissue digestion for both frozen as well as FFPE samples has been recently published by Djidja et al. [127].

Other methods of protein digestion involve tissue blotting through a PVDF membrane with trypsin immobilized on the surface, followed by capture of the resulting peptides onto a second PVDF membrane, which maintains some degree of spatial resolution. This procedure is referred to as the molecular scanner. The lack of sensitivity and spatial resolution resulting from the blotting process

in this approach result in limited pratical applicability. Protein digestion typically yields peptides in the range of 400-3500 Da, a range where instrumental sensitivity is higher than that for intact proteins. The mass spectrum of trypsin digested tissue is more complicated in the low mass region, due to simultaneous detection of peptides and overlapping signals from ionized lipids, matrix clusters, and smaller biomolecules.

On-tissue digestion results in the detection of multiple peptides derived from a number of proteins present in the tissue section. Protein identification can be performed using tandem MS instruments which have capabilities for efficient fragmentation of selected peptides, allowing the identification of the original protein. However, the chemical and molecular complexity of tissue may deliver multiple peptides at each nominal mass [48].

2.1.3. Matrix Application

Matrix solution must be applied on the surface of the tissue before MALDI and ME-SIMS analysis. The matrix solution consists of three components: (a) an organic solvent such as methanol or acetonitrile, (b) an organic acid (the matrix) such as sinapinic acid (SA), and (c) trifluoroacetic acid (TFA). The organic solvent extracts the molecules from the tissue and quickly evaporates, allowing matrix crystal formation from the weak organic acid. The extracted molecules are incorporated into growing matrix crystals. The addition of TFA increases the amount of available protons for ionization and augments the number of intact pseudomolecular ions formed from the surface. During MSI analysis, the surface of the sample is probed with an appropriate laser beam or primary ion beam. The energy of the beam is absorbed by the matrix crystals, which evaporate quickly, releasing the trapped molecules. The matrix plays an active role in the ionization of the analytes. The ionized molecules are typically singly charged [M + H]+. The choice of matrix (organic acid) applied on the tissue section depends on the mass range analyzed and chemical properties of analytes. Many different types of matrices are used for MALDI-MSI. An overview of the matrices

used for MSI can be found in a number of MALDI and sample preparation reviews. They commonly include derivatives of benzoic acid, cinnamic acid, picolinic acid, and Sinapinic acid (3,5-dimethoxy-4-hydroxycinnamic acid) is routinely used for higher *M*w proteins while R-cyano-4- hydroxycinnamic acid (CHCA) is more common for lower *M*w molecules such as peptides. For phospholipids and drug analysis, matrices such as 2,6-dihydroxyacetophenone (DHA) or DHB are used. The matrices can also be used in combination, such as SA in combination with 20% DHB, which provided good crystallization and a relatively homogeneous matrix layer across all organ tissues and resulted in detection of hundreds of protein signals from analyzed tissues. More effective matrix systems for MSI experiments are being developed. For example, a new class of ionic solid and ionic liquid matrices for MALDI-MSI has been developed. Solid ionic matrices are obtained from the equimolar reaction mixture of acidic crystalline matrices such as CHCA, SA, or DHB with different bases such as aniline or *N*,*N*dimethylaniline. Lemaire et al. performed MALDI imaging on rat brain sections comparing the ionic matrix CHCA/ aniline with regular CHCA [57]. The application of an ionic matrix resulted in higher signal intensity and sensitivity, better image quality and peptide localization, reproducibility, and higher resistance to laser ablation. The organic matrices absorb the energy of the laser beam in the UV-wavelength range, resulting in efficient desorbtion and ionization of the matrix material. The ionization of the matrix and related clustering processes create strong background signals in the low mass region of the spectrum, which complicates the MALDI-MSI analysis of low *M*w compounds. In order to lower the chemical noise at low mass ranges, higher molecular weight porphyrin based matrices (in the mass range from 566.70 to 1531.96 Da) have been used for MALDI analysis of vitamins and drugs. Gold nanoparticles (AuNPs) with a size range of 2-10 nm can also be used as new generation matrices for high resolution imaging. They do not ionize easily but allow desorption and ionization of analytes, with minimum background signal coming from the matrix itself. The background interference from matrices occurs as a result of their high concentration in comparison to analyte concentrations and the fact that clusters of matrix molecules also ionize and are detected together with analytes.

Recently, a new matrix, containing the coumarin moiety (7-mercapto-4-methylcoumarin), was used for MSI analysis of small molecular compounds such as choline alkaloids from the areca nut with decreased background interference in the mass range below *m*/*z* 600. The concentration of the matrix in solution must be carefully considered before matrix application. If the concentration is too low, the analyte may diffuse from its original position before crystallization or there will not be a sufficient amount of organic acid to form proper crystals. Too high a matrix concentration could result in rapid crystal formation and a limited time for analyte extraction and incorporation. Depending on the specific application, the matrix concentration range is 10-30 mg/mL SA for protein analysis and 10-20 mg/mL CHCA for peptide analysis. Solvent combinations consisted of acetonitrile, ethanol, methanol, isopropanol, and acetone in different solvent/water proportions. Two solvent solutions, 50:50 acetonitrile/water and 50:50 ethanol/water, were recommended as good general solvents for different types of tissue samples [48]. More non polar solvents such as methanol or isopropanol can be used to analyze more hydrophobic surface molecules. As this study showed, the TFA concentration also affects the MS signals and corresponding results of direct tissue analysis. This study found that a concentration range of 0.3-1% TFA maximizes the total number of proteins analyzed. However, in most current MSI protocols used to analyze different classes of biomolecules, TFA is used at a lower concentration of 0.1%. Hydrophobic proteins, such as membrane-bound or transmembrane proteins, are generally not easily extracted and cannot be detected during MSI analysis. Methods for dissolving molecules in organic/water solutions are ineffective for this class of molecules. For tissue imaging and profiling, the application of MS-compatible detergents to the tissue surface significantly enhanced detection of membrane/lipophilic proteins. The size of the crystals can influence the sensitivity of MSI detection. Usually, too small crystals lead to lower sensitivity for detecting intact biomolecules in MALDI-MSI. In ME-SIMS small crystals assist in obtaining higher spatial resolution. ME-SIMS only samples the top 50 nm of the matrix surface and sputters less than 1% of the surface area in the static SIMS mode whereas MALDI typically ablates much more material both in depth and in surface area [126]. Ultimately,

the choice of matrix crystal size is determined by a combination of desorption and ionization technique used, required spatial resolution, and required sensitivity. In order to obtain bigger crystals, a sufficiently long incubation time is required. Longer incubation allows the solvent to extract the biomolecules of interest from the tissue surface into the droplet prior to crystal formation. There are two parameters that influence the formation of matrix crystals: the speed of solvent evaporation and the time of matrix incubation. Slower solvent evaporation leads to bigger crystals [128]. This process depends on the solvent to water ratio. The higher the concentration of the solvent, the faster its evaporation. Slow crystallization can also be achieved by keeping the sample after matrix deposition at 4 °C for 1 h. This process results in lower noise mass spectra, as already pointed out by Stoeckli et al. [129]. The matrix incubation time should be sufficient for effective solvent evaporation after each round of its application; too fast matrix application leads to analyte diffusion, due to an excess of solvent solution present on the surface of the tissue. The amount of solvent applied on the tissue should allow efficient extraction of biomolecules without diffusion of analytes. On the other hand, too big crystals (100 μm) cover a large area of the tissue. As a result, molecules are extracted from many cells at a time and the spatial resolution of the MS image is negatively affected. For example, a 100-nL droplet dries to form a 900-μm diameter crystalline spot and extracts proteins from about 1000 individual cells [49]. Smaller matrix spots are necessary to increase the spatial resolution of the image, since it is limited by two key parameters: spot size and laser beam diameter. Larger spots require larger sample step sizes between laser shots, while smaller spots allow decreased sample step sizes. With spot diameters smaller than the laser beam, the imaging resolution is generally limited to the laser beam diameter (50-150 μm). Smaller matrix spots and better coverage of the tissue with the matrix material were obtained by applying a thin layer of mechanically ground SA particles on the surface of the tissue section [51]. The seeded matrix produced more homogeneous ion signals throughout each matrix spot and reduced the number of droplets required to obtain matrix spots with good crystal coverage. The crystallization process is heavily influenced by the presence of salts and surface-active compounds such as

carbohydrates, lipids, or excessive amounts of hemoglobin. The local concentration of these interfering substances may lead to differences in the crystallization process, crystal heterogeneity, decreased signal quality, and formation of analyte-rich matrix crystals called “sweet spots” or “hot spots” as well as crystals formed exclusively by matrix and containing no or very little analytes. Rinsing of the tissue section with ethanol prior to matrix application removes salts from the sample’s surface and improves the crystallization process. It has been demonstrated that different salt/matrix compositions locally lead to the formation of different pseudomolecuar ion types and different degrees of fragmentation. Another important aspect of effective matrix crystallization is the choice of the matrix, since different matrices give different crystal patterns. Evaluation of the three most common matrices, SA, CHCA, and DHB, showed that the pattern of SA crystallization is the most uniform and provides an even layer of crystals over the spotted area [121]. In comparison, DHB formed crystals on the rim of the drying droplet which may compromise the quality of the image. With high repetition rate lasers (typically 200 Hz or more), the fast and accurate generation of averaged molecular profiles for each spot on the tissue surface became possible.

Matrix Application Methods.

The matrix solution can be deposited on the tissue section as individual droplets (spotted) or as a homogeneous layer (coated). The method of matrix deposition depends on the spatial resolution required for the analysis. Both methods are focused on homogeneous crystallization of the smallest possible crystals trapping the largest amount of analytes without any diffusion of molecules. Both methods, spotting and spraying, can be performed either manually or automatically. Automated devices offer better reproducibility and control over extraction processes, which allows comparison between different samples. Both spotting and spraying parameters must be experimentally optimized for every tissue type, since the quality of MSI depends on matrix coverage, wetness of the surface during matrix application, and thickness of the crystal layer, with all of these parameters

being surface dependent. In both cases, multiple passes of matrix application are necessary to coat the entire tissue, but excess amount of matrix (overcoating) can suppress the analyte signal. The matrix layer can be monitored under a microscope until an even coating with small crystals is achieved. To check the homogeneity of the matrix coating and to correct for uneven matrix distributions, an internal calibrant, typically a peptide in the same mass range as the analyte of interest, can be added to the matrix solution. Matrix deposition methods developed at the FOM-Institute for Atomic and Molecular Physics (AMOLF) for different matrix deposition devices and high-resolution MSI were reviewed by Altelaar and Heeren in 2009 [130]. Here, the most popular spotting and spraying devices currently available for MSI are presented.

Spotting.

The spotting of the matrix solution onto the tissue section limits diffusion of the analytes to the spot size. Manual spotting can be done using a micropipet that delivers microliter (μL) droplets generating spots of approximately millimeter size. Robotic spotting deposits picoliter (pL) droplets and provides a spot size of around 100-200 μm, which allows MSI at a resolving power of approximately 200 μm [131]. Two popular automated spotting devices utilize two different types of droplet ejectors: inkjet-style piezonozzles and focused acoustic dispensers. General matrix deposition guidelines for both types of spotting devices have been described. Both ejectors can release 100 pL droplets that dry on the tissue to a 100-150 μm diameter spot. The resolution of MSI analysis is in this case limited by the size of matrix spots, which is generally larger than the size of the focused laser spots. Smaller, closely spaced droplets are best for high resolution images and effectively limit analyte migration to the area covered by the droplets, but they are harder to generate and evenly sample with the desorption laser. Larger droplets spread on the sample surface, increase the possibility of analyte diffusion within the matrix spot, and are better suited to profiling rather than imaging. Spotting devices allow multiple rounds of droplet deposition, which can be performed at the same location to increase analyte extraction from the tissue. A number of devices

are available for generating and accurately depositing droplets onto a surface. Matrix spotting devices such as CHIP (Shimadzu) robotic spotting, are equipped with inkjet-style piezonozzles, which were first applied to the fabrication of microarrays of DNA, proteins, and other bioactive molecules. Another automated method for matrix deposition, a desktop inkjet printer with a six-channel piezoelectric head that delivered 3 pL droplets, was presented by Baluya et al. in 2007 [132]. The comparison of different matrix deposition methods, such as electrospray, airbrush, and inkjet, showed that the mass spectral images gathered from inkjet-printed tissue specimens were of better quality and more reproducible than those from specimens prepared by the electrospray and airbrush methods. The significant limitation of inkjet dispensers is the clogging of the capillary when spotting highly concentrated matrix solutions. Focused acoustic dispensers utilize acoustic energy to generate very small droplets of matrix on tissue sections. Matrix solution is kept in a reservoir which is constructed from an acoustically transparent membrane that is coupled to a piezotransponder by way of a column of water. The sound wave produced by the transponder reaches the surface of the matrix solution in the reservoir, which ejects droplets of matrix with a volume of approximately 120 pL. These droplets are then collected on the tissue section held inverted over the matrix reservoir. Since the droplets are ejected from a large surface reservoir, there is no possible clogging. A robot capable of acoustic droplet ejection (RapidSpotter; Picoliter Inc., Sunnyvale, CA) is being used to eject picolitersized matrix droplets onto the surface of the tissue, effectively coating the section. This technique results in a crystal surface similar to that of electrosprayed surfaces, but it allows multiple rounds of precise droplet deposition. This matrix application method deposits droplets which can remain wet longer and minimizes molecule delocalization to the area of droplet. Another spotting device, an Acoustic Reagent Multispotter (Labcyte Inc., Sunnyvale, CA), consists of an acoustic ejector, a translational stage with a lateral precision of 3 μm, and video telescopes integrated under software control [54].

The matrix spotters can also be divided into contact and noncontact deposition devices. Contact deposition methods require a pin or capillary to physically contact the sample for droplet

deposition, which can introduce cross-contamination. The reproducibility of spotting small amounts of liquid using pins or microcapillaries can be low. Noncontact printing devices such as piezoelectric, thermal ink jet, solenoid valves, and pulsed field ejectors do not have these limitations. Microdroplets are ejected from small capillaries onto the tissue by applying pressure pulses without any contact between capillary and the sample.

Spraying. Spray coating is employed to cover the surface of the sample with a fine distribution of small droplets of matrix solution. After drying of these droplets, a homogeneous thin film of solid matrix crystals is formed. Spraying devices deposit a matrix mist on the tissue surface, which results in much smaller droplets than those generated by spotting devices. This approach provides smaller crystal sizes (100 μm) and allows higher image resolution. Both manual (pneumatic sprayer, airbrush, or thin-layer chromatography (TLC) sprayer) and automated (robotic pneumatic sprayer, vibrational sprayer, electrospray) spray coating methods have been developed. Automated methods yield more reproducible results and provide more uniform application conditions. Currently, one fully automated vibrational sprayer system (ImagePrep, Bruker Daltonik GmbH, Bremen, Germany) is commercially available. The spray coating delivers smaller crystal sizes but less reproducible matrix deposition and higher chance of analyte diffusion in comparison to spotting application methods if the surface is wetted too much. The advantage of spray coating is the size of the crystals formed, which are typically around 20 μm, not larger than the diameter of the focused laser beam. A more even coating can be obtained when the final spray consists of only solvent, allowing predeposited matrix crystals to redissolve and recrystallize, which increases the incorporation of analytes in the final crystals. The smallest crystal size, ,5 μm, can be obtained using electrospray deposition, which has been shown to yield subcellular resolution in ME-SIMS experiments [54]. Both spotting and spraying of the matrix take place at RT, but spotting needs more time than spraying, which can cause degradation of some molecules during the matrix application process. Additionally, matrix application by coating covers the whole surface of the

tissue section with a layer of matrix solution and requires a more careful application protocol than spotting.

Alternative Matrix Application: Solvent-Free and Matrix-Free Methods.

Some other matrix application methods for MSI have been tested. One of them is sublimation, which was successfully used for matrix application and resulted in the formation of very small crystals. A protocol using sublimation for matrix deposition was reported in 2007 and provided a homogeneous coating of matrix that allowed the generation of high resolution phospholipid images from tissue [133]. The sublimation apparatus is relatively simple and became commercially available. The key advantage of sublimation deposition in comparison to other matrix application techniques is the elimination of diffusion of the analyte molecules because no solvent is used during the matrix deposition step. Another advantage is the increased purity of the matrix and the reduction of the crystal size. Sublimation of matrix for imaging of peptides and proteins requires rewetting of the surface to enable surface extraction of these analytes. Another alternative matrix application method optimized for detection of proteins involved cocrystallization of matrix with analyte acquired through placing a tissue section upon a drop of SA matrix dissolved in 90% ethanol and 0.5% Triton X-100.4 After solvent evaporation, a seed layer of sinapinic crystals was added as a dispersion in xylene, followed by application of additional layers of SA added as solutions in 90% ethanol followed by 50% acetonitrile. An increased mass range between 25 kDa and 50 kDa of proteins was obtained from tissue sections such as kidneys, heart, lung, and brain of different rodent species. Some variants of matrix application methods, such as covering the complete area with a large matrix volume at 4 ̊C followed by a drying step at RT or complete immersion of the sample in a matrix solution followed by a drying step, were tested, but both caused extensive protein diffusion. However, the first method yielded very strong ion signals while the second provided a very thin layer of crystals and modest signal intensity. Carbon nanotubes (CNTs) are another

desorption and ionization method with potential application for MSI [9]. They are generated *in situ* by chemical vapor deposition. This method gives minimal interference, but this has not been shown to work on proteins or peptides. Nanostructure-initiator mass spectrometry (NIMS) employed clathrates. Clathrate nanostructures provided a spatial resolution comparable to MALDI-MSI, while maintaining the soft nature of MALDI. In this method, "initiator" molecules trapped in nanostructured surfaces (clathrates) release and ionize intact molecules adsorbed on the surface.

This surface can be used together with both ion and laser beam irradiation. Finely ground matrix particles which were filtered directly onto the tissue through a 20 μm stainless steel sieve are another variant of a dry-coating, solvent-free matrix deposition employed in MSI. However, dry matrix deposition resulted in simpler and faster sample preparation with virtually no analyte delocalization. This approach provided highly reproducible results and eliminated the variation caused by operator differences. Another method of solvent-free matrix deposition involved coating of the tissue section with a thin layer of seed matrix, but in that case, a painter's brush was used to distribute the ground matrix, such as SA, on the tissue surface. Excess material was removed using a gentle blow of compressed air in a laboratory hood. Observation of the tissue under a microscope indicated a high density dispersion of 0.3-3 μm particles across the section [9]. The experiment comparing dry coating and regular coating using airbrush showed that the solvent free matrix application technique was more beneficial for MALDI imaging of lipids, since solvent was necessary for extracting peptides from tissue samples.

2.1.4. Staining

Staining of MSI tissue sections helps to correlate the data obtained from imaging experiments with tissue histology. Staining can be done either before or after an MSI experiment. If staining is performed before MS measurements, the protocol must contain MS friendly histological dyes such as cresyl violet or methylene blue. H&E staining protocols, which are the most commonly used staining protocols in clinical pathology, cannot be used prior to MSI analysis, since these dyes affect the quality of the mass spectra. H&E staining can be performed after MSI measurements, following matrix removal from the surface of the sections. Matrix removal can be achieved by immersing the glass slide in a 70% ethanol solution for approximately 1 min followed by dehydration of the section in a graded ethanol series before H&E staining. The morphology of the sample must also be visualized before tissue profiling experiments, since only specific regions of the heterogeneous sample are subject to analysis. When staining cannot be performed, e.g. the tissue section was mounted on a steel plate, correlation of the MSI data with the sample morphology of the sample can be accomplished by using two adjacent sections: one for histology (on a glass slide) and one for MSI analysis. However, visual coregistration between both sections can be complicated due to differences in the structure of adjacent tissue sections. Morphologically and functionally distinct regions of heterogeneous tumor samples are interesting objects for MSI analysis for medical diagnostics. Studies of different regions of lung and breast tumor sections resulted in the detection of many differences on the biomolecular level [10]. In both cases, the adjacent H&E stained tissue sections were used to select the regions of interest (ROIs) prior to profiling.

2.1.5. Contaminants

After successful tissue preparation, the sample is introduced and analyzed in a mass spectrometer, which results in detection of hundreds of different ions. The correct identification of detected peaks is the next biggest challenge. The increasing sensitivity of MSI instruments allows detection of molecules from the tissue present at very low concentration. Along with the biomolecules, many contaminants introduced during sample preparation steps will be ionized and detected as well. Among the most often detected contaminants of biological samples are the impurities present in the solvents used for tissue washing and matrix deposition, salt adducts, keratin, or polymers such as OCT or polyethylene glycol (PEG). A recently published review of common MS contaminants contains a broad list of unwanted ions of different origin [135] The contaminants are classified into two groups. The first group contains proteinaceous interferences or contaminants, which include e.g. enzymes used in sample preparations, keratins, and other abundant, involuntarily introduced proteins or instrument induced peptide fragment interferences. Non proteinaceous interferences or contaminants such as matrix clusters in MALDI-MS, adducts, solvents and polymeric interferences, plasticizers, and additives have been grouped in a second category of contaminants. Ion mobility MS, high-field asymmetric waveform ion mobility spectrometry (FAIMS), and matrix-free laser desorption/ ionization techniques including desorption/ionization on silicon (DIOS), DESI, or direct analysis in real time (DART) are some techniques that are helpful in minimization or elimination of certain background interferences [135]. In addition to that, all steps of tissue preparation should be carefully performed, which includes the use of gloves and clean lab glassware. Every MS analysis should also include blank tests such as system-, solvent-, method-, matrix-, and equipment blanks.

2.2. MSI Instrumentation and Processing Tools

2.2.1. Mass Analyzers

Technological improvements in mass spectrometric instrumentation have enabled various high throughput peptide and protein screening applications in a large variety of samples. Proteomics as a scientific field that has emerged over the past decade has been a major driving force. Approaches such as shot-gun proteomics, quantitative proteomics, top-down proteomics, and chemical proteomics have all developed out of mass spectrometric innovations. Imaging mass spectrometry is taking the same advantage of these innovative technological developments. In this section we will discuss some of these innovations from a more instrumental perspective, highlighting their respective benefits in MALDI or SIMS analysis of tissue.

2.2.2. Software for MSI

Data collected from MS imaging yield high resolution molecular profiles across the tissue with data files of up to a few gigabytes which requires complex visualization software. MSI software controls data acquisition and processing in order to generate ion images. A comparison of several recently developed imaging mass spectrometry software packages was presented by Jardin-Mathe´ et al. in 2008 [75]. Here, we will present a couple of examples of imaging software.

Biomap. Biomap (Novartis, Basel, Switzerland, www.maldi-msi.org) is an image processing application. BioMap was originally developed by Rausch for the evaluation of MSI data in biomedical research, and due to multiplemodifications, it can now support many more imaging data formats, including optical, positron emission tomography (PET), computed tomography (CT), near-infrared fluorescence (NIRF), and MSI [73]. BioMap was written in IDL (Research Systems, Boulder, CO). Visualization is based on multiplanar reconstruction, allowing extraction of arbitrary slices from a 3D-volume. Other features linked to visualization are overlaying of two individual data sets or displaying the ROIs. It allows displaying the mass spectrum from selected single points or ROIs on the generated image. Another mode is to select on the mass spectrum the analyte of

interest and to calculate by integration over the corresponding peak its distribution on the scanned area. Routines for baseline correction of spectra, spatial filtering, and averaging of spectra enhance the information obtainable from a data set. The software provides visualization and a storage platform, which can be easily extended by various software packages, individually designed for the analysis of specific data sets.

FlexImaging. FlexImaging 2.0 (Bruker Daltonics GmbH, Bremen, Germany, www.bdal.com) software is used for acquisition and evaluation of MALDI-TOF imaging data. This software allows color-coded visualization of the distribution of any ion detected during MSI and overlaying of the optical and MS images. Integrating statistical classifications such as hierarchical clustering, PCA, or variance ranking, the software provides "Class Imaging", which allows the classification of tissue types and determination of the class.

3. Applications of Mass Spectrometric Imaging

3.1. Application of MSI in Pathology

MSI has been applied in a vast spectrum of disease pathology. A number of diseases, such as Parkinson's disease, Alzheimer's disease, Fabry's disease, muscular dystrophy, kidney diseases, nonalcoholic fatty liver disease (NAFLD), Tay-Sachs/Sandhoff's disease, and cardiovascular disease, have been investigated by the MSI technique. Similarly, many cancer types, such as breast cancer, prostate cancer, ovarian cancer, lung cancer, glioma, and colon cancer liver metastasis, were analyzed using MSI [9]. As the demand to understand cancer biology is constantly increasing, the number of projects being carried out in this field and the spectrum of applied techniques are also dramatically expanding. In this regard, MSI becomes a practical tool to study cancer biology. The availability of tumor tissue samples (biopsies, resected tumors, and xenograft models) increases the practicability of MSI in cancer biology, as they make good samples for MSI analysis. Many molecular complexities, such as the transformation of cells from normal to malignant as well as the involved pathways, are important scientific questions at present. A number of MSI studies were

carried out to compare the protein or lipid profiles obtained from normal and tumor tissue.The objective of this comparative analysis is to distinguish cancer from normal tissue as well as classify different grades or subtypes of cancer on a molecular level. In this section of the review we present the application of MSI in current medical research. In the first of the presented applications, a large series of quantitative element maps (such as Fe, Cu, Zn, and Mn) were produced in native brain sections of mice subchronically intoxicated with 1-methyl-4-phenyl-1,2,3,6-tetrahydropyridin (MPTP) as a model of Parkinson's disease by a newly developed LA-ICP-MS imaging technique. Significant decreases of Cu concentrations in the periventricular zone and the fascia dentata at 2 h and 7 days and a recovery or overcompensation at 28 day, most pronounced in the rostral periventricular zone (+40%), were observed. In the cortex, Cu decreased slightly to -10%. Fe increased in the interpeduncular nucleus (+40%) but not in the substantia nigra. Some other model of neurodegenerative disease was recently investigated using MSI. The analysis of the Scrapperknockout (SCR-KO) mouse brain showed two types of neurodegenerative pathologies: spongiform neurodegeneration and shrinkage of neuronal cells. PCA revealed numerous alterations and their position in the KO mouse brain. In another study, TOF-SIMS was used to image the distribution of biochemical compounds on tissue sections of steatotic liver [136]. Fatty liver or steatosis is a frequent histopathological change, which is a precursor for steatohepatitis that may progress to cirrhosis and in some cases to hepatocellular carcinoma. The analysis of steatotic vesicles disclosed a selective enrichment in cholesterol as well as in diacylglycerol (DAG) species carrying long alkyl chains and demonstrated that DAG species C30, C32, C34, and C36 carrying at least one unsaturated alkyl chain were selectively concentrated in the steatotic vesicles. Moreover, investigations performed on the nonsteatotic part of the fatty livers despite exhibiting normal histological features revealed small lipid droplets corresponding most likely to the first steps of lipid accretion. Similar experiments were performed using TOF-SIMS with a bismuth cluster ion source to map lipids *in situ* at the micrometer scale and to simultaneously characterize their molecular distribution on liver sections obtained from patients suffering from NAFLD. Accumulation of

triacylglycerols (TAG), DAGs, monoacylglycerols, and fatty acids, with the apparition of myristic acid, together with a dramatic depletion of vitamin E and a selective macrovacuolar localization of cholesterol, were observed in steatosis areas of fatty livers compared to control livers. Finally, the analysis revealed lipid zonation in normal human liver and accumulation of very similar lipids to those detected in areas of fatty livers, which were not characterized as steatotic ones by the histological control performed on serial tissue sections. MSI potentially could be employed in early detection of steatosis, even before the pathological changes are detectable by histological examination. In another example, MALDI-MSI was involved in studying the specific molecular profiles of ovarian cancer interface zones (IZ), which are the regions between tumors and normal tissues. Unique profiles were identified for the tumors, the normal zone, and the IZ. Analysis identified two interfacespecific proteins, plastin 2 and peroxiredoxin 1 (PRDX 1), which were differentially regulated between zones. The results were confirmed by fluorescence microscopy, which revealed high expression levels of plastin 2 and PRDX 1 along the IZ of ovarian tumors. This comparative proteomics study suggested that the IZ is different from the adjacent tumor and normal zones and that plastin 2 and PRDX 1 may be interface markers specific to ovarian tumors. Cancer biology was also investigated by DESI-MSI used to image differential expression and the distribution of different classes of lipids in thin tissue sections of canine spontaneous invasive transitional cell carcinoma of the urinary bladder (a model of human invasive bladder cancer) as well as adjacent normal tissue from different dogs. The tumor and adjacent normal tissue showed differences in the relative distributions of the lipid species. Increased absolute and relative intensities for at least five different GPLs and three free fatty acids in the negative ion mode and at least four different lipid species in the positive ion mode were seen in the tumor region of the samples in all four dogs. In addition, one sphingolipid species exhibited increased signal intensity in the positive ion mode in normal tissue relative to the diseased tissue. The same imaging technique was also used for the profiling and imaging of arterial plaques [9]. Sodium (in positive ion mode) and chloride (in negative ion mode) adducts of diacyl glycerophosphocholines (GPChos),

sphingomyelins (SMs), and hydrolyzed GPChos were detected. Additionally, cholesteryl esters were detected via adduct formation with ammonium cations. Finally, cholesterol was imaged in the atheroma by doping the charge labeling reagent betaine aldehyde directly into the DESI solvent spray, leading to *in situ* chemical derivatization of the otherwise non-ionic cholesterol. The results revealed lipid rich regions of two different lipid profiles within the arterial walls. These lipid rich regions likely correspond to the areas of the tissue where lipoprotein particles accumulated. It is also possible that the different lipid distributions may correlate with the stability or vulnerability of that particular region of the plaque. The MS profiling technique has been applied to detect the highly expressed proteins in human oral squamous cell carcinoma of tongue biopsy. In this study two distinct molecules at approximately 4500 Da and approximately 8360 Da were detected in cancer tissue. To study pancreas pathology, different regions of the pancreas of both control and obese mice were imaged by MALDI-MSI and peptide-specific profiling was performed [9]. The distribution of C-peptide of insulin and glicentin-related polypeptide displayed a striking resemblance with Langerhans islet's histology. Recently, a new strategy in MSI was developed to use 9-year-old rat brain tissues of a Parkinson's disease animal model stored in FFPE blocks. The method employed MALDI tissue profiling, combining the use of automatic spotting of the MALDI matrix with *in situ* tissue enzymatic digestion. The analyses confirmed that ubiquitin, transelongation factor 1 (eEF1), hexokinase, and Neurofilament M were down-regulated, as previously shown in human or animal models of Parkinson's disease. In contrast, peroxidoredoxin 6, F1 ATPase, and R-enolase were up-regulated. In addition, three novel putative biomarkers were uncovered from protein libraries: eEF1 and collapsin response mediator 1 and 2. Finally, the identity of CRMP-2 protein was validated using immunocytochemistry and MALDI imaging based on the different ions from tryptic digestion of the protein. TOF-SIMS was used to obtain high-resolution ion images in ischemic retinal tissues. Marked changes in Ca2+ distribution, compared with other fundamental ions, such as Na+, K+, and Mg2+, were detected during the progression of ischemia. Furthermore, the Ca2+ redistribution pattern correlated closely with TUNEL-positive

(positive for terminal deoxynucleotidyl transferase-mediated 2′-deoxyuridine 5′- triphosphate nick end-labeling) cell death in ischemic retinas.

After treatment with a calcium chelator, Ca2+ ion redistribution was delayed, resulting in a decrease in TUNEL-positive cells. Results showed that ischemia-induced Ca2+ redistribution within retinal tissues was associated with the degree of apoptotic cell death, which possibly explains the different susceptibility of various types of retinal cells to ischemia. MSI quickly became a very important tool for molecular histology. Pathologists have already recognized its potential and started exploring biological material collected from patients and stored in hospital tissue banks. Since these banks usually contain a large number of different samples, it became clear that MSI analysis of such material must be automated. The development of an automated setup for high throughput molecular histology MSI has been recently presented by McDonnell et al. [137]. This device consists of a controlled environment sample storage chamber, a sample loading robot, and a MALDI time of flight/time of flight (MALDI TOF/TOF) mass spectrometer, all controlled by a single user interface. The automated set up has the positional stability and experimental reproducibility necessary for its clinical application. A clear distinction between tumurous tissue and healthy tissue is observed, indicating the applicability of MSI as a medical diagnostic imaging tool. An additional example in tumor biology is employed to study a MCF7 xenograft breast cancer model [127]. Both of these examples employ MSI to provide detailed molecular insight into tumor biology. Along with advances in instrumentation, MSI became well recognized in the medical community.

3.2. Application of MSI in Biological Sciences

MSI has numerous applications in the field of biological sciences. Direct tissue analysis from any type of biological material made this technique a powerful tool for life sciences.

Here, we present some examples of MSI being applied to investigate biological samples of different origin. An MSI technique was applied to investigate a novel family of antimicrobial peptides, named raniseptins present in the dorsal skin of a frog (*Hypsiboas raniceps*). These studies demonstrated that the mature raniseptin peptides are in fact secreted as intact molecules within a defined glandular domain of the dorsal skin. *De no*Vo MS/MS sequencing and direct MALDI imaging experiments of the skin from another frog (*Phyllomedusa hypochondrialis*) identified 18 bradykinin related peptides (BRPs) along with their PTMs. Calf and mature bovine lenses were imaged by MALDIMSI methods to obtain the distribution of lens R-crystallins and their modified forms. The results from this study shed light on the physiological significance of the modified forms of the two R-Crystallin subunits. Another study, involved MSI to investigate the distribution of the age-related changes of human lens R-Crystallin including a novel L52F R-ACrystallin mutation in a cataractous lens [9]. Application of this technique to lens biology enhanced the understanding of R-Crystallin protein processing in aging and diseased human lenses. Ocular lens and retinal tissues were used as model samples for developing a new MALDI-MSI tissue preparation protocol for integral membrane proteins. Molecular images of full-length Aquaporin-0 (AQP0) and its most abundant truncation products were obtained from bovine and human lens sections. This tissue preparation protocol was also successfully applied to image the distribution of the G-protein coupled receptor, opsin, in the rabbit retina. In addition, both fresh and formaldehyde-fixed mammalian lenses were analyzed by direct profiling of two relevant phospholipid classes, phosphatidylcholines (PCs) and SMs [138]. Neuropeptides are another class of biomolecules which can be investigated using an MSI technique. Neuropeptide distributions

directly from rat, mouse, and human pituitary tissue sections were obtained using MALDI-MSI in microscope mode, from crustacean neuronal tissues using an MALDI Fourier transform mass spectrometer (MALDI-FTMS) instrument, and from a wide variety of invertebrate samples such as tissues and ganglia, single neurons, or single vesicles using MALDI-MSI. Distributions of peptide isoforms belonging to 10 neuropeptide families were investigated in the brain of the Jonah crab (*Cancer borealis*). This study revealed the spatial relationships between multiple neuropeptide isoforms of the same family as well as the relative distributions of neuropeptide families. In addition, a MALDI ion trap was used to visualize neuropeptides from the dissected tissue of the house cricket (*Acheta domesticus*). Tissue imaging together with tandem MS allowed successful identification of neuropeptides present in the corpora cardiaca and allata of the insect. MSI was applied to obtain distributions of ganglioside molecular species in the mouse hippocampus. In this study, the location of age-dependent C20-GD1 accumulation was successfully characterized. Another study of the gangliosides inside mouse brain tissue sections demonstrated that the N-fatty acyl chains of gangliosides were differentially distributed in mouse hippocampal regions, whereby the gangliosides with an N-C18 acyl chain were enriched in the CA1 region, while gangliosides with an N-C20 acyl chain were enriched in the dentate gyrus. In this study, an ionic liquid matrix was used for MSI of gangliosides, which provided excellent sensitivity for ganglioside detection without significant loss of sialic acid residues. Another class of lipids detected from rat brains was mapped by MSI to study the normal functioning of the brain. The differential distribution of PCs such as PC(32:0), PC(34:1), and PC(36:1) in different parts of the rat brain was successfully investigated by Mikawa et al. by using MALDI-MSI. PC(32:0) and PC(34:1) were more abundantly observed in the gray matter areas than in the white matter areas, while PC(36:1) was evenly distributed throughout the central nervous system. In addition, PC(32:0) and PC(34:1) were mostly detected in the granular layer of the olfactory bulb, piriform cortex, insular cortex, and molecular layer of the cerebellum, regions known for high neuronal plasticity. In another study, the cell-selective distribution of polyunsaturated fatty acid-containing glycerol phospholipids in the mouse

brain was presented [139]. The results showed that arachidonic acid- and docosahexaenoic acid-containing PCs were seen in the hippocampal neurons and cerebellar Purkinje cells, respectively. MALDI-MSI was also used to study the spatial distribution of metabolites from the cyanobacteria *Lyngbya majuscula* 3L and JHB, *Oscillatoria nigro*-V*iridis*, *Lyngbya bouillonii*, and a *Phormidium* species as well as the sponge *Dysidea herbacea*. The same ionization technique was employed to detect high concentrations of the marine alkaloid, norzoanthamine, present in the epidermal tissue in the colonial zoanthid *Zoanthus* sp.. MSI was used to investigate the biological processes occurring in the reproductory system of small rodents. For example, MALDI-MSI provided global and time-correlated information on the local proteomic composition of the sexually mature mouse epididymis. Tissue sections, cells collected by LCM, and secretory products were analyzed, which resulted in detection of over 400 different proteins. In another study, MALDI-MSI technology was used to characterize the spatial and temporal distribution of phospholipids species associated with mouse embryo implantation. The ion images showed that linoleate- and docosahexaenoate-containing phospholipids localized to regions destined to undergo cell death, whereas oleate-containing phospholipids localized to angiogenic regions. Molecular images revealed the dynamic complexity of lipid distributions in early pregnancy and shed light on the complex interplay of lipid molecules in uterine biology and implantation. Also, the molecular composition, relative abundance, and spatial distribution of a large number of proteins expressed during the periimplantation period were investigated by MALDI-MSI. For the first time, *in situ* proteome profiles of implantation and interimplantation sites in mice in a regionand stage-specific manner with the progression of implantation were obtained. Cytosolic phospholipase A (2alpha) null females that show implantation defects were also investigated, which provided new insights regarding uterine biology. TOF-SIMS equipped with a gold ion gun was used to image mouse embryo sections and analyze tissue types such as brain, spinal cord, skull, rib, heart, and liver [9].

3.3. Application of MSI in Proteomics/Peptidomics

Here, we briefly discuss the issue of peptide and protein detection directly from tissue sections. Topics such as bottom-up and top-down on-tissue proteomics, on-tissue protein digestion, and single-cell MALDI-MS profiling will be discussed [48]. Mass spectrometry evolved into an indispensable tool for proteomics research. The demand for spatial information of detected proteins and peptides pushed the boundary of mass spectrometry capabilities and started a new era of MSI. Three strategies for protein identification and characterization are currently employed in proteomics: bottom-up proteomics, which analyzes proteolytic peptide mixtures, middle-down proteomics, which analyzes longer peptides, and top-down strategies, which analyze intact proteins. It became clear that rapidly developing MSI instrumentation should allow detection, identification, and characterization of proteins directly from biological tissue also in terms of their interactions with other molecules, PTMs, and different isoforms expressed inside the cells. In terms of the bottom-up approach, the proteins present in biological tissue must be first subjected to *in situ* digestion by proteolytic enzyme. The protocol designed for MSI was published by Groseclose et al. in 2007 [141]. The method for on-tissue protein digestion involved a tissue washing step with organic solvents capable of removing lipids. Otherwise, the strong lipid signals in the same mass range as that of the obtained peptides interfere with peptide detection and identification. After removal of lipids, a tissue section should be sprayed or spotted with the solution of proteolytic enzyme, most commonly trypsin, and after the incubation time covered with matrix (usually DHB or CHCA). The top-down approach allows detection of intact proteins directly from tissue sections. The upper mass range of the instruments used for MSI is the detection limiting factor. Therefore, efficient detection and identification of proteins with *M*w 30 kDa needs to be improved. MALDI also suffers from mass dependent sensitivity drop-off, which means that bigger proteins must be present at sufficient concentration in order to be detected and analyzed. One of the solutions for the

sensitivity issue could be Tag-Mass. The complexity of the sample and high *M*w of the analyzed proteins, which very often limits detection of biomolecules directly from tissue sections, can be reduced by simultaneous extraction, separation, and digestion of proteins from the tissue section while preserving their relative location. To reduce the complexity of the sample, contact blotting of fresh cut tissue sections on a surface of C18-coated resin beads or on a polymeric conductive membrane can be performed. The chemical properties of the blotting surface determine which analytes are detected during MSI. Typically, hydrophobic surfaces are used because they can be washed with water in order to remove salts before matrix application. More complex surfaces, such as Teflon plates or antibodies bound to surfaces, were also tested for extraction of specific proteins or a class of proteins from the tissue. While the concept of blotting is quite straightforward, the process involves transfer of the proteins from the tissue into the methanol sprayed MALDI target, which requires diffusion of molecules, which can lead to loss of spatial resolution in the imaging experiment. The molecular scanner approach, introduced by Hochstrasser and co-workers, combined both a blotting step and enzymatic digestion [141]. The molecular scanner was initially developed for 2D gels. It allows protein separation using 2D-PAGE with parallel digestion of the separated proteins and transfer of obtained peptides onto a membrane while keeping their relative positions. The membrane is then sprayed with a matrix solution and analyzed in a mass spectrometer. One of the interesting applications of MALDI-MSI for analyzing intact proteins directly from tissue sections was presented by Dani et al. in 2008 [142]. MSI was applied to study *Anopheles gambiae* antennae, with the aim of analyzing the expression of soluble proteins involved in olfaction perireceptor events. Profiling of the proteins on the antennae surface, revealed distinct protein profiles between male and female antennae, and imaging experiments showed differences in the localization of some of the detected proteins. High resolution measurement and top-down MS/MS experiments resulted in the identification of two proteins: a 8 kDa protein which matched with an unannotated sequence of the *A. gambiae* genome and odorant binding protein 9(OBP-9). This work showed that MALDI-MS profiling is a technique suitable for the analysis and

comparison studies of small and medium proteins in insect appendices. A similar approach was used for comparison of the peptide profiles of the sea slug (*Aplysia californica*) neurons using MALDI-MSI which revealed distinct peptide profiles for each neuronal subtype analyzed and identification of previously unknown peptides. In this study, individual F cells were isolated based on their position, size, and pigmentation and Tungsten needles were used to transfer each cell onto a MALDI target plate containing 0.5 mL of DHB solution.

Single-Cell MALDI-MS Profiling

A review presenting single-cell MALDI-MS peptide profiling from individual cells and other mass-limited tissue samples was published by Li et al. in 2000 [3]. The most recent review presents the history of single-cell mass spectrometry with the emphasis on live single-cell MS. Single-cell MALDI-MS has multiple advantages, such as the following: (1) compatibility with crude mixtures; (2) minimal sample clean up; (3) no need for tagging or preselecting the peptide of interest; (4) simple instrumentation; (5) high sensitivity; (6) complementary information to immunochemical methods; and (7) compatibility with PTMs. One important characteristic of single-cell MALDI-MS is its ability to directly profile intact cell and tissue samples without any purification of peptides or proteins. Simplified sample preparation preserves spatial and biomolecular information within the cells, reducing degradation processes, dilution of biomolecules, or contamination from adjacent cells, which can have different sets of peptides or proteins. Among the disadvantages would be the following: (1) too low sensitivity of instruments to probe the entire content of a single cell and (2) too small size of the cell, making it hard to probe with a laser. The first MALDI-MS profiling analyses of peptides in single neurons were done by van Veelen et al. in 1993, Jime´nez et al. in 1994 [37,38]. Neuropeptides were directly detected in single neurons and the neurohemal area of peptidergic (neuroendocrine) systems in the *Lymnaea* brain. The study of neuroendocrine systems revealed that processing of the complex prohormone expressed in this system occurred entirely in

the soma. In addition, novel as well as previously identified peptides were detected. These experiments demonstrated that MALDI-MS was promising and a valuable approach to study of the synthesis and expression of bioactive peptides, with potential application to single-cell studies in vertebrates, including humans. Since then a number of single-cell MALDI-MS experiments was performed on cells of different origin, such as crayfish, insects, red blood cells, single neurons, mouse bone marrow-derived mast cells, and individual rat pituitary cells. The review article published by Jime´nez and Burlingame provided an overview of MALDI as a tool for the direct analysis of peptide profiles contained in single cells from invertebrate (the pond snail), vertebrate species (*Xenopus* and rat), and tissue biopsies with a special emphasis on the sample handling required for each application [43]. MALDI-MS was successfully applied for profiling the proteome of single cells, but imaging is still not possible due to currently available laser spot sizes, which at present can be focused to a minimal diameter of 20 μm. Development of lasers capable of probing single cells, together with improved matrix application methods, deliver- ing small crystals containing highly concentrated analytes, will open the gate for MALDI-MS imaging of single cells.

Obviously, single cells are routinely analyzed by TOF-SIMS, but the detection limit (upper mass 1000 Da), extensive in source fragmentation of secondary ions and lack of MS/MS capabilities of TOF-SIMS instruments, limits at present its application in proteomic studies.

The first application of MALDI-MSI to proteomics was presented by Caprioli et al. in 1997 [20]. The analysis of regions of rat splenic pancreas and rat pituitary revealed many peptides and proteins detected from the C-18 blotted target. The next paper showed direct profiling of proteins present in tissue sections for several organs of the mouse where over 100 peptide/protein signals in the 2000-30 000 Da range were observed after blotting of the tissue sections on a conductive polyethylene membrane and coating with SA.. Later, MALDI-MSI was used to determine peptide distributions directly from rat, mouse, and human pituitary tissue sections with high-resolution MSI, which allowed localization of neuropeptide distributions within different cell clusters of a pituitary tissue section. MALDI-MS was also employed to detect and structurally characterize small cardioactive

peptides in two functionally related neurons, which form a network involved in the modulation of heartbeat in freshwater snails *Lymnaea*. MALDI-MS was also used to study the intricate processing pattern of a preprohormone expressed in neurons of this gastropod mollusk. Isolated cells and tissues, including egg-laying hormone-releasing cells, from the central nervous systems of the model marine mollusks *Aplysia californica* and *Pleurobranchaea californica* were used to demonstrate the salt removal method and detect several neuroactive peptides previously characterized by conventional biochemical methods. MALDI-MSI was applied to the study of amyloid peptide distribution in brain sections from a mouse model of Alzheimer's disease [143]. A combination of MS profiling and LCM of normal breast stroma, normal ductal epithelium, ductal carcinoma *in situ*, and invasive ductal carcinoma microdissected from a single frozen section was presented by Palmer-Toy et al. in 2000 [144]. Each tissue type, when analyzed separately, revealed characteristic peaks. Several prominent peaks in the 4500-7000 Da range distinguished the breast stroma from the ductal epithelium while highmass peaks in the mass range of 45 to 60 kDa were characteristic only for the invasive carcinoma. A recent review focused on four state of the art proteomic technologies applied in the discovery of potential tumor markers, namely, 2D difference gel electrophoresis, MALDI-MSI, electron transfer dissociation mass spectrometry, and a reverse-phase protein array technique, presenting progress in proteomic technologies from 1997 to 2008 was published by Wong et al. in 2009 [9].

3.4. Application of MSI in Metabolomics

The functional levels of biological cells or organisms can be separated into the genome, transcriptome, proteome, and metabolome. Here, we concentrate on applications of MSI for metabolomics. The term metabolism is derived from the Greek word *metabole´*, meaning change. Metabolome is defined as the total quantitative collection of low *M*w compounds (metabolites) present in cells or organisms which participate in metabolic reactions required for growth,

maintenance, and normal function. The metabolome is composed of small *M*w organic and inorganic species, generally of a mass less than 1500 Da. The number of metabolites is generally 10-fold smaller compared to that of genes; for example, the yeast *S. cere*V*isiae* has a genome encoding more than 6600 genes and contains 584 identified metabolites. But the number of metabolite molecules present within one cell can vary from just a few (signalling molecules) to millions (glucose). The concentration of metabolites depends on the metabolic state of the investigated cell. Metabolites can be of endogenous origin (synthesized or catabolized within the cell or organism) or of exogenous derivation (pharmaceuticals or food nutrients).

Metabolomics is currently a rapidly developing discipline for the study of microbial, plant, and mammalian metabolomes. A recent review focused on the collection of analytical data for metabolomic studies was published by Dunn in 2008 [145]. A review presenting the capabilities of current MSI techniques for imaging metabolite molecules and a summary of representative MSI studies of both endogenous and exogenous metabolites was recently published by Sugiura and Setou [146]. Here, some of the MSI applications for metabolomic studies of animals, plants, sponges, and cyanobacteria are presented. MSI has been recently employed for detection and identification of 13 primary metabolites, such as adenosine monophosphate (AMP), adenosine diphosphate (ADP), adenosine triphosphate (ATP), uridine diphosphate (UDP), or *N*-acetyl-D-glucosamine (GlcNAc), directly from rat brain sections using a 9-aminoacridine matrix. The combination of MALDI and SALDI, enabled successful MSI of low mass species from mouse heart and brain tissues with improved detection sensitivity. Two imaging instruments (MALDI-TOF and MALDI-FTICR) were used to image two HIV protease inhibitors, saquinavir and nelfinavir, in Mono Mac 6 cells. A sublimation/deposition device for homogeneous matrix deposition was constructed which allowed imaging of these HIV protease inhibitors at clinically relevant concentrations. MALDI-TOF and cluster-TOF-SIMS imaging approaches were used to study the localization of lipids (cholesterol, cholesterol sulfate, vitamin E, glycosphingolipids) on skin and kidney sections of patients affected by the Fabry disease. A number of plant metabolites,

such as amino acids, sugars, and phosphorylated metabolites, in wheat seeds were imaged by using a combination of two matrices, CHCA and 9-aminoacridine. MALDI-MSI was also used to image the distribution of the pesticide nicosulfuron (parent compound and a phase 1 metabolite) in plant tissue following root and foliar uptake. The spatial distributions of natural products with potential therapeutic applications were characterized by a MALDI-MSI approach. In this study, a number of metabolites from the cyanobacteria *Lyngbya majuscula*, *Oscillatoria nigro*-V*iridis*, *Lyngbya bouillonii*, and a *Phormidium* species were identified. In addition to known natural products such as curacin A and curazole, a large number of unknown ions colocalized with the different cyanobacteria. MSI proved to be useful as a strategy for *de no*V*o* drug discovery. The same technique was used to observe the secondary metabolites found within the sponge *Dysidea herbacea*. These data demonstrated the potential of MSI for providing spatial distribution of natural products, from single strands of cyanobacteria to the very complex marine assemblage of a sponge [9].

3.5. Application of MSI in Lipidomics

Lipids, important components of the cells, serve as the building blocks of cellular membranes (phospholipids, cholesterol), participate in many signaling pathways (diacylglycerol, ceramide, glycolipids, steroids, or prostaglandins), and are stored as an energy source (triacylglycerols). Various different types of lipids, such as glycerophospholipids, sphingolipids, sterol lipids, prenol lipids, saccharolipids, waxes, and fat-soluble vitamins, are found in biological systems. Glycerophospholipids, the key components of the cellular membranes and also important constituents of serum lipoproteins and pulmonary surfactant, are the most abundant lipids in the brain, and they play a role in metabolism and cell signaling. In glycerophospholipids, two hydroxyl groups of the glycerol are esterified by two different fatty acid chains. The third hydroxyl group of the glycerol backbone is esterified by phosphate. The phosphate group can be further esterified by

inositol, glycerol, choline, serine, or ethanolamine. In the case of phosphatidic acid, phosphate remains in its unesterified form. Different subclasses of glycerophospholipids contain different types of bonds between the glycerol backbone and the fatty acid chain, e.g. acyl, alkyl, or alk- 1′-enyl. The fatty acid chains in biomembranes usually contain an even number of carbon atoms, which can be saturated (e.g., 16:0, 18:0) or unsaturated (e.g., 16:1, 18:1,18:2). Sterols are another important lipid constituent of biological membranes. For example, cholesterol is part of cellular membranes in animals, where it regulates the cellular membrane fluidity but also serves as a secondary messenger in developmental signaling. Researchers interested in lipid biology may visit a comprehensive Lipid Metabolites and Pathways Strategy Web site for more information about different classes of lipids and most recent discoveries in this field of science [147]. Almost all types of ionization sources used for MSI have been successfully applied in the field of lipid imaging. Lipids were imaged using MALDI, DESI, SIMS, and also the recently developed nano-PALDI82 ionization method. In general, most lipids present in tissues ionize easily due to their polar head groups (e.g., phosphocholine [M + H]+ *m*/*z* 184, phosphoinositol [M + H]- *m*/*z* 241, phosphoethanolamine [M - H]- *m*/*z* 140318). Phosphatidylcholines, sphingomyelins, and cholesterol ionize in positive ion mode, while phosphatidylinositols, phosphatidylserines, and sulfatides ionize in negative ion mode. Phosphatidylethanolamine (PE) can be analyzed in both positive as well as negative ion mode. Most biological samples subjected to MSI have a rich lipid content which manifests in a strong ion signal around *m*/*z* 800. A commonly observed phospholipid in tissues is phosphatidylcholine PC (16:0/18:1) with an ion [M + H]+ at *m*/*z* 760 having the elemental composition of C42H83NO8P. Phosphatidylcholines are at present the most commonly detected and imaged lipid class. They dominate mass spectra due to the presence of the positively charged quaternary ammonium group in the choline head. Collisional activation and fragmentation of all phosphatidylcholines yield a major product of phosphocholine (PC) at *m*/*z* 184. However, when a phosphatidylcholine molecular species is cationized with either Na+ or K+, closely related but structurally quite different ions at *m*/*z* 147 and 163, respectively, are observed [148]. In fact,

these product ions became very characteristic MS features by which cationized PC can be easily identified. Lipids can also generate abundant negative ions. For phospholipids, such as PE, phosphatidylserine (PS), phosphatidic acid (PA), phosphatidylglycerol (PG), and phosphatidylinositol (PI), this is due to the presence of the phosphodiester moiety, which can exist as a very stable gas phase anion. Other lipids, such as sphingomyelin (SM) (phosphodiester), sulfatides (sulfuric acid ester), and bacterial lipids related to lipid A (phosphate esters), also yield quite abundant [M - H]-molecular anions. For some polyphosphate esters, doubly charged ions [M - 2H]2- can also be observed [148]. Phosphatidylinositol and lysophosphatidylinositol (LPI) yield a specific fragment ion at *m*/*z* 241; plasmenylethanolamine (PlsEtn) and PE yield one at *m*/*z* 196.141 The MS analysis of cellular membranes results in the detection of signals from hundreds of different phospholipids molecular species. In contrast, cholesterol is present in the plasma membrane as a single molecular species. During the MALDI desorption/ionization process, cholesterol undergoes dehydration, which results in detection of the [M + H - H2O]+ ion at *m*/*z* 369.3, instead of [M + H]+ at *m*/*z* 387.3, [H + NH4]+ at *m*/*z* 404, or [M + Na]+ at 409.3 [33]. A review of matrices used for the analysis of cellular phospholipids has been recently published by Kim et al. [149]. Matrices such as 30 mg/mL DHA in 50:50 ethanol/water,11 5 mg/mL CHCA in 50:50 acetonitrile/0.1% TFAaq, and 40 mg/mL DHB in 20 mM potassium acetate, 70:30 methanol/0.1% TFAaq were used for imaging of lipids. The lipid spectra can be simplified by addition of potassium acetate or LiCl320 to the matrix solution, which results in the formation of exclusively potassium or lithium adducts of lipids, respectively. By changing the concentration of alkali metal salts in the matrix solution, it is also possible to selectively ionize either polar or nonpolar lipids. The presence of alkali metal salts in the matrix solution enhanced the detection of polar lipids, while a salt-free matrix solution was suitable for the detection of nonpolar lipids. The selection of the matrix must be tailored to the type of tissue examined and the class of lipids being analyzed. For MSI analysis of lipids in a lens, PNA (*p*-nitroaniline) at a concentration of 20 mg/mL resulted in improved sensitivity as compared to DHB. The ionic liquid matrix offered excellent

sensitivity for detection of gangliosides without significant loss of sialic acid residues. The matrix application method should be carefully selected as well. The optimal matrix application should not cause any diffusion of lipids from their original position in the tissue section. Various matrix application methods have been examined for MSI of lipids. Matrix application by direct sublimation of an organic matrix described by Hankin et al. provides multiple advantages [133]. Such a matrix deposition method prevents diffusion of the lipids, delivers extremely small matrix crystal sizes, and results in a substantial increase in sensitivity. Because no solvent is needed, this method provides enhanced purity of matrix applied to the sample and uniformity of deposition. In terms of the tissue sample preparation method, the use of OCT is not recommended before lipid imaging due to a significant reduction in the quality of the mass spectra. Current, nonmass spectrometric approaches for phospholipids analysis include an extraction step and subsequent identification of the main phospholipid classes by either 31P MRI (magnetic resonance image) spectroscopy or chromatographic separation followed by mass spectrometric detection. In comparison to these techniques, MSI offers a quick and easy method of lipid analysis. A review presenting MALDITOF MS as a technique suitable for all known lipid classes together with its advantages and disadvantages in comparison to other established lipid analysis methods was discussed by Schiller et al. in 2004 [150]. A review presenting massspectrometry- based strategies for lipid analysis, including imaging, was published in 2007 by Isaac et al. [151]. Here, we will present some MSI applications for lipid analysis. Detection and imaging of lipid molecules was mostly studied using rodents brains. For example, whole normal rat brain sections were investigated by imaging technology to observe the distribution of three types of PCs such as PC(32:0), PC(34:1), and PC(36:1). Age-dependent changes in the distribution and amount of PCs molecular species in a rat brain were also evaluated. Atlases of lipid distributions in rat brain and mouse brain have been constructed. MSI was also successfully applied to rodent brain sections analyzed by intermediate-pressure MALDI on a linear ion trap (LIT) instrument and by gold cluster focused ion beam TOF-SIMS. Specific examples in the detection of phospholipids, sphingolipids, and glycerolipids were

presented with images of mouse brain and kidney tissue slices. The localization of specific lipids and osmium oxide (OsO4), a stain commonly used for unsaturated lipids in electron and optical microscopy of cells and tissues, was independently monitored in mouse adipose tissue by using TOF-SIMS with Bi cluster primary ions. TOF-SIMS was also utilized to address the issue of localization of lipids and inorganic ions in healthy rat aorta and human atherosclerotic plaque [152]. Several frozen vessels bearing atherosclerotic lesion were analyzed by cluster TOF-SIMS to map lipid content at micrometric resolution. Debois et al. performed the first *in situ* lipidomic analysis of human liver using TOF-SIMS imaging directly on tissue sections [153]. *In situ* detection and structural analysis of phosphatidylcholine species in rat brain tissue was performed using a MALDI TOF/TOF mass spectrometer. Initial profiling of lipids in tissue was conducted by MALDI-TOF and allowed for the assignment of phosphatidylcholine species. To confirm the structure, lithium adducts of phosphatidylcholine species were analyzed by MALDI-MS/MS and yielded fragments that allowed for the identification and positional assignment of acyl groups in phosphatidylcholine species. The *in situ* analysis of two relevant phospholipid classes, phosphatidylcholines and sphingomyelins, in slices of fresh or fixed bovine lenses was also performed. A new technical variation of NIMS has been recently presented by Patti et al. for analysis of carbohydrates and steroids, which can be challenging to detect with traditional mass spectrometric approaches. The cation-enhanced NIMS was used to image the distribution of sucrose in a *Gerbera jamesonii* flower stem and the distribution of cholesterol in a mouse brain [154]. The advantages of imaging using ion mobility prior to MS analysis were demonstrated for profiling of human glioma and selective lipid imaging from rat brain. Lipids have been implicated in a number of human disease states, including cancer and cardiovascular disease. Different MSI ionization sources and mass analyzers offer a variety of possibilities for lipid analysis and practical tools to study lipidomics.

3.6. Application of MSI in Pharmacokinetic Studies

Pharmacokinetic studies are performed to examine the absorption, distribution, metabolism, and excretion of drugs in laboratory animals or humans. This procedure is mandatory for drug approval by the Food and Drug Administration (FDA). Pharmacokinetic studies employ many methods, such as whole-body autoradiography (WBA), tissue homogenization, and analysis by high performance liquid chromatography tandem mass spectrometry (HPLC MS/MS), and in the past decade also MSI. WBA requires the compound of interest to be radioactively labeled. The compound is then administered to animals, which are sacrificed after different postdose time points. Whole-body sections of these animals are then exposed to a radioactivity detector or film, which allows visualizing the spatial radioactivity distribution. The WBA technique is used during early stage drug development, which provides many benefits, including parallel sample processing, standardized procedures, high sensitivity, and applicable quantification. However, this method has two major limitations, such as the expensive, time-consuming synthesis of radiolabeled drugs (labeled with e.g. 3H, 14C) and the incapability to distinguish between a parent drug and its metabolites[118]. While the first leads merely to more complexity and increased cost for each experiment, the last cannot be overcome by this technology and additional analysis of tissue homogenates by HPLC-MS is required. At present, WBA and MSI are two imaging techniques often used together to obtain the most reliable data for drug distribution in small animals. MALDI imaging itself is an excellent tool for visualizing small molecules in tissue sections. Many biologically or pharmacologically relevant compounds are less than 1 kDa in size and can be easily detected by MS. These include both exogenous and endogenous molecules, such as pharmaceutical compounds and their metabolites, drugs of abuse, environmental toxins, and endogenous metabolites. In pharmacokinetics, were demonstrate the use of MALDI-MSI by employing this technique to detect the anticancer drug paclitaxel in a human ovarian tumor and the antipsychotic drug spiperone in spiked sections of rat liver tissue. The development of new MALDI-MS imaging methods adapted

to animal whole-body sections allowed a specific and simultaneous detection of multiple analytes based on their molecular weights and fragmentation patterns [118]. This technique has potential to reveal data related to the drug's metabolism as well as obtain information on the organism's response to drug treatment. On the other hand, MALDI low-molecular-weight imaging suffers from the interference of the ions derived from the matrix. This problem was overcome by applying tandem MS for imaging of drugs in tissue sections. For example, one study examined a distribution of a drug (SCH 226374) with a calculated protonated monoisotopic *M*w that differed from the *M*w of the SA matrix cluster ion by less than 0.2 amu. In this case, collisionally activated dissociation (CAD) was employed to fragment the drug ion at *m*/*z* 695 into a dominant fragment ion at *m*/*z* 228. The SA cluster ion at *m*/*z* 695 fragmented into noninterfering ions at *m*/*z* 246 and *m*/*z* 471. Thus, MS/MS was used to indirectly localize the SCH 226374 compound in a mouse tumor sample. Another example of MALDI-MS/ MS used to image drugs in tissue was performed on clozapine (*m*/*z* 327) [102]. The MALDI-MS/MS image of the clozapine fragment ion (*m*/*z* 192) showed the most intense signal in the ventricle area, which was in agreement with autoradiography results. The role of the instrument as well as the method used for sample preparation is crucial with respect to the image quality obtained. MSI sample preparation procedures, including sample collection, the choice of matrix, extraction solvent, and matrix application method, must be optimized for each drug individually due to the wide variety of structures, solubility, and physicochemical properties of drug compounds.The matrix solution typically contains one or multiple matrices at different concentrations, organic solvent, water, and TFA. Standard matrix coating involves spraying saturated CHCA in 50:50 ACN/ 0.1% TFAaq with a pneumatic TLC sprayer. Some other matrices, such as DHB (40 mg/mL) in 75:25 methanol/water19 or CHCA (25 mg/mL) in 70:30 ethanol/0.1% TFAaq, were also successfully used for imaging of different drug compounds. To improve the signal intensity in the low mass range, a thin (5 nm) layer of gold can also be sputter deposited on top of the dried matrix layer. In contrast to MALDI methods, DESI offers pharmacokinetic studies direct, high-throughput measurements of tissue sections at AP without any prior chemical treatment

of the sample. This method was used to map the distribution of clozapine directly from rat brain, lung, kidney, and testis after an oral dose of 50 mg/kg. Two reviews presenting various applications of MSI for drug imaging, biomarker discovery, and mapping were published by Rubakhin in 2005 [106]. The distribution of the anticancer drug SCH 226374 in mouse tumor tissue and rat brain was published by Reyzer et al. in 2003 [105]. MALDI images were obtained by using the tandem mass spectrometric technique of selected reaction monitoring (SRM) to specifically monitor the drug under study. The SRM experiment is accomplished by specifying the parent mass of the compound for MS/MS fragmentation and then specifically monitoring for a single fragment ion. Such an approach minimized the potential for ions arising from either endogenous compounds or the interfering matrix ions. In another application of MALDI-MSI, the absorption of an antifungal agent, ketoconazole, into skin was examined by the use of an indirect tissue blotting approach. This method can be used to study the absorption of a wide range of xenobiotics into skin. Additionally, some preliminary data from a combined solventassisted transfer/derivatization approach to sample preparation were also described. The distributions of chlorisondamine, a neuronal nicotinic ganglionic blocker, and cocaine into rat brains were examined. Both compounds were detected in the brains via MALDI-MSI using CHCA and DHB as the matrices for chlorisondamine and cocaine, respectively. Tandem MS was employed to confirm the identity of the protonated ions. The use of MALDI-MSI to study drug distribution in a whole-body mouse section was performed for the first time by Rohner et al. in 2005 [155]. The first results showed a good correlation between WBA and MALDI-MSI data. This approach was extended by protein imaging to produce wholebody images showing the location of drug, drug metabolites, and endogenous markers for various organs of the body. In this study, olanzapine (brand name Zyprexa) was subjected to imaging. Zyprexa is generally used to treat mood disorders such as schizophrenia and acute mania in bipolar patients. MSI analysis of tissues from olanzapine dosed rats revealed the temporal distribution of the drug and metabolites, which was in agreement with previous quantitative WBA studies. MALDI-MS/MS analyses were performed on the whole-body sections to detect

simultaneously olanzapine (*m*/*z* 313) and its fragment ion (*m*/*z* 256) and two first-pass metabolites, *N*-desmethylolanzapine (*m*/*z* 299) together with its fragment ion (*m*/*z* 256) and 2-hydroxymethylolanzapine (*m*/*z* 329) and its fragment ion (*m*/*z* 272). Both metabolites were detected in the liver and bladder, which was consistent with previous autoradiographic data and with the known metabolic pathways in rats. Detection of proteins from organs present in a whole-body sagittal tissue section showed the potential of MSI for the analysis of novel therapeutics with subsequent studies of therapeutic and toxicological processes at the molecular level. Some practical aspects of MALDI-MSI for drug and metabolite imaging in whole-body sections were described by Stoeckli et al. in 2007 [118] In another study, Atkinson et al. applied MALDI-MSI to analyze the distribution of the bioreductive anticancer drug banoxatrone (AQ4N) in H460 lung tumor xenografts. In this study, imaging resulted in localization of the prodrug and its active form as well as ATP and the colocalization of the active reduced form of the drug in the hypoxic region of the tumor [114]. In another MSI application, the anticancer drug vinblastine was imaged in rat whole-body sections by MALDI-MS. Vinblastine is a chemical analogue of vincristine which was first isolated from the Madagascar periwinkle plant. The mechanism of action of these alkaloids is to arrest cell growth during the metaphase through binding to tubulin and inhibiting microtubule assembly. The distribution of the vinblastine precursor ion *m*/*z* 811.4 together with several product ions, including *m*/*z* 793, 751, 733, 719, 691, 649, 524, and 355, was shown. IMS was employed to remove the interfering matrix ions. FTICR images of the antitumor drug imatinib (*m*/*z* 494.2664) and its des-methyl metabolite (*m*/*z* 480.2506) in mouse brain glioma were shown by Cornett et al. in 2008 [156]. The image showed almost none of the presumed imatinib ion distributed outside of the glioma, which indicated that this ion did not accumulate in normal brain. In another study, clioquinol (CQ) was administrated to a mouse model of Alzheimer's disease to study its potential therapeutic effect. CQ is known to interfere with brain metal metabolism and ameliorate disease pathology through a mechanism that is not fully understood. The MSI results showed that CQ was mainly localized within the cortex and the hippocampus, which are brain areas primarily involved

in cognitive functions. Recently, imaging of the HIV protease inhibitors saquinavir and nelfinavir in Mono Mac 6 cells by two types of mass spectrometry techniques, MALDI-TOF and MALDI-FTICR, was performed by Dekker et al. in 2009 [157]. A sublimation/deposition device for homogeneous matrix deposition was constructed which allowed imaging of these HIV protease inhibitors at clinically relevant concentrations. MALDI-MSI has also been applied to assess the distribution of a novel potential therapeutic compound in whole-body sections of mice. Peptides display potent biological activity, such as somatostatin mimetics, and are resistant to the digestion by proteases and peptidases Imaging experiments allowed the detection and localization of the drug and its metabolites, the monocysteine and monomethionine complexes, in kidney sections, where they localized exclusively in the cortex, suggesting that the drug did not penetrate deeply into the organ. MALDI-MSI technology provides molecular images of resected organs or whole-body sections from small animals. It has attracted great interest of scientists interested in drug delivery and metabolism monitoring. It provides *label free* tracking of both endogenous and exogenous compounds with spatial resolution and molecular specificity. In combination with WBA, this technology significantly improves the analysis of novel therapeutics. MSI is a powerful technique which provides deeper insight into therapeutic and toxicological processes such as metabolic changes or side effects often associated with drug administration.

3.7. MSI 3D Imaging

MSI provides two-dimensional distributions of multiple ions detected from biological samples. This technique has been recently extended to the third dimension. It provides 3D distributions of the selected molecules detected by MSI from biological samples. A stack of 2D MS images of a selected ion acquired from the same sample can be stitched together to reconstruct a 3D distribution map of that ion. This extension of a conventional MS imaging experiment provides more comprehensive information about the spatial distribution of selected molecules inside the whole

sample. To perform MSI 3D reconstruction, the sample is cut into serial sections which are processed under identical conditions and imaged in MS. The acquired images are stitched together by software such as Image J336 to obtain the 3D distribution of a particular ion. Here, we present some practical aspects of 3D MSI, its applications and future perspectives of this youngest modification in the MSI family. In terms of the sample, at the beginning of 3D MSI, the rodent brain was the most commonly chosen organ. This was due to its small size, well-defined internal/external structure, and an anatomical atlas which was used as reference for the methodology development. Imaging of two lipids, PS (18:0/22:6) and ST (sulfatide) (24:1), allowed a full visualization of the graymatter region as well as the white-matter region in the total volume of the brain. This allowed a complete view of substructures, such as the corpus callosum and anterior commissure, throughout the brain volume. Cross-sectional views of the 3D models can be used to investigate distributions of many additional molecules detected by MSI. The coregistration of MSI proteomic data from the whole mouse head with *in* V*i*V*o* MRI data was reported by Sinha et al. in 2008 [158]. A detailed procedure describing how to make 3D volume reconstructions of MALDI-MSI data was published by Andersson et al.[159]. On a subcellular scale, 3D MSI images of the mitotic spindle from T98G human glioblastoma tumor cells were acquired by TOF-SIMS. This study demonstrated that 3D SIMS imaging was essential for the analysis of mitotic cells, where specialized regions such as the mitotic spindle were hidden beneath the cell surface. Another study applied TOFSIMS to visualize the 3D distribution of phosphocholine and inorganic ions in single cells. Unlike *in* V*i*V*o* tomographic imaging techniques, 3D MALDI-MS images require the specimen to be sliced into thin serial sections. Sectioning can lead to tissue tearing and deformation. Therefore, correlating consecutive 2D images to obtain a 3D reconstruction must be performed carefully. To properly reconstruct a 3D volume from 2D MSI data, the images must be coregistered. The coregistration can involve inter- and/or intrasection registration. The intersection registration provides alignment of optical images of the tissue sections, while the intrasection registration aligns

the MALDIMSI data to the corresponding optical image. Another coregistration technique involves the use of fiducial markers [9].

The imaging of the sample includes the region containing the markers used as orientation and alignment points during the 3D reconstruction process. One of the advantages of 3D MSI is the possibility to correlate distributions of the multiple biomolecular ions with physiological and structural information observed by *in* V*i*V*o* imaging techniques, such as CT, PET, and magnetic resonance spectrometric imaging (MRSI). These *in* V*i*V*o* imaging techniques are limited to a few molecules and cannot show protein distributions. Of the current techniques, MSI can image the widest range of molecules.

Advantages of MSI

MSI offers a unique tool box for sample surface analysis. Several methods offer high spatial resolution biomolecular analysis. The achievable spatial resolution depends on the ionization technique used; for example, typically MALDI allows probing spots as small as 25 μm in diameter, while a NanoSIMS ion beam can be focused to the size of 50 nm in diameter. With a typical mammalian cell size of 10 μm, MALDI collects spectra covering approximately four cells per image point while SIMS can probe subcellular structures. Special approaches such as the utilization of a high resolution 1 μm coaxial objective or 600 nm microscope mode imaging can be used to overcome some of these spatial resolution limitations. However, these instruments are not widely available yet, and the experiments at extremely high spatial resolution can suffer from the lack of sensitivity. Modern mass spectrometers are capable of separating and detecting ions with very high mass resolution. Resolving power (m/dm) 50% in excess of 105 is routinely available on commercial instruments. High mass resolving power can be used to reveal spatial features that remain hidden with low resolution technologies. Ion mobility separation (IMS) combined with mass spectrometry allows the gas-phase separation of isobaric ions or molecules with similar nominal mass during an MSI experiment. MSI takes full advantage of high sensitivity MS instrumentation to image molecules present at very low concentrations inside the cells. At present the instruments are

capable of detecting molecules present in concentrations as low as 500 attomol, which facilitates detection of components from a single cell. The sensitivity of MS instruments was estimated by spotting a protein solution (insulin) on brain tissue, which resulted in detection of a minimal signal obtained from a spot of insulin at a concentration of 12 fmol/mm. With the laser spot diameter of 50 μm, this resulted in an absolute detection level of 25 attomol per image point. This sensitivity is in a range where it can be used to detect biomolecules present in tissue sections. In order to visualize different classes of biomolecules present inside the cells, the instruments must be able to detect a broad range of ions, from very low *M*w ions such as drugs and metabolites to large *M*w ions of intact proteins. In theory TOF mass analyzers can mass separate all ions without molecular weight limits. MS instruments can also be used for imaging unknown compounds present in the biological sample without any *a priori* knowledge or labels. This is a key advantage of MSI, as unknown molecules can subsequently be identified using tandem mass spectrometry. For this purpose, an ion of interest (parent ion) is fragmented and its fragments (daughter ions) are mass analyzed. This type of analysis is also known as tandem MS, MS*n*, or MS/MS because it involves two or more mass spectrometers: the first mass spectrometric separation is used for the selection of the ion of interest, prior to fragmentation in the collision cell, and the second mass spectrometer is used to mass analyze the fragments generated. Tandem MS can also be utilized for MSI analysis. Another advantage of MSI is that molecules are detected directly from the biological sample without complicated preparation steps. Normally the protocol for MSI requires a short tissue wash followed by matrix application for MALDI and ME-SIMS [22]. Conventional SIMS typically uses no sample surface modification whatsoever. The time of sample analysis is also a crucial aspect of any imaging technique. In the case of MSI, the image acquisition time depends on the selected spatial resolution, the repetition rate of the MALDI laser, and the area sampled. The data acquisition of an average imaging experiment lasts from minutes to several hours depending on the instrumentation utilized. The process is fully automated and normally does not require any supervision.

Limitations of MSI

The sensitive nature of MSI instruments requires that the samples remain stable at room temperature . Unfortunately some molecules degrade at RT within a couple of minutes. The sample preparation process must be carried out as fast as possible without exposing the samples to the air, moisture, or high temperature. Also, all types of sample treatment, including cutting, washing, digestion, or matrix application, possess the risk of sample contamination and molecular diffusion, which can affect the reproducibility of the data, complicate their analysis, or affect the quality of the image. The spatial resolution of a MALDI image can also be affected by the matrix crystal size, which typically is above 10 μm. The image quality can be compromised by the presence of matrix clusters and their alkali metal ion adducts, which complicates detection of compounds in the 500-1400 Da range. SIMS does not require matrix or any sample washing steps, but its extensive in-source fragmentation limits the size of the ions detected to 1000 *m*/*z*. Biological tissue represents an extremely complex and challenging sample for direct analysis by MSI. The multiple molecules present in a tissue section (e.g., proteins, lipids, oligonucleotides, carbohydrates, small organic molecules, matrix ions, and salts) can negatively influence each others' desorption and ionization efficiency and prevent optimal detection. The presence of ion-suppressing phenomena differentially attenuates the ionization process and can limit the number of detected molecules. Ionization suppression occurs when one analyte is present in great excess over another or ionizes more easily than others. For example, components such as lipids, carbohydrates, and salts can promote adduct formation and modes of image acquisition, and their application in MSI, are briefly discussed. In this section, we will also explore and explain the difference between profiling and imaging modes of MSI.

4. Methods and materials

Sample preparation not only influences sensitivity, but also affects the type of scientific problems that can be addressed with imaging MS. Sample preparation for imaging mass spectrometry includes a number of steps that can drastically affect the outcome of an experiment [128]. As a

general rule we can distinguish four different steps in the preparation of a sample before : tissue collection and embedding, tissue sectioning and mounting, washing and surface modifications. Hearts from adult Sprauge-Dawley rats were dissected and stored at -80 ° C until analysis. Thin (12 µm) tissue sections were prepared and thaw mounted onto an ITO slide. (Figure 1)

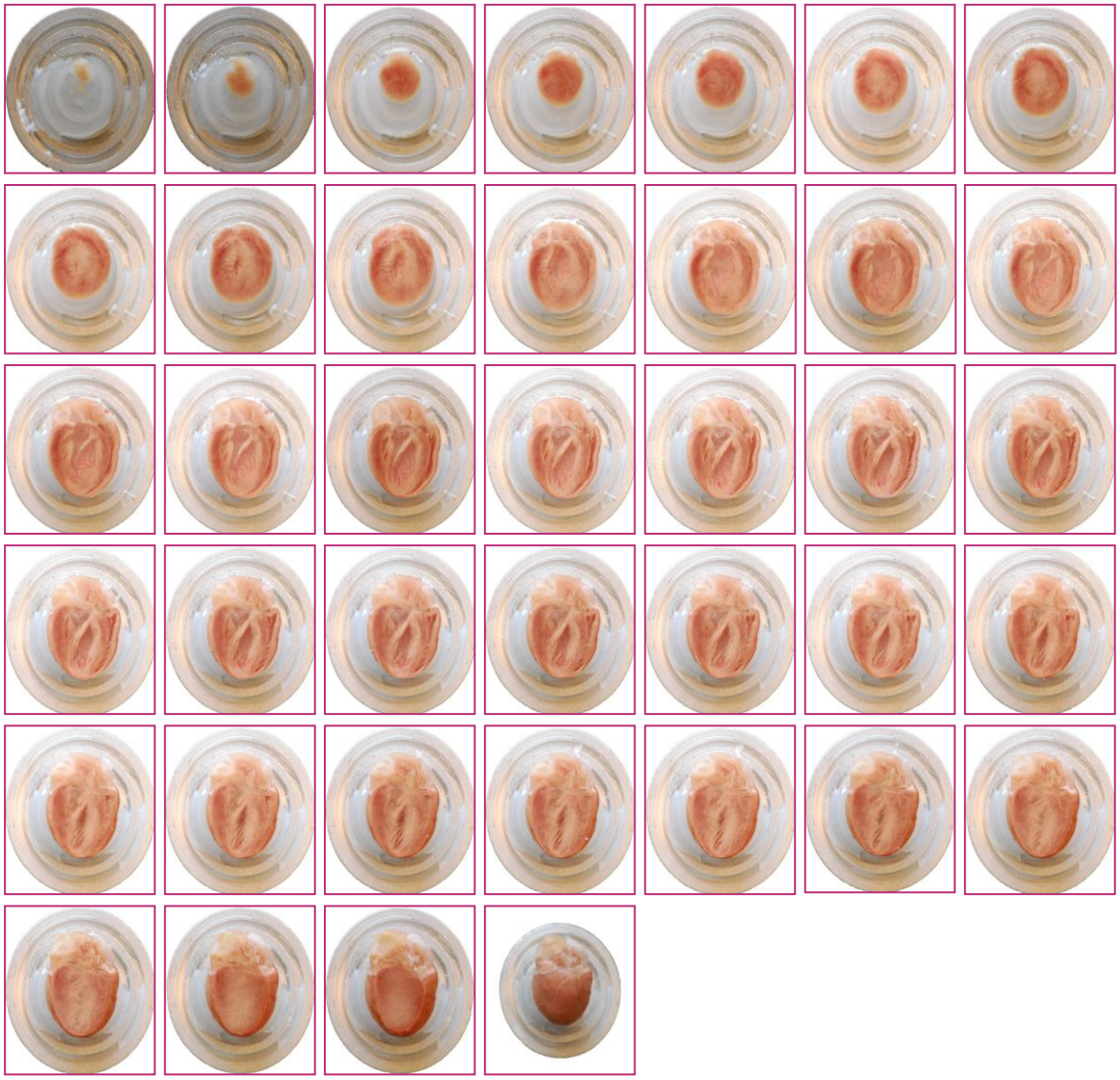

468
276
144
132
72
48
72
72
36
156
48
48
84
72
72
48
108
180
168
144
132
108
156
132
120
204
240
228
516
408
420
312
288
432
348
492
456
840

Fig.1(a) Anatomic features from an entire rat heart. 1 (b) micron distance beetwen SIMS sections

Several rat heart tissue section were done before properly protocol obtained.

In The 12 μm thickness ensures that enough analyte molecules are available for extraction and no problems occur with the insulating properties of tissue[121]. 1-nm layer of gold was deposited on an unwashed tissue section before measurement by SIMS. Sample metallization as a means to improve organic molecular ion yields was introduced [55].

After a series of ethanol/water wash step ,α-cyano-4-hydroxycinnamic acid (HCCA) matrix solution was applied on the tissue section, with subsequent analysis by MALDI-MSI. A good example of the influence of sample preparation on MS-based biomolecular tissue imaging with MALDI-MSI and (ME-)SIMS is provided by Heeren et al. [55] and describes both SIMS and MALDI related sample preparation issues. Significantly improved signal intensity has been reported following the washing steps [128];

We used a brief (30 sec) 70% ethanol wash that can be used to wash away both cell salts and debris, followed by a (30 sec) 95% ethanol wash to help complete tissue dehydration and to temporarily fix the tissue and prevent subsequent degradation of the proteome. The process for obtaining high quality MALDI-MSI mass spectra relies fundamentally on effective MALDI matrix deposition on the sample. For MALDI-MSI of peptides and proteins, as for standard MALDI-MSI, the choice of matrix is normally determined by the mass range over which the experiment is to be performed [132,133]. In our experiments for lower molecular weight masses (ions, lipids and peptides) and for higher molecular masses (proteins), a TOF mass spectrometer in reflectron mode and 10 mg/ml HCCA, 50:50 ETOH:H2O/0.1% TFA. The matrix application method should be carefully selected as well. Automated vibrational spray coater (ImagePrep by Bruker Daltonics) is used : produces a homogeneous matrix layer, with small crystals and in a closed system. All MALDI experiments were performed using an Ultraflex II MALDI-TOF instrument in two mass ranges: low (m/z 100 to 4000) and medium (m/z 4000 to 40000). MALDI mass spectra were acquired using an Ultraflex II TOF–TOF mass spectrometer (Bruker Daltonics, Billerica, MA, USA) with a solid-state UV laser capable of a variable repetition rate. Positive-ion mass spectra were collected at 100 Hz in the

reflectron mode with a delay time of 20 ns and an acceleration voltage of 25 kV. All mass spectra were externally calibrated and data analyses were performed with the FlexAnalysis and FlexImaging software packages (Bruker Daltonics). Additionally, BioMap (Novartis, Basel, Switzerland) was used for region-of-interest analyses by importing the imaging file produced by the FlexImaging software. (figure 2)

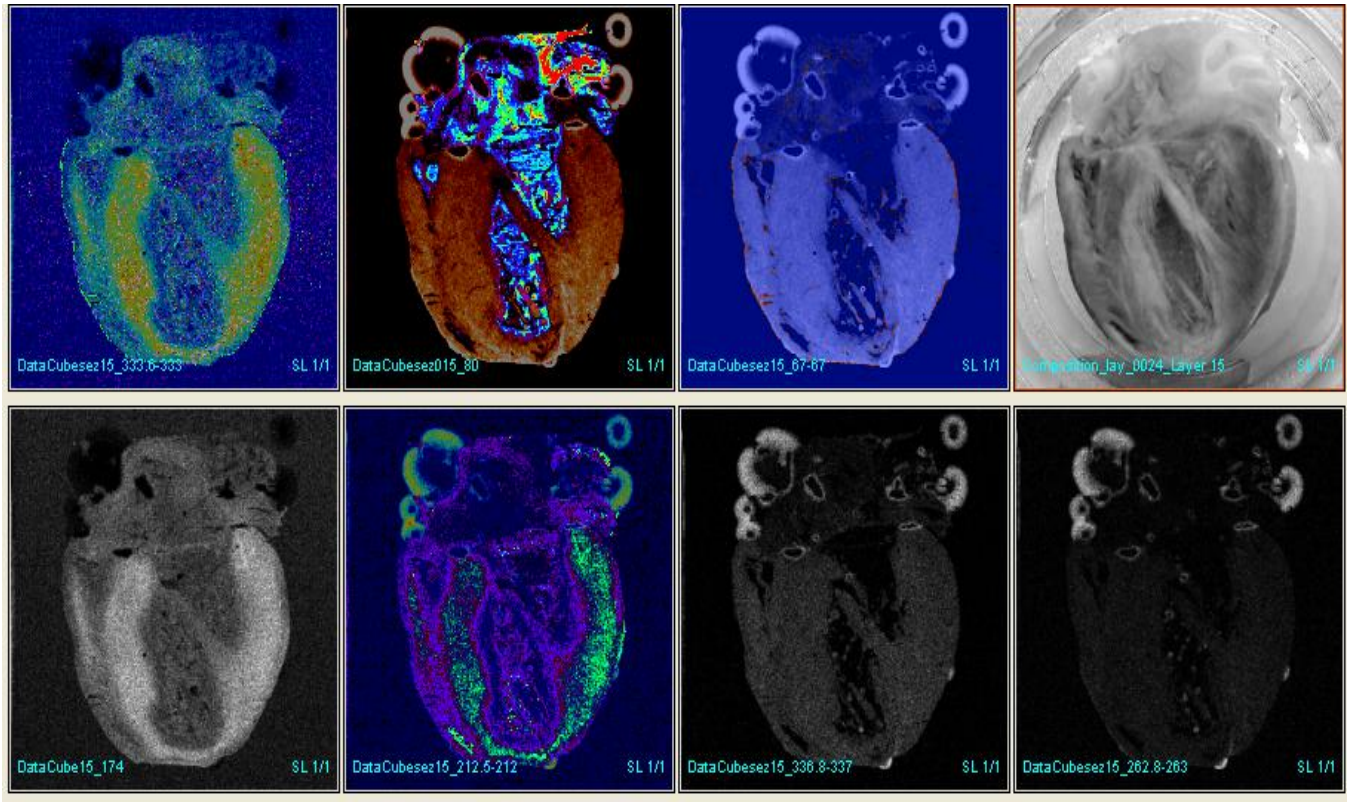

Fig. 2. BioMap images

All SIMS experiments were performed on a Physical Electronics (Eden Praire, MN) TRIFT-II time-of-flight SIMS (TOF-SIMS). To correlate heart's molecular profile with morphological features, the tissue sections were stained with H&E after SIMS and MALDI analysis. Many of the basic requirements are taken from well-established histological methods (see for example www.ihcworld.com/) to the point where the tissue would be fixed.

The amount of data generated in our work is tremendous. The most basic and in many cases still the most insightful way of exploring MS imaging is manual. Peaks of interest can be selected in the

total image spectrum and an intensity profile image or selected ion current (SIC) image of that peak can be made. Most package look at the data from a spectral point of view. Bionformatics plays a central role in doing this. The purpose of our work is to look at the data from an imaging point of view and with the use of DataCubeExplore has been possible. Program load data into memory from an imaging point of view rather than from a spectral point of view. To realized the first 3D reconstruction of the rat heart based on molecular information by SIMS 38 datacube were acquired resulting in total of 42949672960 spectra in raw files around **250 Gbyte** of measurement data. While several structures of the heart can be observed in the 38 individual 2D sections analyzed by SIMS-MS imaging, a full view of these structures in the total heart volume can be achieved only through the construction of the 3D heart model.

From a single image, no depth can be computed without a prior information. In such a context we used a developed software tool, the volume explorer, based way to deal 3D perception from multiple images. Advanced simulations are integrating increasingly larger data sets. It is essential to explore the use of high performance computing to assure tractable methods of investigating computational data. Because these data combine information from different structures, it is important to research advanced interface technology and develop more intuitive methods for interaction with large data sets. Advanced intuitive interfaces are needed to integrate these vast amounts of data into a single coherent simulation. These interfaces will facilitate exploration and interaction and will increase understanding of complex data.

Three dimensional reconstructions of individual mass spectral peaks can be simultaneously displayed using a Red-Green-Blue (RBC) colour scheme in which each colour represents a specific molecular feature (Figure 3). With the recording of large amounts of data, data analysis gets increasingly complicated. PCA is a common statistical technique for finding patterns in data of high dimension and expressing the data in such a way as to highlight their similarities and differences by transforming a number of (possibly) correlated variables into a (smaller) number of uncorrelated variables called principal components (PC) So, the first principal component accounts for as much

of the variability in the data as possible, and each succeed component expresses for as much of the remaining variability as possible [160].

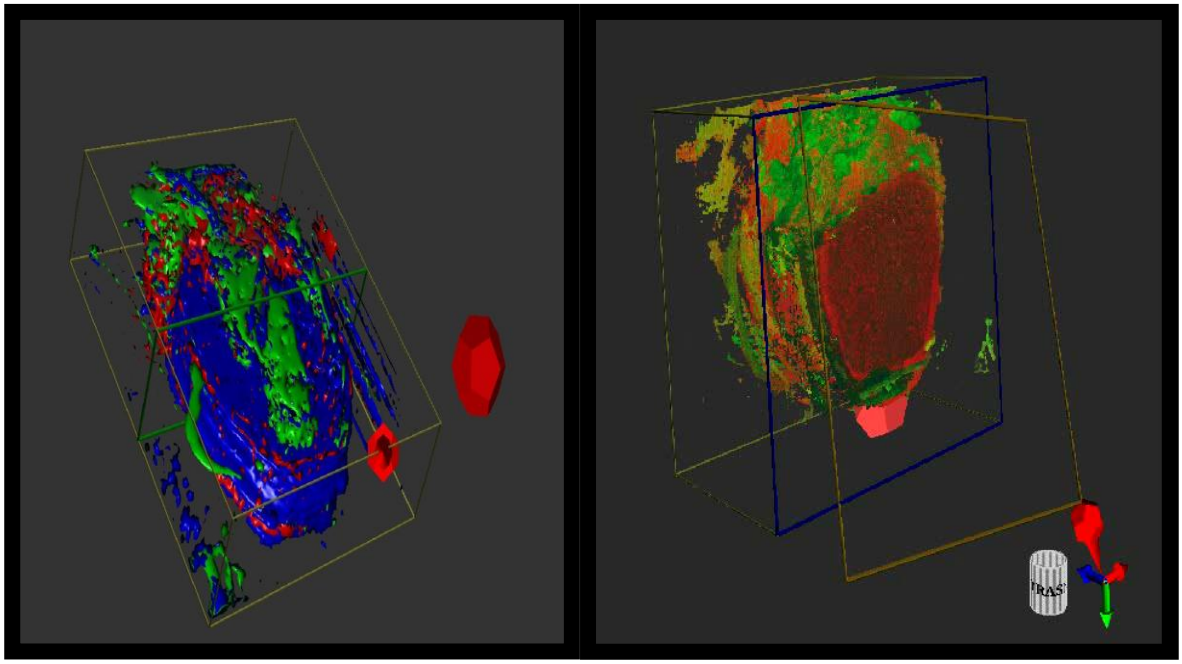

Figure 3 (a)(b). 3D Reconstruction of the heart showing 3D-spatial distributions of different ions: 145 m/z, 23 m/z ,39 m/z

The pre-processing of the data before PCA analysis is important so it transforms the data into a format that will be more easily and effectively processed for our purpose. PCA with VARIMAX optimization were both used for this purpose [161]. Score plot that are a result of PCA are used for visualization as the molecules reflect the combination of relevant spectral features.

5. Results

In our work surface rastering of heart tissue sections generated multiple secondary ions in a mass range up to 1500 m/z. High-resolution (8192x8192 pixels) SIMS images of total ions and H&E stained images of the morphological structures of the heart is show in figure 4.

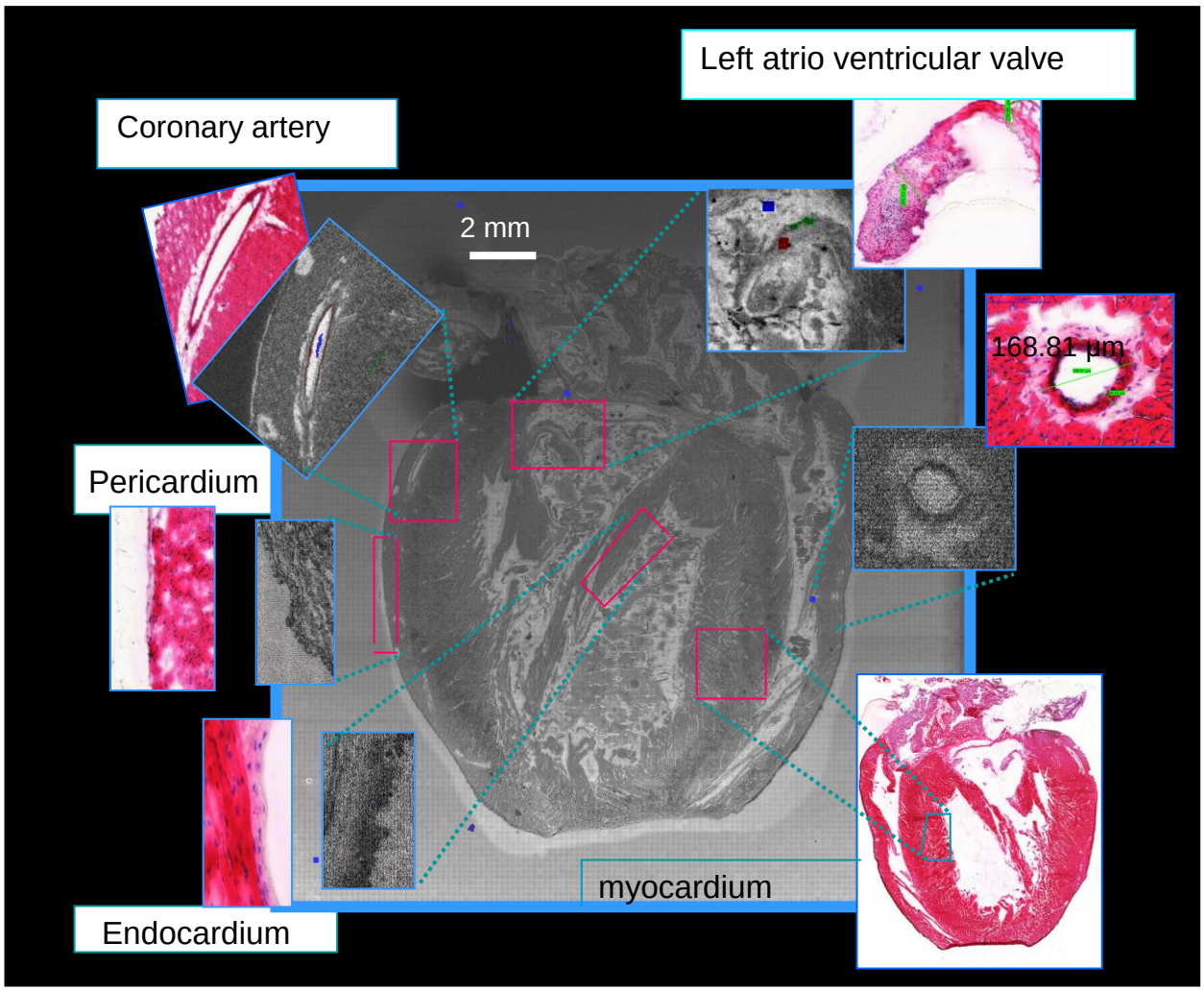

Figure 4. High-resolution (8192x8192 pixels) SIMS images of total ions and H&E stained images of the morphological structures of the heart.

Several distinctive MS peak and correlate image patterns were observed in the negative-ion mode for the heart sections analyzed depending on the region of the heart under investigation after PCA and VARIMAX optimization (figure 5 to 15).

Ion masses of **Left and Right ventricle, Right atria and Endocardium** (**VC- 4**) :

High correlation

1,03	158,89	196,82	209,84	238,88
12	174,89	197,02	210,07	250,88
13,02	184,07	197,82	210,85	252,89
14,04	193,87	198,07	212,87	394,13
15,01	195,79	198,92	222,86	

low correlation

12,25	57,07	121,92	173,86	251,13
13,23	57,43	125,06	175,06	266,89
23,99	71,06	128,07	177,09	276,88
25,01	71,23	129,11	211,8	278,89
26,04	86,05	140,91	214,89	292,9
27,01	91,24	141,92	221,85	320,87
28,06	93,74	150,07	223,87	393,69
39,33	115,07	153,01	225,86	418,69
40,05	116,09	154,08	234,82	431,68
46,96	117,07	156,08	237,87	983,48
48	118,82	157,88	238,88	
49,28	119,89	160,93	248,71	

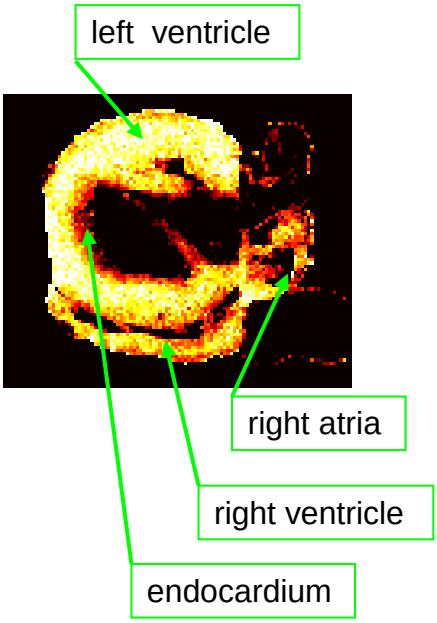

Figure 5

Ion masses of **pericardium**, **endocardium, right atria and aorta wall** (**VC+13**

High correlation

124,94

Low correlation

140,91	282,9
202,89	288,87
205,97	304,87
244,72	581,98

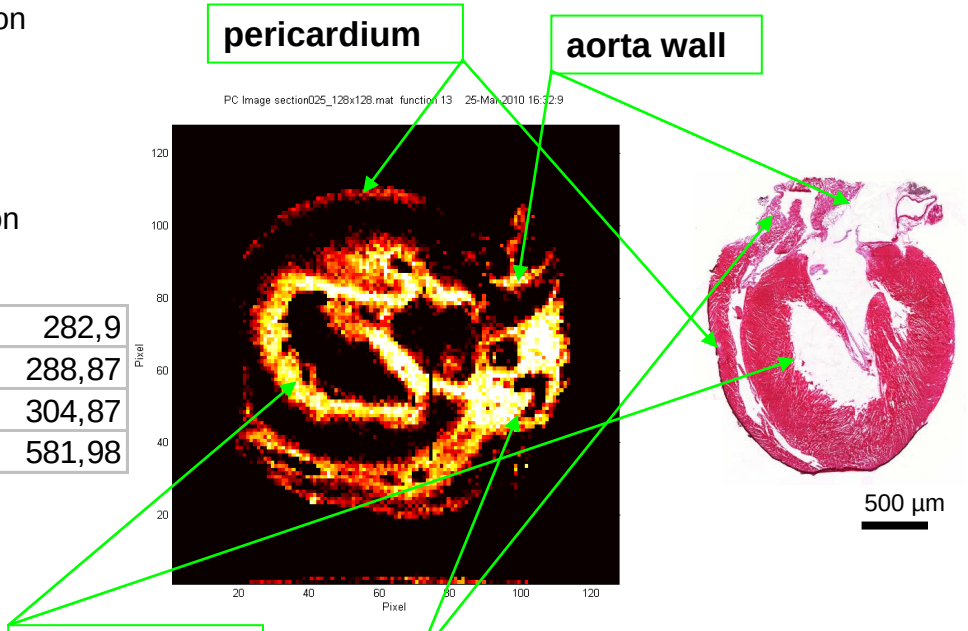

Figure 6

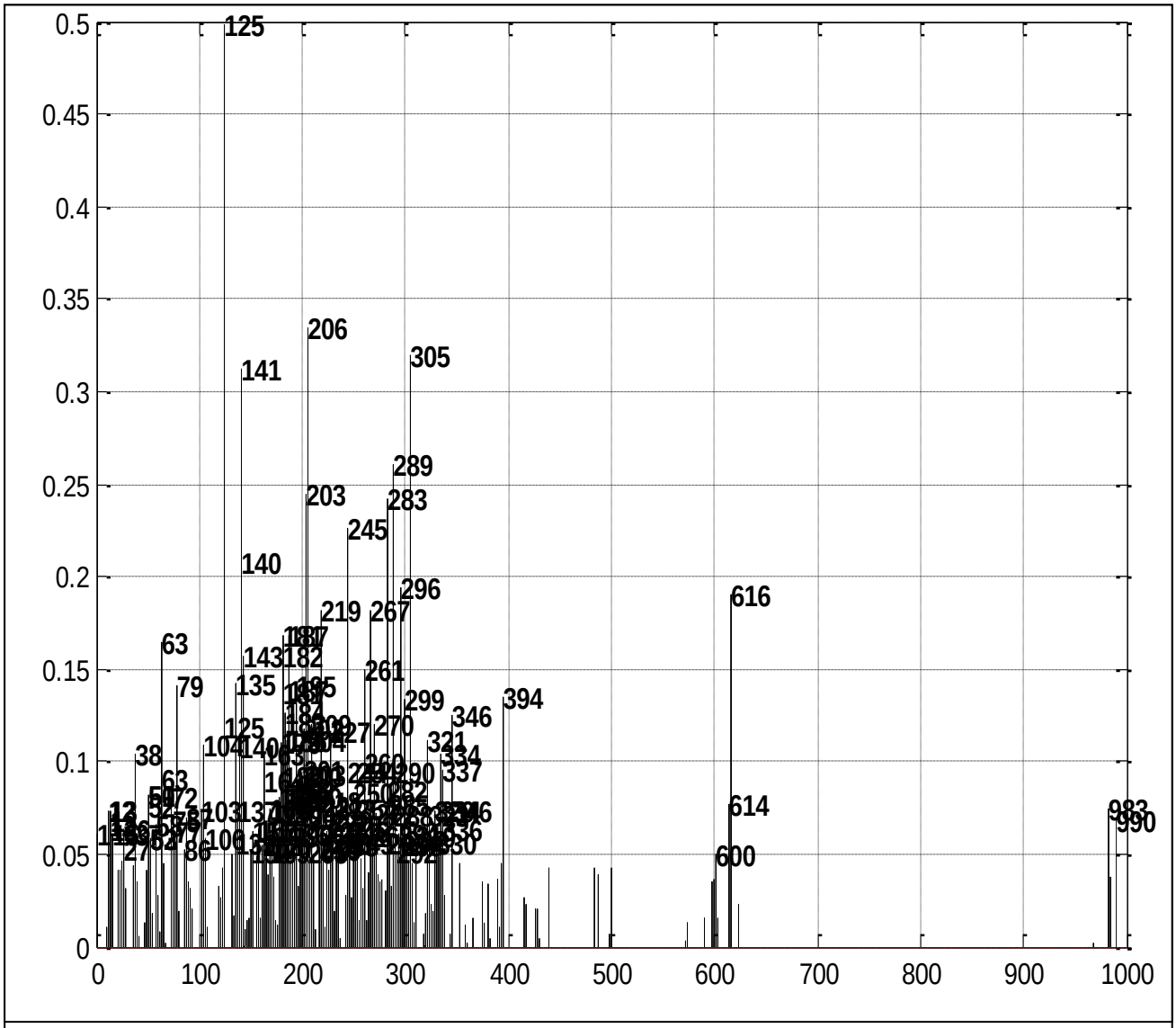

Figure 7. Spectral results of the most indicative PCA results after VARIMAX optimization. VC +13 show signal for various lipid including diacyl glycerols (m/z 550-610).

Ion masses of **aorta wall**, **left** and the **right atria, semilunar valve, atrioventricular valve, left and right ventricule**(**VC+3**) : **A:** High correlation, **B:** low correlation

A

25,01	107,44	128,07	146,08	161,08	181,07	322,89
77,04	108,1	131,07	147,07	162,06	187,06	367,18
77,23	109,08	132,09	149,05	163,07	189,07	368,18
86,05	112,84	133,06	151,07	163,89	197,02	369,19
91,07	115,07	140,01	152,08	165,06	198,07	370,17
91,24	116,09	141,07	153,1	165,9	199,09	385,16
92,08	117,07	141,92	154,08	167,08	201,05	386,16
93,07	118,08	142,24	155,04	169,08	203,04	430,16
95,09	119,07	142,91	156,08	173,07	205	968,04
97,07	120,09	143,07	157,07	174,09	215,06	968,31
103,04	121,08	143,89	158,89	175,06	254,12	
105,07	122,1	144,08	159,09	177,09	268,09	
106,09	123,07	145,08	159,9	178,05	282,13	
107,08	126,04	145,37	160,1	179,06	296,14	

B

12	74,05	116,82	175,88	204,05	254,9	324,87	577,28
13,02	75,04	125,06	176,09	205,97	256,09	352,18	578,25
14,04	79,08	126,04	177,91	210,07	263,15	353,69	578,38
17,07	79,24	127,09	179,85	210,85	265,15	354,15	579,99
21,01	81,08	129,86	180,9	211,8	269,75	364,16	580,2
23,6	85,09	130,08	181,86	212,87	270,74	366,19	603,26
23,99	88,06	130,85	183,04	214,11	271,06	394,13	603,38
28,06	92,27	131,86	185,07	214,89	272,08	416,08	604,24
30,04	93,74	133,85	186,08	215,87	273,78	428,15	604,4
36,69	93,95	136,1	188,06	216,08	274,85	429,16	606,01
37,68	94,09	137,07	190,08	217,03	275,8	432,1	607,02
40,05	97,93	140,91	191,04	219,86	278,89	522,26	983,16
40,71	99,08	147,99	192,89	222,86	279,15	546,25	983,48
43,06	100,05	155,89	193,87	224,88	279,93	547,25	
51,04	101,07	157,88	195,1	229,06	282,9	548,26	
52,53	102,26	158,1	195,79	235,85	283,06	549,26	
53,06	104,25	160,93	196,82	238,88	284,85	549,37	
54,07	107,97	162,02	197,82	239,13	294,1	550,27	
57,07	110,84	162,91	198,92	239,86	300,83	551,27	
59,07	112	168,06	199,89	244,72	301,07	572,24	
60,05	113,06	169,85	200,1	245,71	306,88	573,25	
60,98	113,83	172,08	200,92	247,71	311,72	575,26	

Figure 8

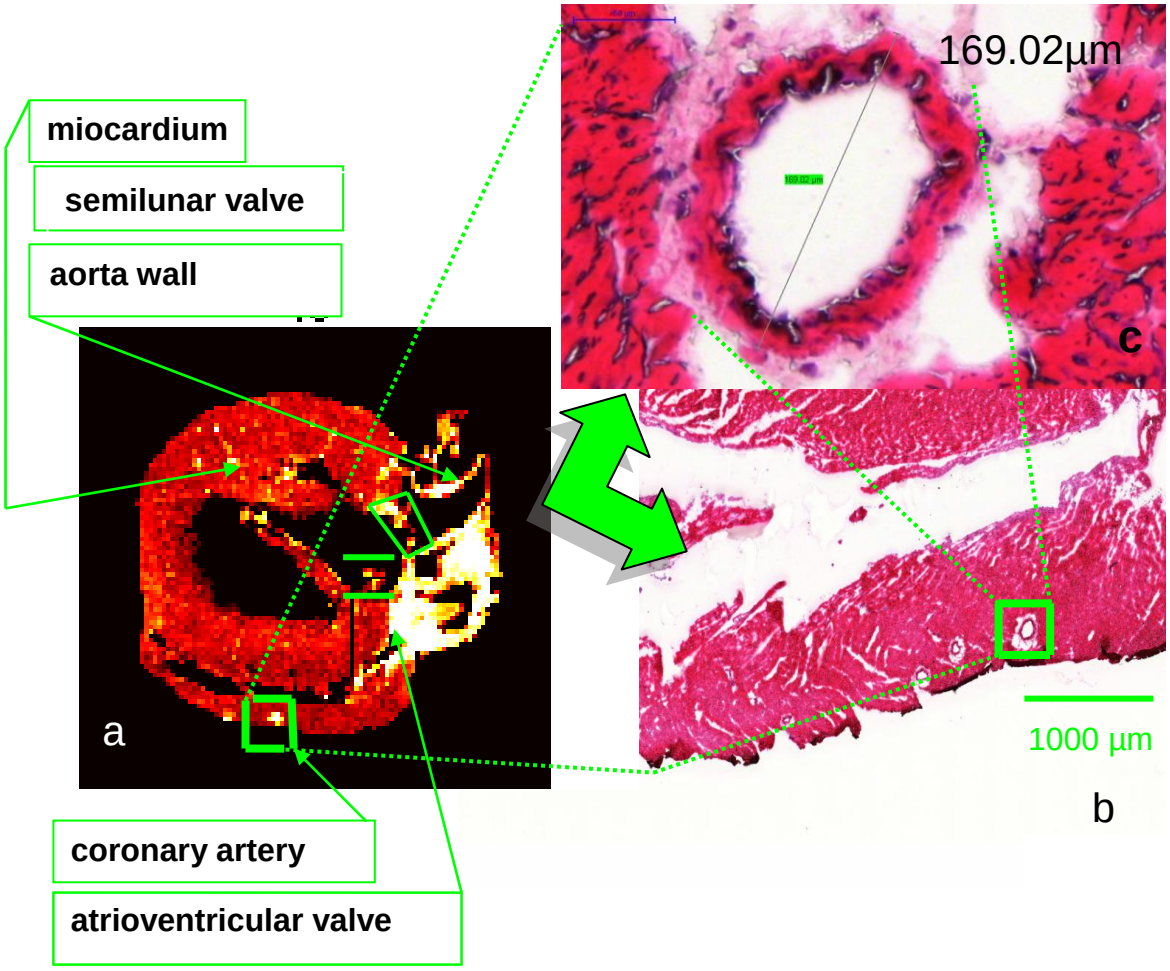

Figure 9.The distributions based on the PCA results (a) give clear image of the different areas that can be characterized with H&E staining (b,c)

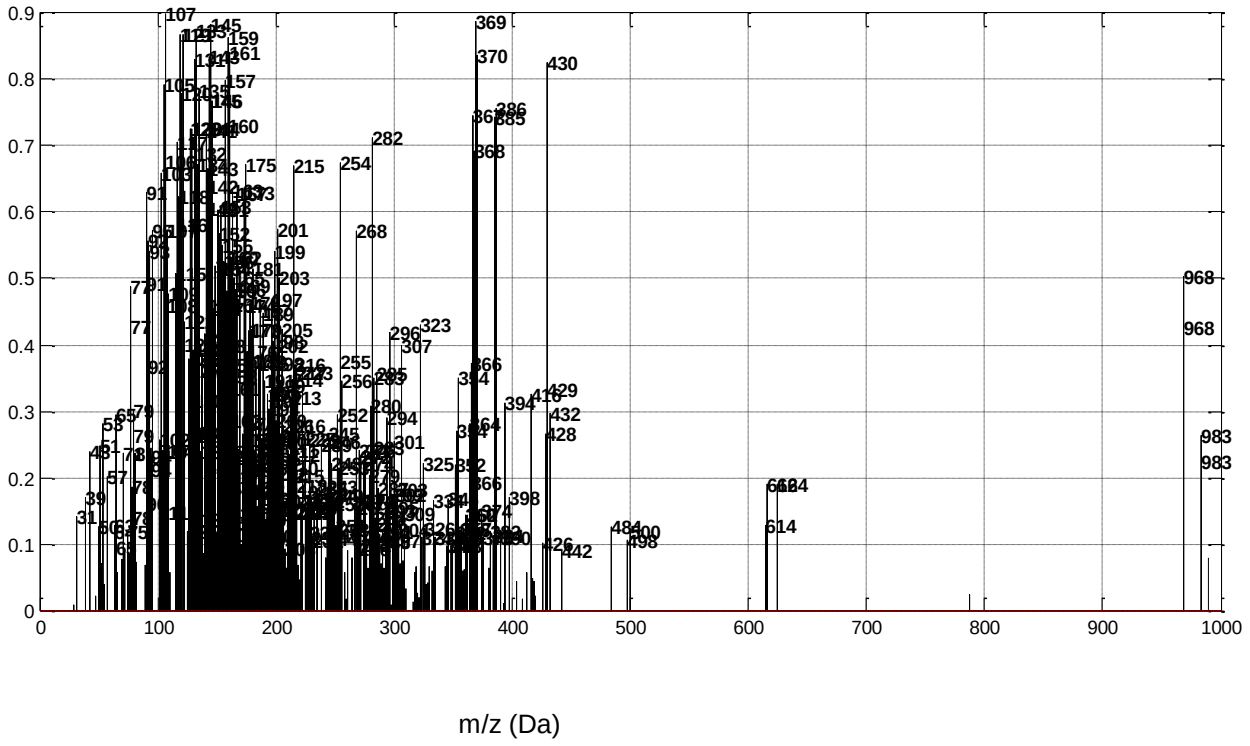

Figure 10. Spectral results of the most indicative PCA results after VARIMAX optimization. VC +3 show signal for cholesterol ((M-OH)+ at m/z 369.1 and M+ at m/z 370.1)

Ion masses of **Pericardium** and **Endocardium Left atria, Right atria and Aorta and atrio ventricular valve** (**VC-8**) :

High correlation:

126,04	174,89	212,87
142,91	180,9	306,88
165,06	183,04	322,89

Low correlation:

37,68	121,92	181,07	284,85	324,87
39,33	124,94	181,86	285,87	
46,96	149,05	184,97	300,83	
58,06	162,06	205	307,11	
63,02	167,08	214,89	308,87	
63,35	177,09	245,71	323,8	

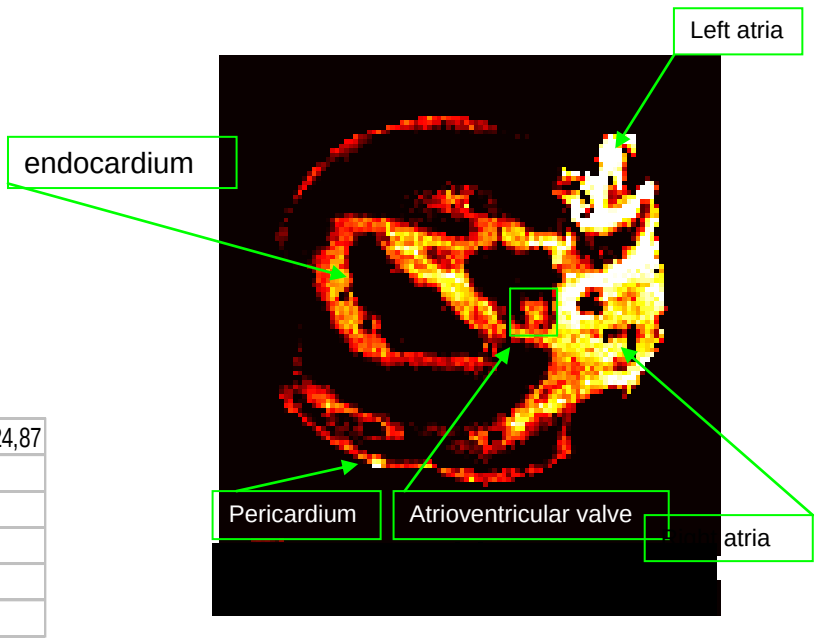

Figure 11

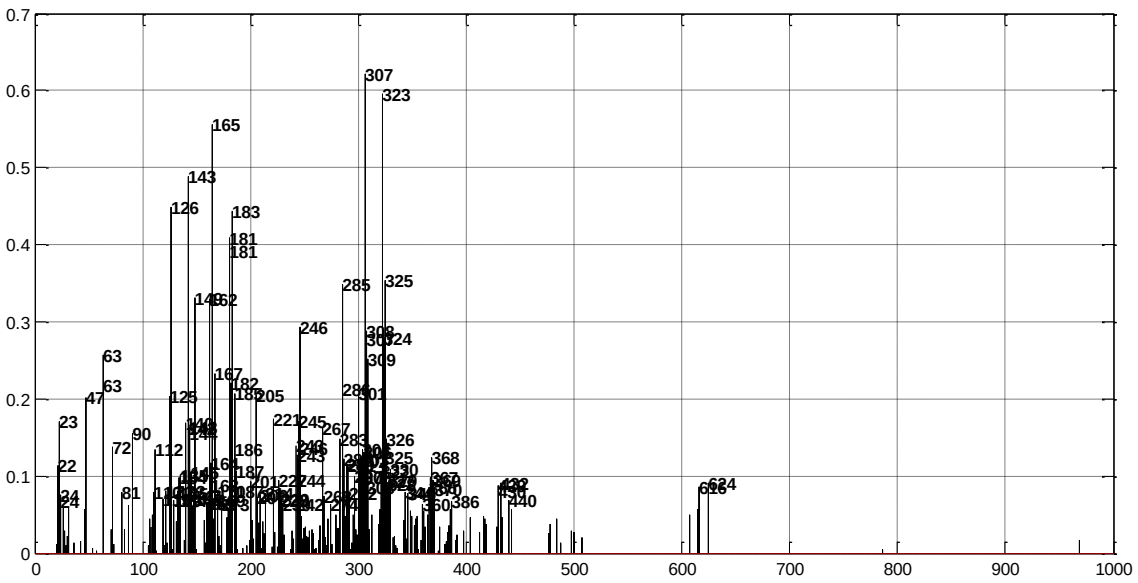

Figure 12. Spectral results of the most indicative PCA results after VARIMAX optimization. VC -8

Ion masses of **Right atria, Left atria** and **Aorta** (**VC + 10**):

High correlation

21.01
36.69

Low correlation

25,01	235,85
40,71	270,74
41,05	304,12
60,05	305,1
74,05	325,11
75,04	328,09
88,06	383,14
112,84	384,16
	406,13

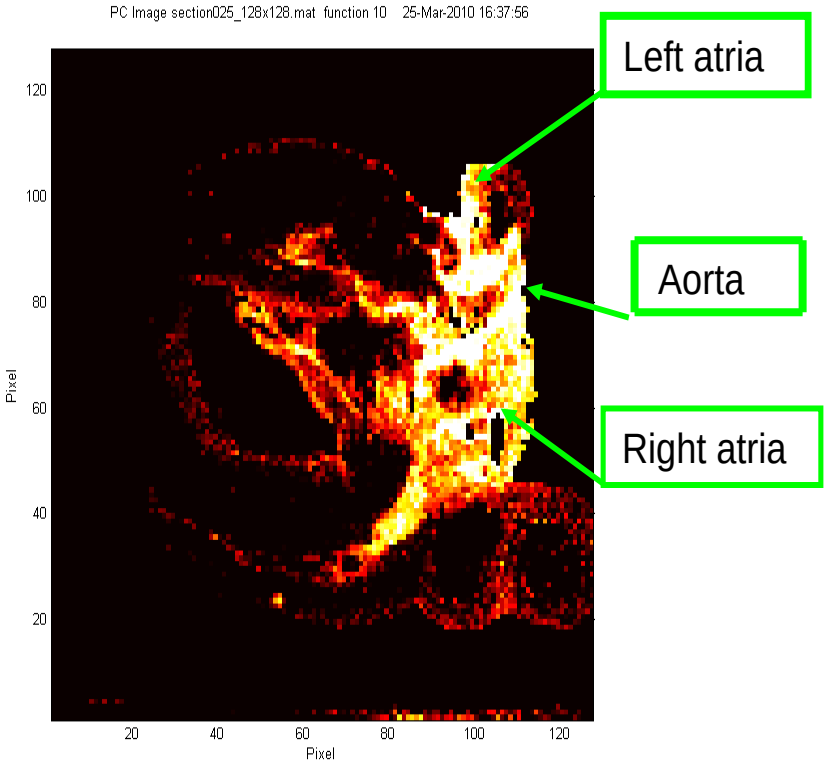

Figure13

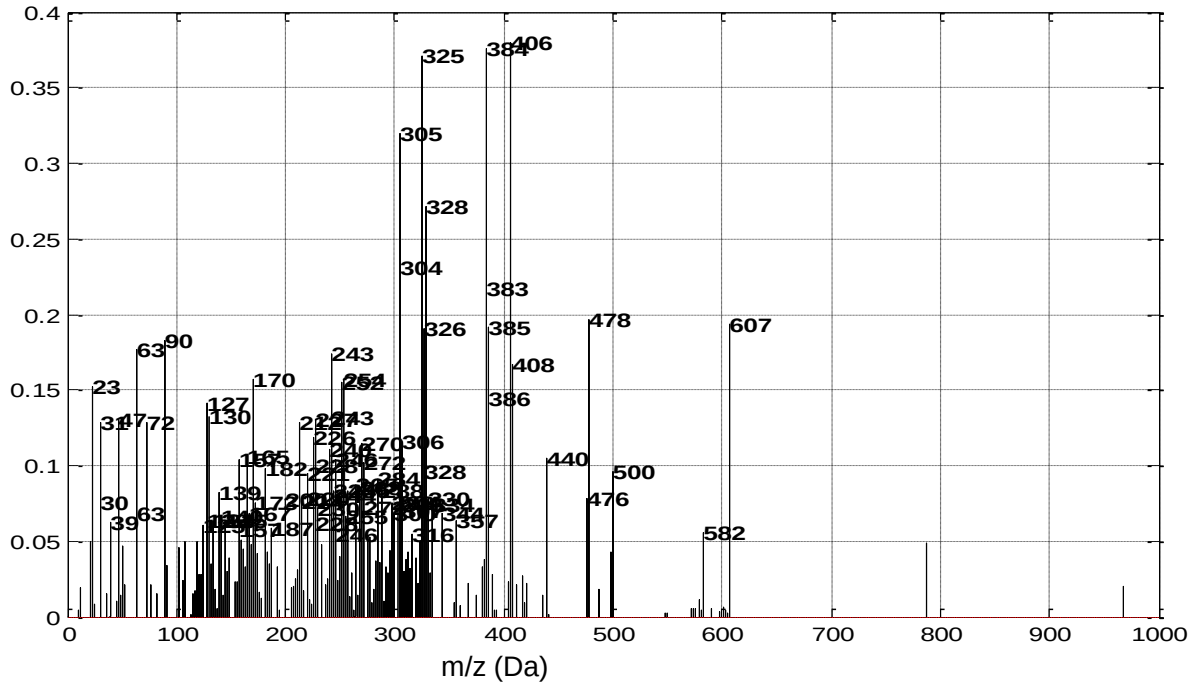

Figure 14. Spectral results of the most indicative PCA results after VARIMAX optimization. VC +10

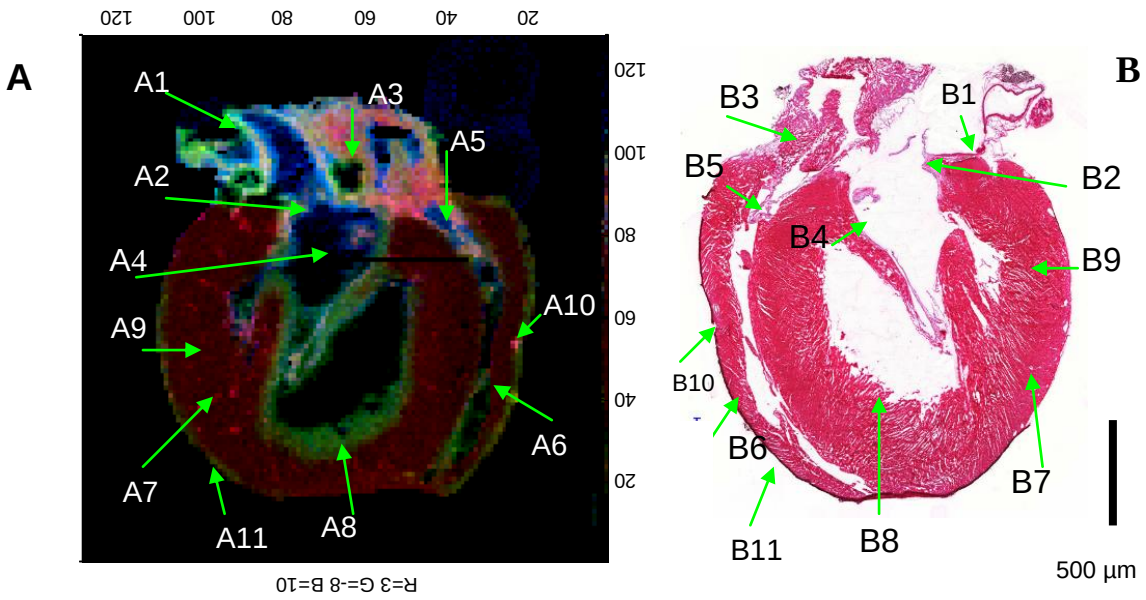

Figure 15. (A): overlay correlate image to VARIMAX data : Red corresponding to the function 3, Green corresponding to the function 8 and blu corresponding to the function 10. (B): H&E staining. A1;B1 aorta, A2;B2 semilunar valve,A3;B3 right atria, A4;B4 left atrioventricular valve, A5;B5 right atrioventricular valve, A6;B6 right

Several localization patterns can be distinguished. The differences are associated with ions and lipids compositions representative of the differents structures of the heart. As shown in figure 16, 20 and 22 the distribution of a wide variety of secondary ions ranging from atomic ions to intact fatty acids has been imaged in the heart.

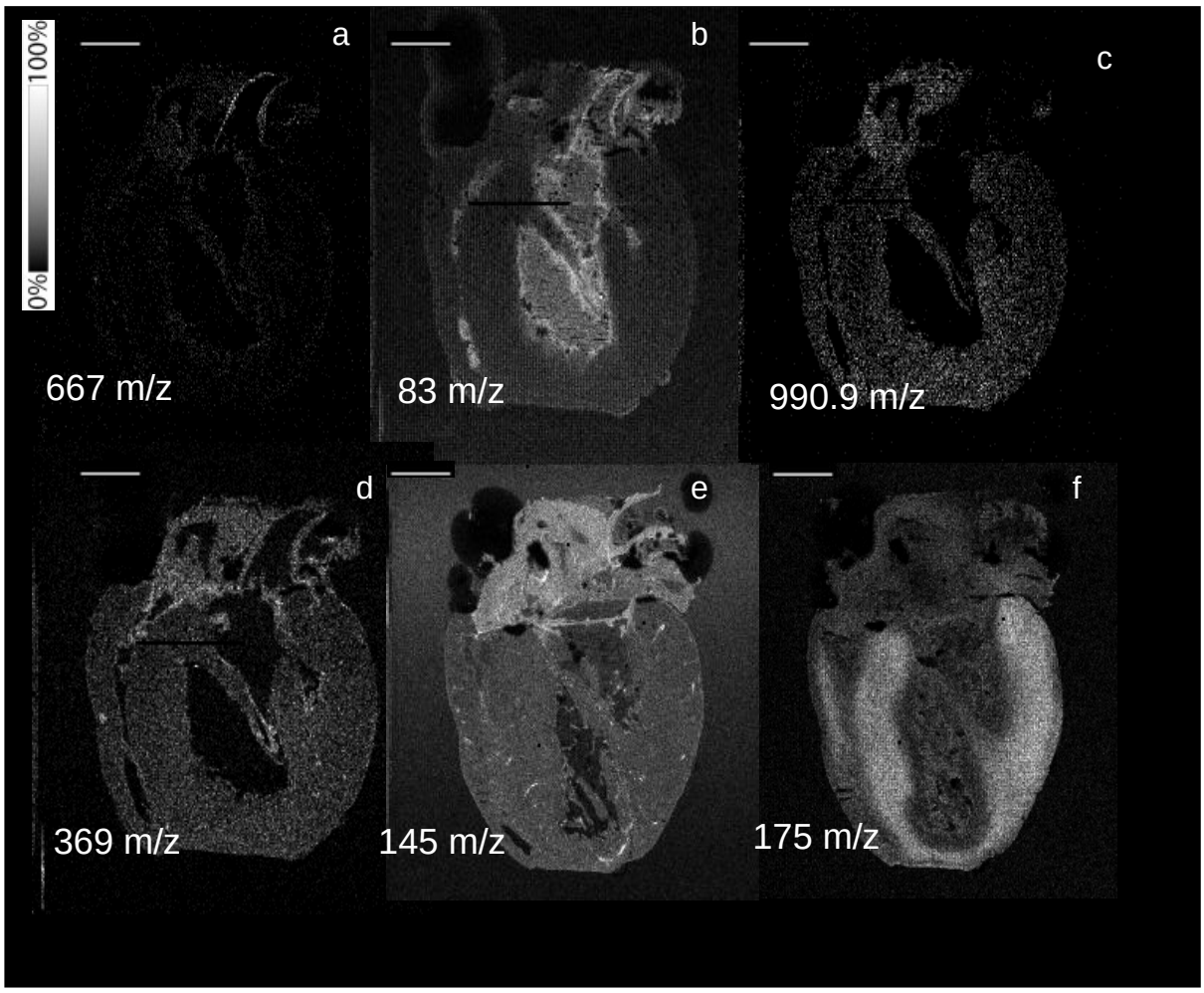

Figure 16. Metal-assisted SIMS images of a sagittal section of a rat heart. Top image (a) shows the high spatial resolution distribution of lipids in the aorta. The image shown are of a m/z 667.1. The distribution of the individual masses are very localized to the differents structure. For instance m/z 83 is localized to the aorta wall aorta, semilunar valve and endocadium whereas is absent from both ventricles and atrias (b). The image c shows the high spatial resolution distribution of lipids at 990.9 m/z in the right atria. The bottom image d shows cholesterol at 369 m/z localized in coronary artery right atria, the aorta wall, the semilunar valve and atrioventricular valve. The image e shows the ion at 145 m/z very localized in pulmonary artery, right atria and atrioventricular valve. The right image (f) shows the distribution of the 175 m/z only in the right and left ventricle. All ion image scale bars = 100 micron

The selected ion images are expected to be highly specific as several peaks are often visible within a single *m/z* range and only a single peak is used to create the ion images (figure 16,17,20 and 22). The ion at m/z 667, (figure 16 a) m/z 83 and m/z 80 (figure 17 a and b) and m/z 840 (figure 22 d) localized very precisely within the wall aorta. The ion at m/z 83 localized in the aorta wall , endocardium and pulmonary valve (figure 16 b). Cholesterol is another lipid that plays a major role

in the membrane structure. Acetyl-CoA derived from fatty acids or pyruvate in mitochondria oxidation is utilized in cholesterol biosynthesis. The synthesies of cholesterol in the aortic wall has been demonstrated in several animals and humans [152,162,163]. Significant peaks in our work are seen at m/z 369 and m/z 385, representing cholesterol [M+H−H2O]+ and [M−H]+ which were used for imaging of cholesterol. The difference in the relative cholesterol content of the lipids of the heart ventricles is also apparent. The cholesterol show high intensity in both atrias, aorta wall, valves and coronary artery but is not present in ventricles surface.((figure 16 d). and (figure 17 e,i)). Choline is an amine originated in the lipids. Choline is vital for the build up signalling functions of cell membranes, and in the formation of phosphocholine [164]. The distributions based on the PCA results give clear image of the different areas of m/z 105 (choline) signal with high correlation. The m/z 105 (choline) signal localizes in both atrias, aorta, pulmonary artery, in the atrioventricular valves and semilunar valves but is not present in ventricles surface as show in figure 9. The intermediate mass region show phosphocholine headgroup at m/z 184, which was used for localization of phosphocholine-containing phospholipids, i.e. sphingomyelin and phosphatidylcholine . The composition of the plasma membrane of most cells is known to be predominantly phosphatidylcholine, a known source of abundant *m/z* 184 [165].

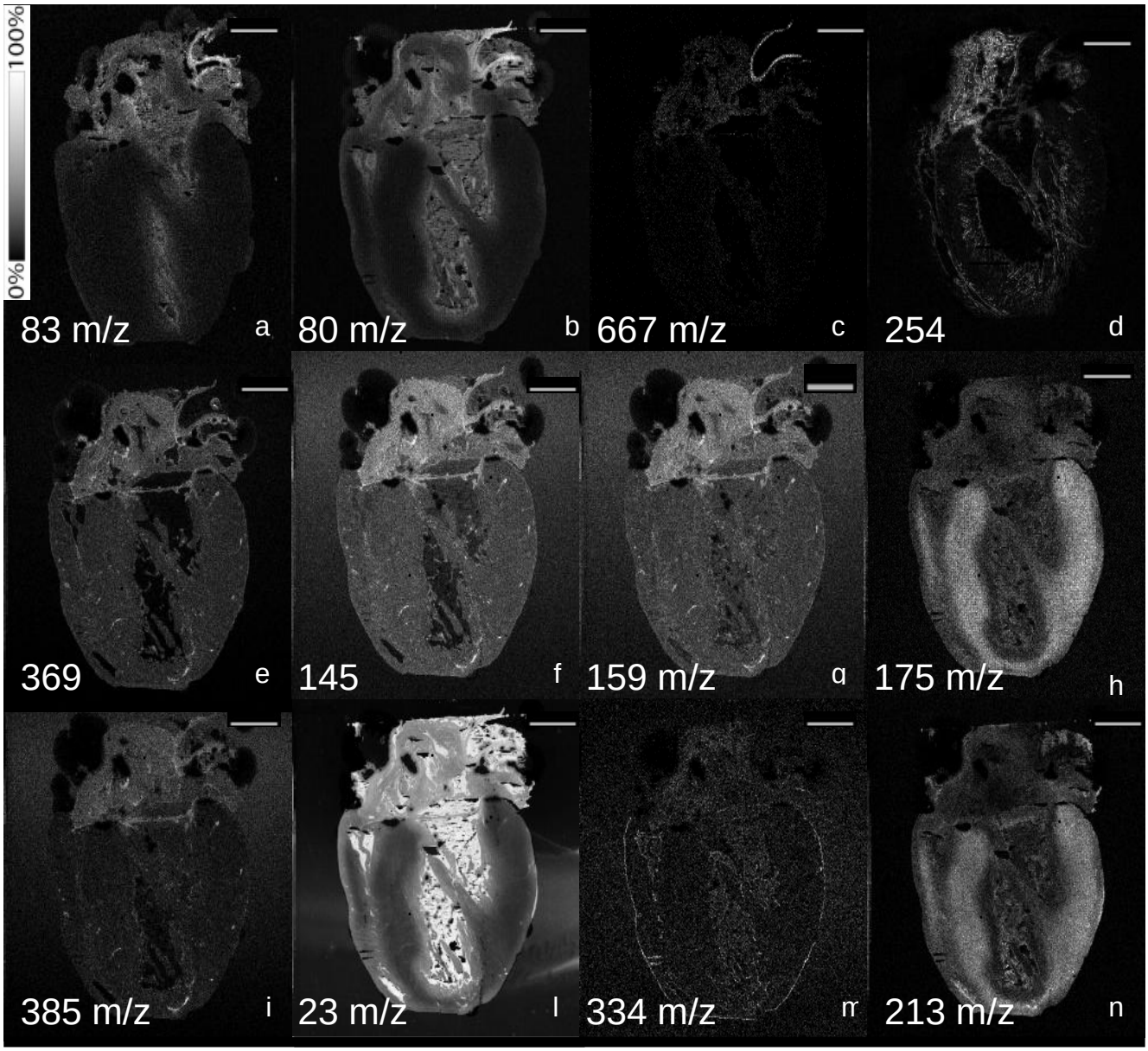

Figure 17. Metal-assisted SIMS images of a sagittal section of a rat heart. All ion image scale bars = 100 micron

The distribution based on the PCA results after VARIMAX optimization show phosphocholine with high correlation localized to left and right ventricle, right atria and endocardium. This ion is not localized in aortic valve, atrioventricular valve and left atria (figure 5) and is certainly not ubiquitous in the heart. DAG is a glyceride with two fatty acids esterfied with a glycerol molecule produced from glycerol-3-phosphate pathway or synthesised from acylation of monoacylglycerol [166]. DAG is not a major component of biological membranes, but plays a significant role in both intermediate metabolism and in signal transduction as a second messenger surface. Several

localization patterns can be distinguished. DAG species with probable identifications as [P–Po]+ (Palmitic, Palmitoleic) at m/z 550, (Palmitic, Oleic) at m/z 578 and [OO]+ (Oleic, Oleic) at m/z 604, could be detected. (figure 8B and 9) .Other significant peaks are seen at 175 m/z as show in figure 1f where this ion is very localized only to left and right ventricle. The data on the molecules content of rat heart tissues are summarized in figure 5,6,7,8,10,11,12,13 and 14. The images of 3D reconstruction show a highly complementary localization between Na+, K+, ion at m/z 145 and ion at m/z 667. Na+ is localized to tissue regions corresponding to atrias, while K+ is strongly localized to tissue regions corresponding to ventricles surface (figure 3). The contrast used in displaying the images was increased to allow better visualization of distinctive areas of the heart. This was also necessary because the software used for the construction of the 3D volumes segments the heart based on color differences. the overlaid 3D model obtained is a representation of the whole heart. With MALDI-TOF in the mass range between m/z 100 and 4000 several masses with highly specific spatial localization were found. (figure 18,19,21 and 23) .

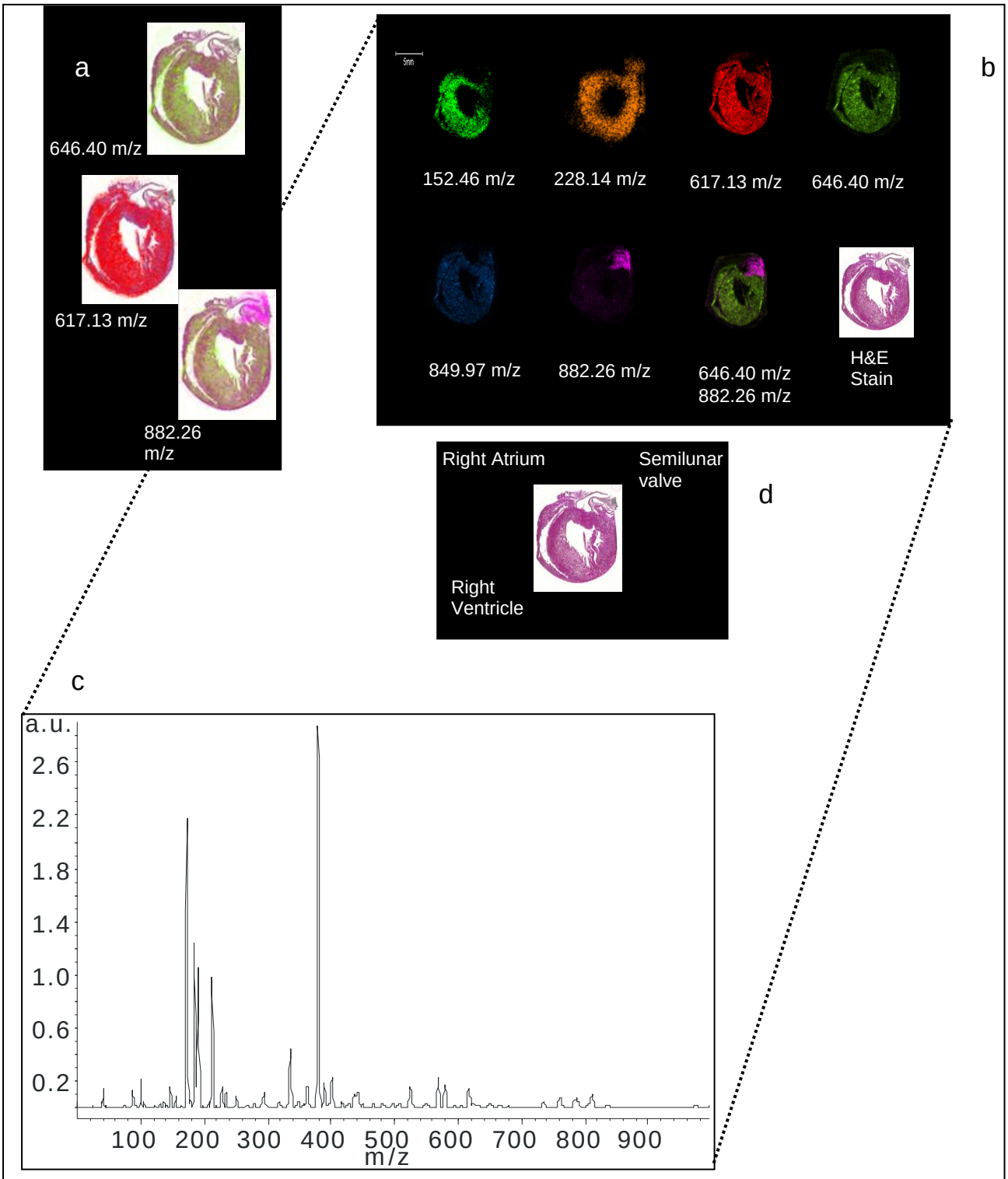

Figure 18. (a) overlay of ion image and H&E stained tissue section (b) MALDI TOF images of a sagittal section of a rat heart . (c) spectrum ion images The right image (d) H&E stained tissue section

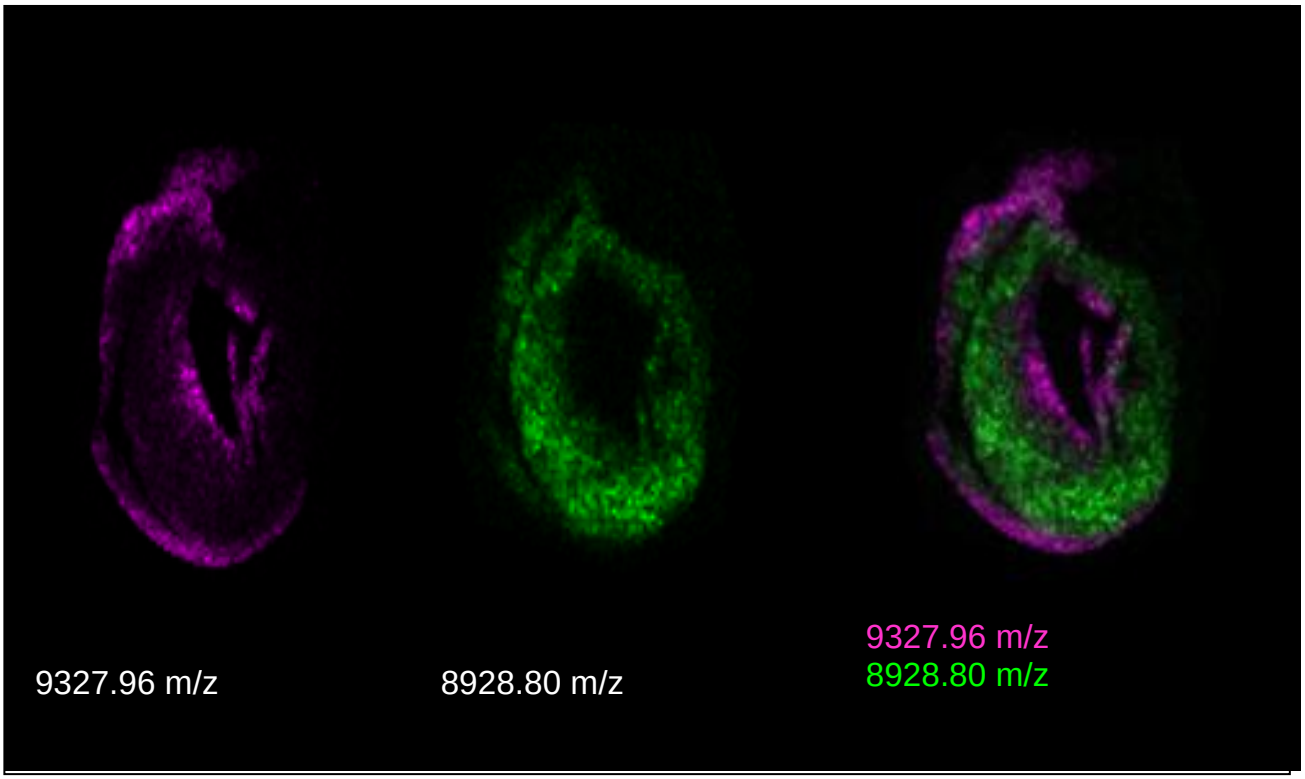

Figure 19. Visualization of proteins detected with MALDI IMS. MALDI IMS offers the ability to reveal regional overlaps of proteins localization by means of visualization of several peaks and their spatial distribution concurrently

The distribution and localization of the individual masses is easily observed, for instance the top image shows *m/z 152.46* is localized to the right ventricle and part of left ventricle, whereas *m/z 228.14* is present only in the left atria and left ventricle. The bottom image shows the high spatial resolution distribution of lipids between 617.13 and 882.26 m/z (figure 18b). Proteins were also found in the mass range between m/z 4000 and 40000 (figure 19and 21a). The protein with m/z 6810.05 was found only in the right atria meanwhile the protein with m/z 8928.80 was found only in the left ventricle (figure 19). Several images with high spatial resolution were obtained. These molecules will be further analyzed with MS/MS analysis, *in-situ* tryptic digestion and traditional proteomics for identification purposes. The data show significant differences in the ions, lipids, peptides and proteins lipid distribution in the various heart structures and emphasize the distinctive pattern of localization in this organ. We have demonstrated that anatomical features evident and identified in optical images, are also evident in corresponding imaging mass spectrometry analysis.

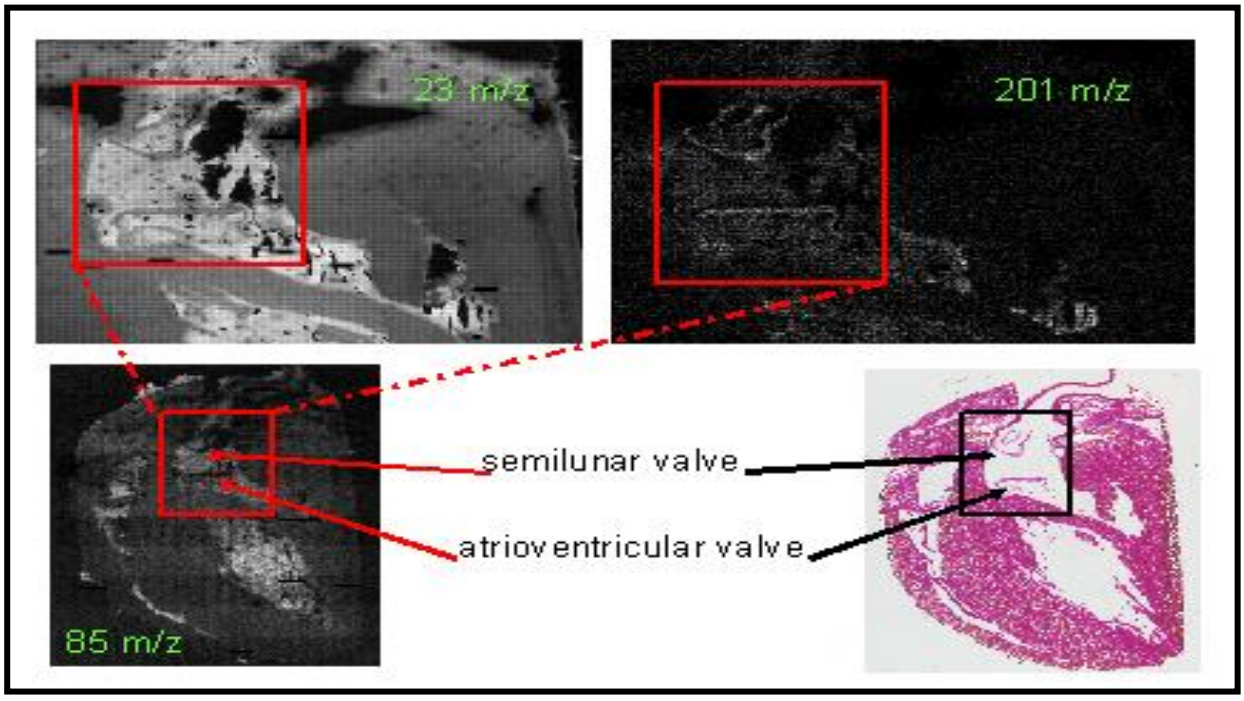

Figure 20. SIMS-MSI images of ions detected from a representative heart valves

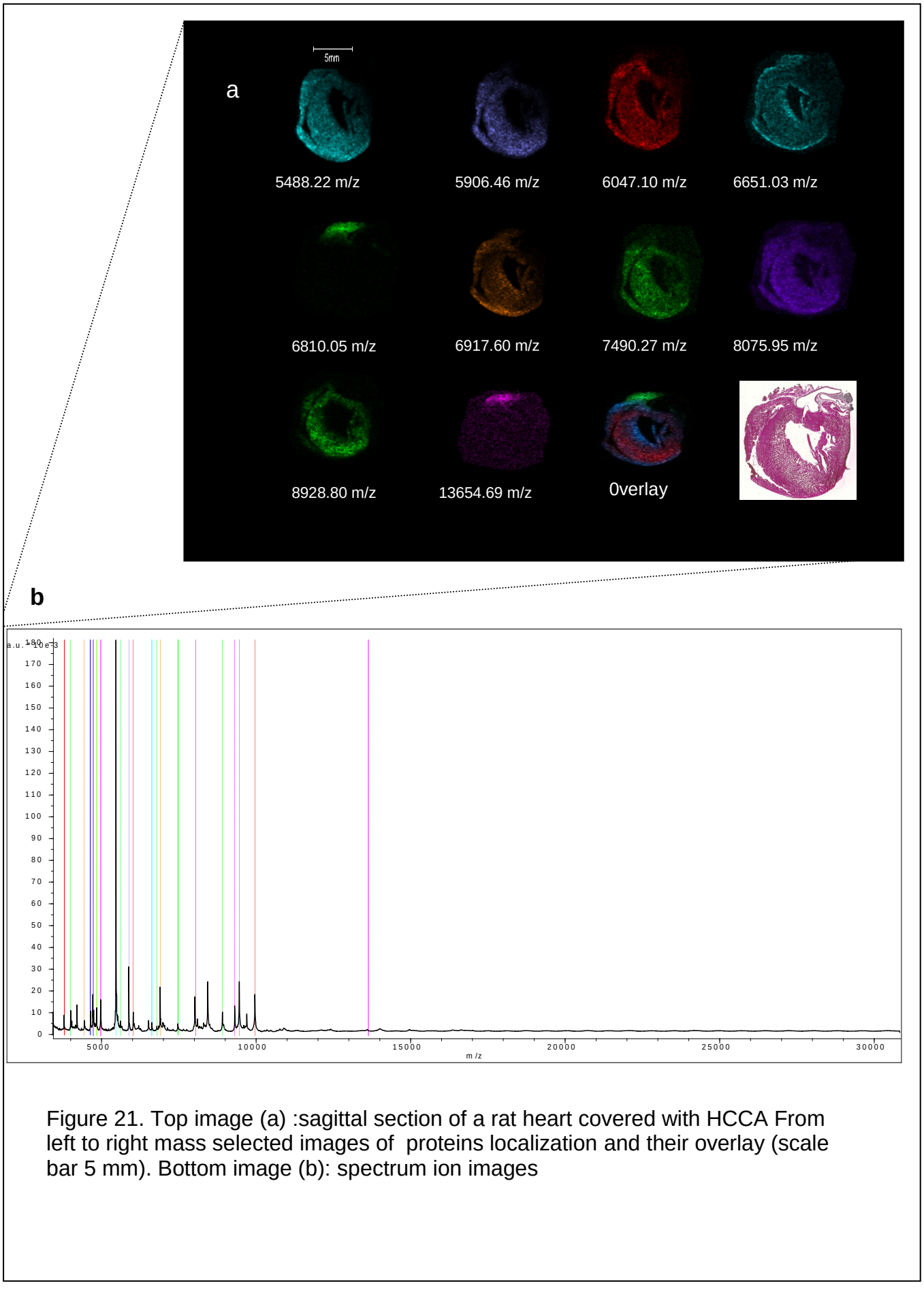

Figure 21. Top image (a) :sagittal section of a rat heart covered with HCCA From left to right mass selected images of proteins localization and their overlay (scale bar 5 mm). Bottom image (b): spectrum ion images

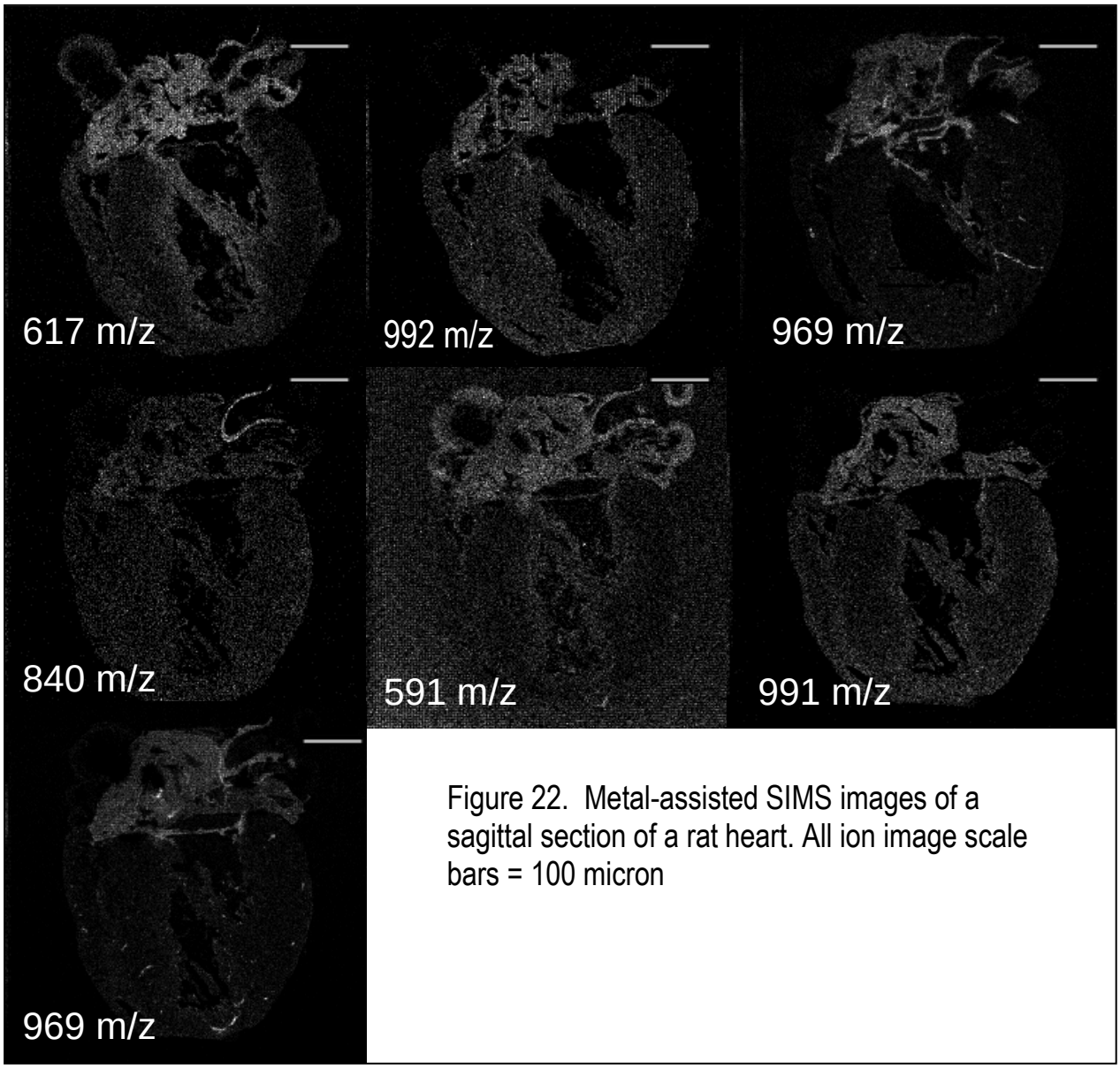

Figure 22. Metal-assisted SIMS images of a sagittal section of a rat heart. All ion image scale bars = 100 micron

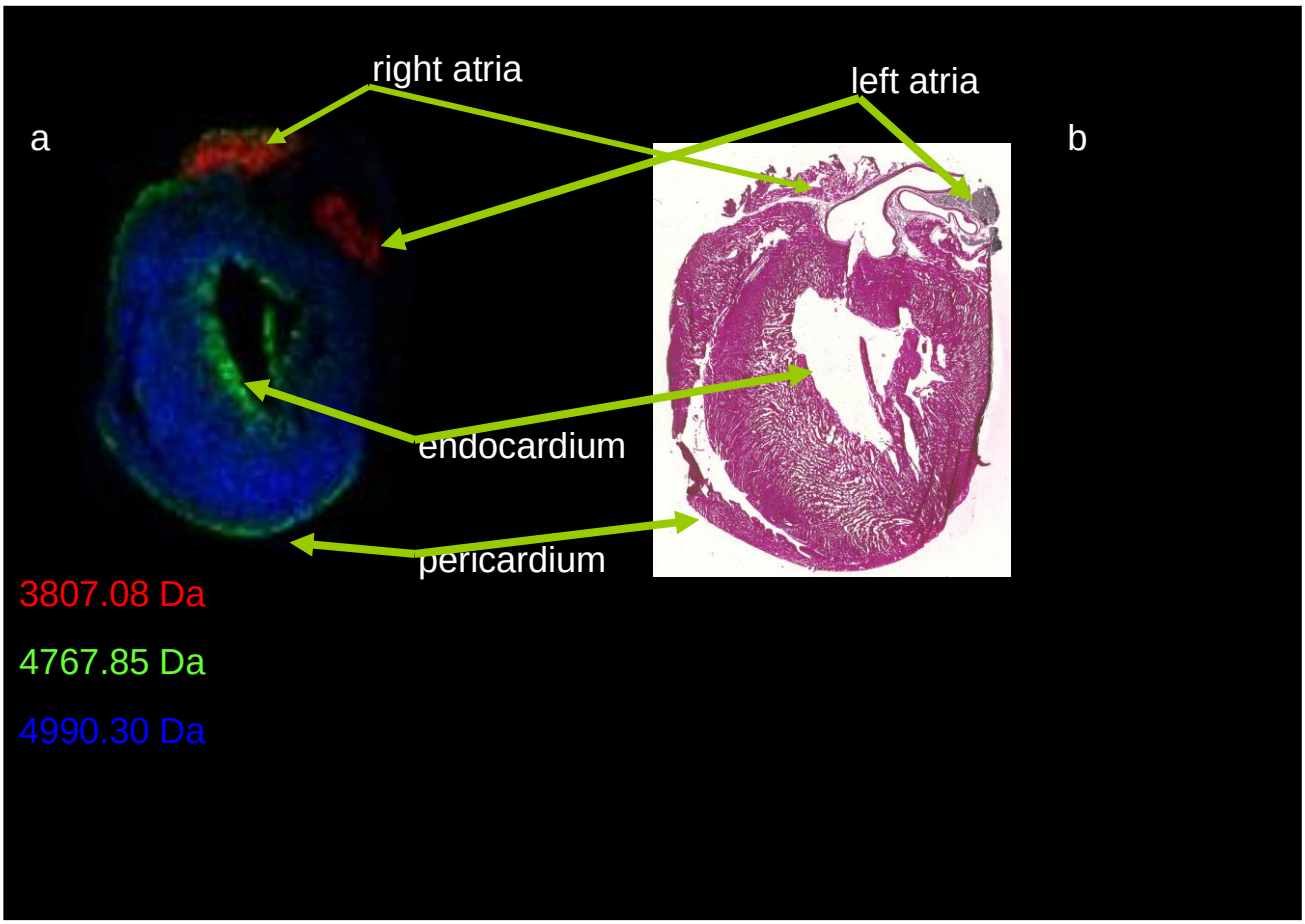

Figure 23. (a) MALD -TOF images of ions detected from a representative rat heart tissue section. (b) H&E stained tissue section after analysis.

6. Discussion

The ability to characterize specific biomolecules is crucial for biological, and especially pathological, investigations. Molecular biology thrives on molecular imaging techniques that aim at the investigation of the relationship between spatial organization, structure and function of molecules in biological systems. Although impairment in calcium homeostasis, abnormal myocyte energetics and myocardial remodelling have been described to be associated with cardiac dysfunction, the underlying molecular mechanisms involved in the transition from normal cardiac function to heart failure remain poorly understood [167]. Insight into these processes and pathways will be important in the development of new therapeutic strategies for treatment and prevention of heart failure. Under normal physiologic conditions, the heart utilizes fatty acids as its chief energy substrate. Because there is limited capacity for triglyceride storage in the cardiomyocyte, the uptake and oxidation of fatty acids is tightly coupled [168]. The accumulation of triglyceride in the heart, caused by a mismatch between the uptake and the oxidation of fatty acids, is associated with a number of pathophysiologic condition. In animal models (rats) of obesity and diabetes, triglyceride accumulation within cardiomyocytes is associated with impaired contractile function . Although it is unclear how lipids induce cardiac dysfunction, accumulation of intramyocardial triglyceride is associated with altered gene expression [169]. The lipid droplet is endured by a core of lipids, which mostly consists of TAG (90-99%) and to a lesser amount of DAG, FFA, phospholipids and monoacylglycerol. The oleic acid (47%) and palmitic acid (19%) are the dominate fatty acids [170-172]. Several distinctive MS peak and correlate image patterns were observed with MALDIMS and SIMSMS for the heart sections analyzed depending on the region of the heart under investigation. Several localization patterns can be distinguished. The differences are associated with ions, lipids, peptides and proteins, compositions representative of the different structures of the heart. The difference in the relative cholesterol content of the lipids of the heart ventricles is also apparent. The

cholesterol show high intensity in both atrias, aorta wall, valves and coronary artery but is not present in ventricles surface. The synthesise of cholesterol in the aortic wall has been demonstrated in several animals and humans but for the first time we detected the cholesterol with difference patterns. Choline also is an amine originated in the lipids. The distributions based on the PCA results give clear image of the different areas of m/z 105 (choline) signal with high correlation. The composition of the plasma membrane of most cells is known to be predominantly phosphatidylcholine, a known source of abundant *m/z* 184 . This ion is not localized in aortic valve, atrioventricular valve and left atria and is certainly not ubiquitous in the heart in our results. DAG is not a major component of biological membranes, but plays a significant role in both intermediate metabolism and in signal transduction as a second messenger surface. The data show significant differences in the lipid distribution in the various heart tissues and emphasize the distinctive pattern of lipid localization in this organ. With MALDI-TOF in the mass range between m/z 100 and 4000 several masses with highly specific spatial localization were found. The MS imaging (MSI) approach can be used to detect and probe the molecular content of tissues in an anatomical contex t. Anatomical atlases based on optical images are widely used for anatomical and physiological reference. A series of secondary ion images obtained from successive tissue sections of rat heart can be used to produce a 3-dimensional (3D) molecular atlas that contains both pieces of information. SIMS provides detailed high resolution molecular images of tissue surfaces. The aim of our study is to provide a molecular basis for the histology of the heart through the local identification of biomolecules by MS. The results reported here represent the first 3D molecular reconstruction of rat heart by SIMS imaging. The application of this method in future studies could be used to identify changing regions within the tissues that are indicative of human heart disease. 3D heart reconstruction provides a knowledge base which could change the face of cardiovascular biology. Further developments are still needed to establish this technology in a clinical setting. For example, standardization of protocols must be undertaken between tissue collection, storage, preparation, and data acquisition. MALDI and SIMS imaging will ultimately provide high resolution molecular

imaging but will also result in direct biomarker identification with statistical validation such that it will become an essential proteomics tool in clinical histopathology. MALDI-MSI and SIMS-MSI will improve tissue classification necessary to perform retrospective studies, will assist clinical studies from the bench to bedside, and will provide a remarkable follow-up procedure. Improved tissue classification using MALDI-MSI and SIMS-MSI on the same heart tissues used by pathologists for diagnosis will speed up the process of molecular diagnosis. Molecular tissue classification after MALDI-MSI and SIMS-MSI based on known biomarkers or using unsupervised multivariable analyses can positively affect patient treatment. Based on the tissue biomarkers identified by MSI, it could be important to follow up the evolution of the heart disease during treatment furthermore in cases where traditional biomarkers cannot be clearly detected in biopsies, MALDI-MSI and SIMS-MSI could become critical to the outcome. At this point, it is obvious that further clinical studies using MALDI-MSI SIMS-MSI technology are required. Nonetheless MALDI-MSI and SIMS-MSI has opened the door to molecular tissue classification, which could be of great use to pathologists with regard to diagnosis but also in drug development and diagnosis coupled with MRI technology. A major advance for MALDI-MSI will be its coupling with positron emission tomography, x-ray, computed tomography instrumentation, and MRI for both preclinical and clinical research. The complementarities between non-invasive tech- niques and molecular data obtained from MALDI-MSI and SIMS-MSI imaging will result in a more precise diagnosis. In clinical studies, the need for information on the spatial localization of pathologically gene-encoded products has become more pressing. The three-dimensional volume reconstructions generated by MALDI-MSI data and SIMS-MSI data (our work) now offer the possibility to compare the molecular data with data obtained using positron emission tomography or MRI. These associations will enhance the use of MALDI-MSI and SIMS-MSI.

7. CONCLUSIONS

In conclusions, this thesis describes for the first time a "omic" analysis of normal rat heart tissues by imaging mass spectrometry for detection and localization of several molecules that will provide a global network map and forms the foundation for the development of an extensive database for rat heart "omic". Furthermore, this "omic" map will help identify differences between profiles of normal and diseased cardiac tissues derived from rat models with complex cardiovascular disease. Understanding the signalling pathways and molecular mechanisms regulating heart structure and function, and the disruptions to these processes in the diseased state, will be critical for the detection of cardiac biomarkers and the development of new therapeutic agents. A series of images obtained from successive sections of animal heart could, in principle, be used to produce a molecular atlas. Such tissue atlases (based optical images) are widely used for anatomical and physiological reference. Advances in our understanding of biologic system and development of powerful new tools that can be applied at both the bench and bedside-genomics, proteomics, transgenic animal models, structural biology, biochemistry, and imaging technologies-offer unprecedented prospect for advancing knowledge of heart human disorders in a translational context. A definitive description of the molecular imaging of the heart is well beyond the scope of this thesis.

7.1 Future Perspectives

MSI is becoming an established tool for imaging of the most complex biological samples. Its key applications are foreseen in a biomedical environment, more specifically in molecular histology. This *ex* V*i*V*o* imaging technique provides a lot of information about the biomolecular composition of the tissue, without the need for labels, complicated sample preparation protocols, or staining procedures. No *a priori* knowledge about the sample is necessary, but for correct interpretation of results some MS knowledge is required. The instrumentation used for imaging has reached a degree of maturation, with ionization sources performing at high resolution and mass analyzers of broad mass range and high sensitivity. MSI is rapidly developing into an imaging tool used by pathologists, biologists, and biochemist. In the future it has the potential to become a routine tool for imaging of tissues dissected during surgerical operations or stored in tissue banks. MSI can help us to understand the link between the localization of certain molecules and their function during pathogenesis, disease progression, or treatment. It can accelerate our efforts to provide more effective therapeutics for a broad range of diseases, such as cancer, cardiovascular disease,neurodegenerative diseases, or age-related problems. Having said this, there are still areas of development needed. To make MSI a routine tool, the method needs to be validated on large patient or sample cohorts. This requires a higher degree of automation than currently available. Automation and robotics developments will improve the throughput of the MSI technologies, allowing a researcher to analyze more samples. The capability of high-throughput imaging also will drive the developments in sample preparation. The sample preparation protocols need to keep up with the speed of the new instruments. This requires automated sectioning, mounting, washing, and surface preparation. These tools are not available today. High-throughput perspectives drastically increase the amount of data generated in MSI experiments. It will soon become difficult to keep all the raw data from a MSI validation study at high spatial resolution. On-the-fly data reduction and feature extraction protocols have to be developed that address this issue. In addition, multimodal imaging

approaches will assist in the validation and acceptance of MSI technology in molecular biology. The increased throughput will also induce a larger demand for 3D MSI. The capabilities are already available, but only a few good examples exist due to the lack of proper processing infrastructure.

These prospective improvements in MSI technology put further strain on the data storage and processing resources. As a result, they pose new challenges for the bioinformaticians working in this field. New desorption and ionization techniques in the ambient environment offer new application possibilities.

8. Abbreviations

ADP adenosine diphosphate
ADRP Adipose differentiation- related protein
AMOLF FOMsInstitute for Atomic and Molecular Physics
AMP adenosine monophosphate
AP atmospheric pressure
APCI atmospheric pressure chemical ionization
AQP0 Aquaporin-0
ATP adenosine triphosphate
AuNPs gold nanoparticles
BRPs bradykinin related peptides
CAD collisionally activated dissociation
CHCA R-cyano-4-hydroxycinnamic acid
CID collision induced dissociation
CMC carboxymethylcellulose
CNTs carbon nanotubes
CT computed tomography
DAG diacylglycerol
DART direct analysis in real time
DESI desorption electrospray ionization
DESI-MSI desorption electrospray ionization-Image mass spectrometry
DHA 2,6-dihydroxyacetophenone
DHB 2,5-dihydroxybenzoic acid
DI desorption ionization
DIOS desorption-ionization on silicon
2D-PAGE 2-dimensional polyacrylamide gel electrophoresis
EPPE ethanol-preserved and paraffin-embedded
ESI electrospray ionization
EVA ethylene vinyl acetate
FAIMS high-field asymmetric waveform ion mobility spectrometry
FDA Food and Drug Administration
FFPE formaldehyde-fixed and paraffin-embedded
FTICR Fourier transform ion cyclotron resonance
FTMS Fourier transform mass spectrometer
GALDI graphite-assisted laser desorption/ionization
GlcNAc *N*-acetyl-D-glucosamine
GPChos glycerophosphocholines
GPLs glycerophospholipids
GTP guanosine triphosphate
H&E hematoxylin and eosin
HPLC MS/MS liquid chromatography tandem mass spectrometry tandem mass spectrometry
HUPO-PSI Human Proteome Organization-Proteomics Standards Initiative
HV high vacuum
ICA in-cell ion accumulation
ICR ion cyclotron resonance
IMS ion mobility separation
IR-MALDI infrared MALDI
ITO indium tin oxide
ITO slides coated glass slides
IZ interface zones

LAESI laser ablation electrospray ionization
LA-ICP-MS laser ablation inductively coupled plasma MS
LC liquid chromatography
LCM laser capture microdissection
LDI laser desorption ionization
LIT linear ion trap
LMIG liquid metal ion guns
LPI lisophosphatidylinositol
LTP lipid transfer protein
LTQ linear trap quadrupole
MALDI Matrix-assisted laser desorption/ionization
MALDI-FTMS Matrix-assisted laser desorption/ionization- fourier transform ion cyclotron resonance
MALDI-MSI Matrix-assisted laser desorption/ionization-image mass spectrometry
MALDI TOF/TOF Matrix-assisted laser desorption/ionization-image mass spectrometry-time of flight/time of flight
META-SIMS meta metallization- secondary ion mass spectrometry
MRI magnetic resonance imaging
MRSI magnetic resonance spectrometric imaging
NAFLD nonalcoholic fatty liver disease
PA phosphatidic acid
PCA principal component analysis
PC principal components
PE Phosphatidylethanolamine
PET positron emission tomography
PG phosphatidylglycerol
PI phosphatidylinositol
PLASs phospholipases A
PlsEtn plasmenylethanolamine
PMI post-mortem interval
PS phosphatidylserine
PTMs post translation modification
ROIs region of interest
RT real time
SA sinapinic acid
SIC selected ion current
SIMS secondary ion mass spectrometry
SRM selected reaction monitoring
TAG triacylglycerols
TFA trifluoroacetic acid
TOF-SIMS secondary ion mass spectrometry-time of flight
UDPuridine diphosphate
WBAwhole-body autoradiography

9. References

[1] McGregor E, Dunn MJ. Proteomics of the Heart Unraveling Disease. *Circ. Res.* 2006;98:309-321.

[2] Mueller DR, Voshol H, Waldt A, et al. LC-MALDI MS and MS/MS–an efficient tool in proteome analysis. *Subcell. Biochem.* 2007;*43*:355–380.

[3] Li L, Garden RW, Sweedler JV. Single-cell MALDI: A new tool for direct peptide profiling. *Trends Biotechnol.* 2000; *18*:151–160.

[4] Suzuki T, Nagai R. Cardiovascular proteomic analysis. J of Chromatography B analyt Technol Biomed Life Sci. 2007; 855; 28–34.

[5] Ping P. *N Engl J Med*. Getting to the Heart of Proteomics. 2009;360;532-534.

[6] Dunn MJ, Corbett JM, Wheeler CH. HSC-2DPAGE and the twodimensional gel electrophoresis database of dog heart proteins. *Electrophoresis*.1997;18:2795–2802.

[7] Li XP, Pleissner KP, Scheler C et al. A two-dimensional electrophoresis database of rat heart proteins. *Electrophoresis*.1999;20:891– 897.

[8] Heeren RMA, McDonnell LA, Amstalden E, et al. Why don't biologists use SIMS? A critical evaluation of imaging MS. *Appl. Surf. Sci.* 2006;*252*: 6827-6835.

[9] Chughtai K, Heeren RMA. Mass Spectrometric Imaging for Biomedical Tissue Analysis. *Chem. Rev.* 2010;*110:* 3237–3277.

[10] Yanagisawa K, Shyr Y, Xu BJ, et al. Proteomic patterns of tumour subsets in non-small-cell lung cancer. *The Lancet*. 2003;362:433-439.

[11] Altelaar AFM, Taban IM, McDonnell LA, et al. High-resolution MALDI imaging mass spectrometry allows localization of peptide distributions at cellular length scales in pituitary tissue sections. *Int. J. of Mass Spectrometry*. 2007;260:203-211.

[12] Russell JC. Editorial O f mice and men, rats and atherosclerosis. *Cardiovascular Research.*. 2003;59: 810–811.

[13] Chaurand P, Norris J L, Cornett DS, Mobley J A, et al. New developments in profiling and imaging of proteins from tissues by MALDI mass spectrometry. J *Proteome Res.* 2006;*5*:2889-2900

[14] Seeley EH, Caprioli RM. Molecular imaging of proteins in tissues by mass spectrometry *Proc. Natl. Acad. Sci. U. S. A.* 2008;*105*:18126-31

[15] Goodwin RJ, Pennington SR, Pitt AR. Protein and peptides in pictures: imaging with MALDI mass spectrometry. *Proteomics.* 2008;*8*:3785-3800

[16] Li L, Sweedler JV. Peptides in our brain: Mass spectrometric- based measurement approaches and challenges. *Annu. Rev. Anal. Chem.* 2008;*1*:451–483.

[17] Walch A, Rauser S, Deininger SD. MALDI imaging mass spectrometry for direct tissue analysis: a new frontier for molecular histology. *Histochem Cell Biol*. 2008;130:421–434.

[18] Fenn JB, Mann M, Meng CK, et al. Electrospray ionization for mass spectrometry of large biomolecules. *Science* 1989:*246*;64-71.

[19] Karas M, Bachmann D, Hillenkamp F. Influence of the wavelengh in high-irradiance ultraviolet laser desorption mass spectrometry of organic molecules. *Anal. Chem.* 1985;*57*:2935-2939.

[20] Caprioli RM, Farmer TB, Gile J. Molecular imaging of biological samples: localization of peptides and proteins using MALDITOF MS. *Anal. Chem. 1997;* 69**:** 4751–4760.

[21] Stoeckli M, Chaurand P, Hallahan DE, et al. Imaging mass spectrometry: a new technology for the analysis of protein expression in mammalian tissues. *Nat. Med. 200;*7:493–496.

[22] Clerc J, Fourre C, Fragu P. SIMS microscopy, problems and perspectives in mapping drugs and nuclear medicine compounds. *Cell Biol. Int.* 1997;*21:* 619-33.

[23] Galle P, Berry JP, Escaig F. Secondary ion mass microanalysis: applications in biology. *Scan Electron Microsc*. 1983;2:827-39.

[24] Benninghoven A, Sichtermann WK. Detection, identification and structural investigation of biology important compounds by secondary ion mass spectrometry. *Anal Chem*.1978;50:1180-1184.

[25] Burns M. Polyatomic interferences in high-resolution secondary ion mass spectra of biological tissues. *Anal Chem*.1981; 53:2149-2152.

[26] Berry JP, Escaig F, Lange F, et al. Ion microscopi of the thyroid gland: a method for imaging stable and radioactive iodine. *Lab Invest*.1986; 55:109-119.

[27] Fragu, P. and Kahn, E. Secondary ion mass spectrometry (SIMS) microscopi : a new tool for pharmacological studies in humans. *Microsc Res Tech*.1997; 36:296-300.

[28] McMahon JM, McCandlish CA, Brenna JT et al. Identification and mapping of phosphocoline in animal tissue by static secondary ion mass spectrometry and tandem mass spectrometry. *Rapid Commun Mass Spectrometry.* 1996;10:335-340.

[29] Seedorf UMF, Voss R, Meyer K et al. Smith-Lemli-Opitz syndrome diagnosed by using time-of-flight secondary-ion mass spectrometry. *Clinical Chemistry.*1995;41:548-552.

[30] McQuaw CM, Sostarecz AG, Zheng L, et al. Investigating lipid interactions and process of raft formation in cellular membranes using ToF-SIMS. *Appl Surf Sci.* 2006; 252: 6716-6718.

[31] Sjovall P, Lausmaa J, Nygren H, Carlsson L et al. Imaging of membrane lipids in single cells by imprint-imaging time-of-flight secondary ion mass spectrometry. *Anal Chem*. 2003;14:3429-3434.

[32] Pacholski ML, Cannon DM, Ewing AG et al. Static time-of-flight secondary ion mass spectrometry imaging of freeze-fractured,frozen-hydrated biological membranes. *Rapid Commun Mass Spectrom*.1998;12:1232-1235.

[33] Chandra S, Morrison GH, Beyenbach KW. Identification of Mg-transporting renal tubules and cells by ion microscopy imaging of stable isotopes. *Am J Physiol.* 1997;273:939-48.

[34] Touboul D, Brunelle A, Halgand F et al. Improuvement of biological time-of-flight-secondary ion mass spectrometry imaging with a bismuth cluster ion source. *Lipid Res*. 2005;46:1388-95.

[35] Fletcher JS, Lockyer NP, Vaidyanathan S et al. TOF-SIMS 3D biomolecular imaging of Xenopus laevis oocytes using buckminsterfullerence (C60) primary ions. *Anal Chem*. 2007;79:2199-206.

[36] Nygren H, and Malmberg, P. Bioimaging. TOF-SIMS of tissue by gold ion bombardment of a silver-coated thin section. *J Microsc*. 2004;215:156-61.

[35] Mccombie G, Staab D, Stoeckli M. Spatial and spectral correlations in MALDI mass spectrometry images by clustering and multivariate analysis. *Anal Chem*.2005;77:6118-6124.

[37] van Veelen PA, Jime´ nez CR, Li KW, et al. Direct peptide profiling of single neurons by matrix-assisted laser desorption ionization mass spectrometry. *Org. Mass Spectrom. 1993;*28**:** 1542–1546.

[38] Jime´ nez CR, Van Veelen PA, Li KW, et al. Neuropeptide expression and processing as revealed by direct matrix-assisted laser desorption ionization mass spectrometry of single neurons. *J. Neurochem. 1994;*62**:**404–407.

[39] Li KW, Hoek RM, Smith F, et al. Direct peptide profiling by mass spectrometry of single identified neurons reveals complex neuropeptide-processing pattern. *J. Biol. Chem. 1994;*269**:**30288–30292.

[40] Li KW, Jime´ nez CR, Van Veelen PA, et al. Processing and targeting of a molluscan egg-laying peptide prohormone as revealed by mass spectrometric peptide fingerprinting and peptide sequencing. *Endocrinology. 1994;*134**:**1812–1819.

[41] Li KW, Van Golen FA, Van Minnen J, et al. Structural identification, neuronal synthesis, and role in male copulation of myomodulin-A of Lymnaea: a study involving direct peptide profiling of nervous tissue by mass spectrometry. *Brain Res. Mol. Brain Res.*1994; 25**:** 355–358.

[42] Dreisewerd K, Kingston R, Geraerts WP, et al. Direct mass spectrometric peptide profiling and sequencing of nervous tissues to identify peptides involved in male copulatory behavior in Lymnaea stagnalis. *Int. J. Mass Spectrom.* 1997;169**:** 291–299

[43] Jime´ nez CR, Burlingame AL. Ultramicroanalysis of peptide profiles in biological samples using MALDI mass spectrometry. *Exp. Nephrol* 1998;6:421–428.

[44] Jime´ nez CR, Li KW, Dreisewerd K, et al. Direct mass spectrometric peptide profiling and sequencing of single neurons reveals differential peptide patterns in a small neuronal network. *Biochemistry.* 1998; 37**:** 2070–2076.

[45] Redeker V, Toullec JY, Vinh J, et al. Combination of peptide profiling by matrix-assisted laser desorption/ ionization time-of-flight mass spectrometry and immunodetection on single glands or cells. *Anal. Chem.* 1998; 70**:** 1805–1811.

[46] Rubakhin SS, Li L, Moroz T P, et al. Characterization of the Aplysia californica cerebral ganglion F cluster. *J. Neurophysiol* 1999; 81**:**1251–1260.

[47] Sweedler J V, Li L, Floyd P, et al. Mass spectrometric survey of peptides in cephalopods with an emphasis on the FMRFamiderelated peptides. *J. Exp. Biol* .2000; 203**:**3565–3573.

[48] Schwartz SA, Caprioli RM. Imaging mass spectrometry: viewing the future. *Methods Mol Biol*. 2010;656:3-19.

[49] Chaurand P, Schwartz SA, Caprioli RM. Imaging mass spectrometry: a new tool to investigate the spatial organization of peptides and proteins in mammalian tissue sections. *Curr. Opin. Chem. Biol. 2002;* 6**:** 676–681.

[50] Fournier I, Day R, Salzet M. Direct analysis of neuropeptides by in situ MALDI-TOF mass spectrometry in the rat brain. *Neuro Endocrinol.* 2003; 24: 9–14.

[51] Caldwell R L, Caprioli RM. Tissue profiling by mass spectrometry:
a review of methodology and applications. *Mol. Cell. Proteomics* 2005;4**:** 394–401.

[52] Jurchen J C, Rubakhin SS, Sweedler J V. MALDI-MS imaging of features smaller than the size of the laser beam. *J. Am. Soc. Mass Spectrom. 2005;* 16**:** 1654–1659.

[53] Maddalo G, Petrucci F, Iezzi F, et al. Analytical assessment of MALDI-TOF imaging mass spectrometry on thin histological samples. An insight in proteome investigation. *Clin. Chim. Acta* 2005; 357**:** 210–218.

[54] Aerni HR, Cornett DS, Caprioli RM. Automated acoustic matrix deposition for MALDI sample preparation. *Anal. Chem. 2006;*78**:** 827–834.

[55] Altelaar AF, Klinkert I, Jalink K, et al. Gold-enhanced biomolecular surface imaging of cells and tissue by SIMS and MALDI mass spectrometry. *Anal. Chem. 2006;* 78**:**734–742.

[56] Crossman L, McHugh N A, Hsieh Y, et al. Investigation of the profiling depth in matrix-assisted laser desorption/ ionization imaging mass spectrometry. *Rapid Commun. Mass Spectrom. 2006;*20**:** 284–290.

[57] Lemaire R, Tabet J C, Ducoroy P, et al. Solid ionic matrixes for direct tissue analysis and MALDI imaging. *Anal. Chem. 2006;*78**:** 809–819.

[58] Lemaire R, Wisztorski M, Desmons A, et al. MALDI-MS direct tissue analysis of proteins: improving signal sensitivity using organic treatments. *Anal. Chem.* 2006*;* 78**:** 7145–7153.

[59] Stauber J, Lemaire R, Wisztorski M, et al. New developments in MALDI imaging mass spectrometry for pathological proteomic studies: introduction to a novel
concept, the specific MALDI imaging. *Mol. Cell. Proteomics.* 2006 5: 247–249.

[60] Wiseman JM, Ifa DR, Song Q, et al. Tissue imaging at atmospheric pressure using desorption electrospray ionization (DESI) mass spectrometry. *Angew.Chem. Int. Ed. Engl.*2006;45**:**7188–7192.

[61] Wisztorski M, Brunet L, Dreiserwer K, et al. Effect of metals coating for UV MALDIa- TOF mass spectrometry imaging (MALDI IMS) and direct tissue analysis in UV/IR MALDI-o-TOF mass spectrometry, in *Proceedings of the 54th ASMS Conference on Mass Spectrometry and Allied Topics, Seattle.* Abstract No. ThP 328, American Society for Mass Spectrometry, Santa Fe, NM.2006 May 30- June 2.

[62] Chaurand P, Schriver KE, Caprioli RM. Instrument design and characterization for high resolution MALDI-MS imaging of tissue sections. *J. Mass Spectrom.* 2007; 42: 476–489.

[63] Cornett DS, Reyzer ML, Chaurand P, et al. MALDI imaging mass spectrometry: molecular snapshots of biochemical systems. *Nat. Methods. 2007;* 4**:** 828–833.

[64] Dreisewerd K, Lemaire R, Pohlentz G, et al. Molecular profiling of native and matrix-coated tissue slices from rat brain by infrared and ultraviolet laser desorption/ionization orthogonal time-of-flight mass spectrometry. *Anal. Chem.2007;* 79**:** 2463–2471.

[65] Garrett T J, Prieto-Conaway MC, Kovtoun V, et al. Imaging of small molecules in tissue sections with a new intermediate-pressure MALDI linear ion trap mass spectrometer. *Int. J. Mass Spectrom. 2007;* 260**:** 166–176.

[66] Groseclose M R, Andersson M, Hardesty W M, et al. Identification of proteins directly from tissue: in situ tryptic digestions coupled with imaging mass spectrometry. *J. Mass Spectrom.* 2007*;* 42**:** 254–262.

[67] Hankin J A, Barkley RM, Murphy R C. Sublimation as a method of matrix application for mass spectrometric imaging. *J. Am. Soc. Mass Spectrom.* 2007;18**:**1646–1652.

[68] Lemaire R, Menguellet SA, Stauber J, et al. Specific MALDI imaging and profiling for biomarker hunting and validation: fragment of the 11S proteasome activator complex, Reg alpha fragment, is a new potential ovary cancer biomarker. *J. Proteome Res.*2007*;* 6:4127–4134.

[69] McLean J A, Ridenour W B, Caprioli RM. Profiling and imaging of tissues by imaging ion mobility-mass spectrometry. *J. Mass Spectrom.* 2007;42:1099–1105.

[70] Taban IM, Altelaar A F, Van der Burgt YE, et al. Imaging of peptides in the rat brain using MALDI-FTICR mass spectrometry. *J. Am. Soc. Mass Spectrom.* 2007;18**:** 145–151.

[71] Chen Y, Allegood J, Liu Y, et al. Imaging MALDI mass spectrometry using an oscillating capillary nebulizer matrix coating system and its application to analysis of lipids in brain from a mouse model of Tay-Sachs/Sandhoff disease. *Anal. Chem.* 2008*;*80**:**2780–2788.

[72] Seeley E H, Oppenheimer S R, Mi D, et al. Enhancement of protein sensitivity for MALDI imaging mass spectrometry after chemical treatment of tissue sections. *J. Am. Soc. Mass Spectrom.* 2008*;* 19**:**1069–1077.

[73] Taira S, Sugiura Y, Moritake S, et al. Nanoparticle-assisted laser desorption/ionization based mass imaging with cellular resolution. *Anal. Chem.* 2008; 80**:** 4761–4766.

[74] Trim P J, Atkinson S J, Princivalle AP, et al. Matrix-assisted laser desorption/ionisation mass spectrometry imaging of lipids in rat brain tissue with integrated unsupervised and supervised multivariant statistical analysis. *Rapid Commun.Mass Spectrom.* 2008;22**:** 1503–1509.

[75] Jardin-Mathe´ O, Bonnel D, Franck J, et al. MITICS (MALDI Imaging Team Imaging Computing System): a new open source mass spectrometry imaging software. *J. Proteomics.* 2008*;*71**:** 332–345.

[76] Chaurand P, Schwartz S A, Billheimer D, et al. Integrating histology and imaging mass spectrometry. *Anal. Chem.* 2004; 76**:** 1145–1155.

[77] Lemaire R, Desmons A, Tabet J C, et al. Direct analysis and MALDI imaging of formalin-fixed, paraffinembedded tissue sections. *J. Proteome Res.* 2007; 6:1295–1305.

[78] Schwamborn K, Krieg R C, Reska M, et al. Identifying prostate carcinoma by MALDI-Imaging. *Int. J. Mol. Med.* 2007*;* 20**:** 155–159.

[79] Brown LM, Helmke S M, Hunsucker SW, et al. Quantitative and qualitative differences in protein expression between papillary thyroid carcinoma and normal thyroid tissue. *Mol. Carcinog.* 2006; 45**:** 613–626.

[80] Chaurand P, Sanders M E, Jensen R A, et al. Proteomics in diagnostic pathology: profiling and imaging proteins directly in tissue sections. *Am. J. Pathol.* 2004;165**:**1057–1068.

[81] Johnson M D, Floyd J L, Caprioli RM. Proteomics in diagnostic neuropathology. *J. Neuropathol. Exp. Neurol.* 2006; 65: 837–845.

[82] Marko-Varga, G, Lindberg H, Lo¨ fdahl CG, et al. Discovery of biomarker candidates within disease by protein profiling: principles and concepts. *J. Proteome Res.* 2005; 4: 1200–1212.

[83] Meistermann H, Norris J L, Aerni H R, et al. Biomarker discovery by imaging mass spectrometry: transthyretin is a biomarker for gentamicininduced nephrotoxicity in rat. *Mol. Cell. Proteomics.* 2006;5:1876–1886.

[84] Skold K, Svensson M, Nilsson A , et al. Decreased striatal levels of PEP-19 following MPTP lesion in the mouse. *J. Proteome Res.* 2006; 5: 262–269.

[85] Stoeckli M, Knochenmuss R, McCombie G, et al. MALDI MS imaging of amyloid. *Methods Enzymol.* 2006; 412**:** 94–106.

[86] Groseclose M R, Massion P P, Chaurand P, et al. High-throughput proteomic analysis of formalin-fixed paraffin-embedded tissue microarrays using MALDI imaging mass spectrometry. *Proteomic.* 2008;8: 3715–3724.

[87] Ronci M, Bonanno E, Colantoni A, et al. Protein unlocking procedures of formalin-fixed paraffin-embedded tissues: application to MALDI-TOF imaging MS investigations. *Proteomics.* 2008; 8;3702–3714.

[88] Stauber J, Lemaire R, Franck J, et al. MALDI imaging of formalinfixed paraffin-embedded tissues: application to model animals of Parkinson disease for biomarker hunting. *J. Proteome Res.* 2008*;*7: 969–978.

[89] Van de Plas R, Ojeda F, Dewil M, et al. Prospective exploration of biochemical tissue composition via imaging mass spectrometry guided by principal component analysis. *Pac. Symp. Biocomput*. 2007;5:458–469.

[90] Djidja M C, Carolan V, Loadman PM, et al. Method development for protein profiling in biological tissues by matrix-assisted laser desorption/ionisation mass spectrometry imaging. *Rapid Commun. Mass Spectrom.* 2008;22:1615–1618.

[91] McCombie G, Staab D, Stoeckli M, et al. Spatial and spectral correlations in MALDI mass spectrometry images by clustering and multivariate analysis. *Anal. Chem.* 2005;77:6118–6124.

[92] Deininger SO, Ebert M P, Futterer A, et al. MALDI imaging combined with hierarchical clustering as a new tool for the interpretation of complex human cancers. *J. Proteome Res. 2008;* 7: 5230–5236.

[93] El Ayed M, Bonnel L, Longuespée R, et al. MALDI imaging mass spectrometry in ovarian cancer for tracking, identifying, and validating biomarkers. *Med Sci Monit*. 2010;16: 233-245.

[94] Chaurand P, Rahman M A, Hunt T, et al Monitoring mouse prostate development by profiling and imaging mass spectrometry. *Mol. Cell. Proteomics.* 2008;7: 411–423.

[95] Din S, Lennon A M, Arnott ID, et al. Technology insight: the application of proteomics in gastrointestinal disease. *Nat. Clin. Pract. Gastroenterol. Hepatol.* 2007;4: 372–385.

[96] Fournier I, Wisztorski M, Salzet M. Tissue imaging using MALDI-MS: a new frontier of histopathology proteomics. *Expert Rev. Proteomic.* 2008*;* 5: 413–424.

[97] Francese S, Dani FR, Traldi P, et al. MALDI mass spectrometry imaging, from its origins up to today: the state of the art. *Comb. Chem. High Throughput Screen.* 2009; 12**:** 156–174.

[98] Norris J L, Cornett D S, Mobley J A, et al. Processing MALDI mass spectra to improve mass spectral direct tissue analysis. *Int. J. Mass Spectrom.* 2007;260**:** 212–221.

[99] Tilz G P, Wiltgen M, Demel U, et al. Insights into molecular medicine: development of new diagnostic and prognostic parameters. *Wien. Med. Wochenschr.* 2007; 157**:** 122–129.

[100] Wisztorski M, Lemaire R, Stauber J, et al. New developments in MALDI imaging for pathology proteomic studies. *Curr. Pharm. Des.* 2007;13**;** 3317–3324.

[101] Reyzer M L, Caprioli RM. MALDI-MS-based imaging of small molecules and proteins in tissues. *Curr. Opin. Chem. Biol.* 2007;11**:** 29–35.

[102] Hsieh Y, Casale R, Fukuda E, et al. Matrix-assisted laser desorption/ ionization imaging mass spectrometry for direct measurement of clozapine in rat brain tissue. *Rapid Commun. Mass Spectrom.* 2006; 20**:** 965–972.

[103] Hsieh Y, Chen J, Korfmacher W A. Mapping pharmaceuticals in tissues using MALDI imaging mass spectrometry. *J. Pharmacol. Toxicol. Methods.* 2007; 55: 193–200.

[104] O'Brien E, Dedova I, Duffy L, et al. Effects of chronic risperidone treatment on the striatal protein profiles in rats. *Brain Res. 2*006; 1113**:** 24–32.

[105] Reyzer M L, Hsieh Y, Korfmacher W. A., et al. Direct analysis of drug candidates in tissue by matrix-assisted laser desorption/ionization mass spectrometry. *J. Mass Spectrom.* 2003; 38**:** 1081–1092.

[106] Rubakhin S S, Jurchen J C, Monroe E B, et al. Imaging mass spectrometry: fundamentals and applications to drug discovery. *Drug Discov. Today.* 2005*;* 10**:** 823–837.

[107] Wang HY, Jackson S N, McEuen J, et al. Localization and analyses of small drug molecules in rat brain tissue sections. *Anal. Chem.* 2005;77: 6682–6686.

[108] Dekker LJ, Van Kampen JJ, Reedijk M L, et al. A mass spectrometry based imaging method developed for the intracellular detection of HIV protease inhibitors. *Rapid Commun. Mass Spectrom.* 2009; 23: 1183–1188.

[109] Hopfgartner G, Varesio E, Stoeckli M. Matrix-assisted laser desorption/ionization mass spectrometric imaging of complete rat sections using a triple quadrupole linear ion trap. *Rapid Commun. Mass Spectrom.* 2009; 23**:** 733–736.

[110] Huamani J, Willey C, Thotala D, et al. Differential efficacy of combined therapy with radiation and AEE788 in high and low EGFR-expressing androgen-independent prostate tumor models. *Int. J. Radiat. Oncol. Biol. Phys.* 2008; 71: 237–246.

[111] Trim P J, Henson C M, Avery J L, et al. Matrix-assisted laser desorption/ionization-ion mobility separation-mass spectrometry imaging of vinblastine in whole body tissue sections. *Anal. Chem.* 2008; 80**:** 8628–8634.

[112] Reyzer M L, Caldwell RL, Dugger T C., et al. Early changes in protein expression detected by mass spectrometry predict tumor response to molecular therapeutics. *Cancer Res.* 2004; 64**:** 9093–9100.

[113] Khatib-Shahidi S, Andersson M, Herman J L, et al. Direct molecular analysis of whole-body animal tissue sections by imaging MALDI mass spectrometry. *Anal. Chem.*2006; 78**:** 6448–6456.

[114] Atkinson S J, Loadman P M, Sutton C, et al. Examination of the distribution of the bioreductive drug AQ4N and its active metabolite AQ4 in solid tumours by imaging matrixassisted laser desorption/ionisation mass spectrometry. *Rapid Commun. Mass Spectrom.* 2007*;*21**:** 1271–1276.

[115] Slaveykova V I., Guignard C, Eybe T, et al. *Chem. Re*V. Dynamic NanoSims ion imaging of unicellular freshwater algae exposed to cooper. *Anal. Bioanal. Chem*. 2009;393:583-589.

[116] Pumphrey GM, Hanson B T, Chandra S, et al. Dynamic secondary ion mass spectrometry imaging of microbial popolations utilizing C-labelled substrates in pure culture and in soil. *En*V*iron. Microbiol.* 2009, *11*:220-229.

[117] Esquenazi E, Yang Y, Watrous J, et al. Imaging mass spectrometry of natural products. *Proc. Nat Prod Rep.*2009;26:1521-1534.

[118] Stoeckli M, Staab D, Schweitzer A. Imaging of a beta-peptide distribution in whole-body mice sections by MALDI mass spectrometry *Int. J. Mass Spectrom.* 2007;18: 1921-1924.

[119] Ronci M, Bonanno E, Colantoni A, et al. Protein unlocking procedures of formalin-fixed paraffin-embedded tissues: application to MALDI-TOF imaging MS investigations *Proteomics.* 2008; *8*: 3702-3714.

[120] Chaurand P, Norris J L, Cornett D S, et al. New developments in profiling and imaging of proteins from tissues by MALDI mass spectrometry. J *Proteome Res.* 2006;*5*: 2889-2900.

[121] Schwartz S A, Reyzer M L, Caprioli R M. Direct tissue analysis using matrix-assisted laser desorption/ionization mass spectrometry: pratical aspects of sample preparation. *J. Mass Spectrom.* 2003; *38*: 699-708.

[122] Crecelius A, Gotz A, Arzberger T, et al. Assessing quantitative post-mortem changes in the gray/matter of the human frontal cortex proteome by 2-D DIGE. *Proteomics* 2008;*8*:1276-1279.

[123] Groseclose M R, Massion P P, Chaurand P, et al. High-throughput proteomic analysis of formalin-fixed paraffin-embedded tissue microarrays using MALDI imaging mass spectrometry. *Proteomics.* 2008; *8*: 3715-3724.

[124] Seeley E H, Caprioli RM. Molecular imaging of proteins in tissues by mass spectrometry. *Proc. Natl. Acad. Sci. U. S. A.* 2008;*105*:18126-31.

[125] Mangé A, Chaurand P, Perrochia H, et al. Liquid chromatography-tandem and MALDI imaging mass spectrometry analyses of RCL2/CS 100-fixed, paraffin-embedded tissues: proteomic evaluation of an alternative fixative for biomarker discovery. *J. Proteome Res.* 2009;*8*: 5619-5628.

[126] Heeren RMA, Ku krer-Kaletas B, Taban IM et al. Quality of surface: The influence of sample preparation on MS-based biomolecular tissue imaging with MALDI-MS and (ME-)SIMS. *The Applied Surface Science*. 2008; 255: 1289–1297.

[127] Djidja M C, Francese S, Loadman PM et al. MALDI-ion mobility separation-mass spectrometry imaging of glucose-regulated protein 78 KDa (Grp 78) in human formalin-fixed, paraffin-embedded pancreatic adenocarcinoma tissue sections. *Proteomics* 2009; *9*: 2750-2763.

[128] Kaletas B K, Van der Wiel I M, Stauber J, et al. Sample preparation issues for tissues imaging by imaging MS. *Proteomics.* 2009; *9*: 2622-2633.

[129] Stoeckli M, Staab D, Staufenbiel M, et al. Molecular imaging of amyloid beta peptides in mouse brain sections mass spectrometry. *Anal. Biochem.* 2002; *311:* 33-39.

[130] Altelaar AF, Heeren RM. Tissue analysis with high-resolution imaging mass spectrometry. *Methods Mol Biol*. 2009; 492:295-308.

[131] Goodwin R J, Pennington SR, Pitt AR. Protein and peptides in pictures: imaging with MALDI mass spectrometry. *Proteomics.* 2008;*8*:3785-3800.

[132] Baluya D L, Garrett TJ, Yost R A. Automated MALDI matrix deposition method with inkjet printing for imaging mass spectrometry. *Anal. Chem.* 2007;*79*: 6862-7.

[133] Hankin J A, Barkley RM, Murphy RC. Sublimation as a method of matrix application for mass spectrometric imaging *J. Am. Soc. Mass Spectrom.* 2007; *18*:1646-1652.

[134] Yanagisawa K, Xu BJ, Carbone DP et al. Molecular fingerprinting in human lung cancer. *Clin Lung Cancer*. 2003;5:113-118.

[135] Keller B O, Sui J, Young A B, et al. Interferences and contaminants encountered in modern mass spectrometry. *Anal. Chim. Acta* 2008;*627*:71-81.

[136] Le Naour F, Bralet M P, Debois D, et al. Chemical imaging on liver steatosis using synchrotron infrared and ToF-SIMS microspectroscopies. *PLoS One* 2009;*4*: 7408-7408.

[137] McDonnell L A, Van Remoortere A, Van Zeijl R J, et al. Imaging mass spectrometry data reduction automated feature identification and extraction *J Am Soc Mass Spectrom. 2001; 21: 1969-1978.*

[138] Rujoi M, Estrada R, Yappert M C. In situ MALDI-TOF MS regional analysis of neutral phospholipids in lens tissue. *Anal. Chem.* 2004, *76*: 1657-1663.

[139] Sugiura Y, Konishi Y, Zaima N, et al. Visualization of the cell-selective distribution of PUFA-containing phosphatidylcholines in mouse brain by imaging mass spectrometry. *J. Lipid Res* . 2009;*50*:1776-1788.

[140] Groseclose MR, Andersson M, Hardesty W M et al. Identification of proteins directly from tissue: in situ tryptic digestions coupled with imaging mass spectrometry. *J. Mass Spectrom.* 2007;*42*: 254-262.

[141] Binz P A, Muller M, Walther D, Et al. A molecular scanner to automate proteomic research and to display proteome images. *Anal. Chem.* 1999;*71*: 4981-4988.

[142] Dani F R, Francese S, Mastrobuoni G, et al. Exploring proteins in Anopheles gambiae male and female antennae through MALDI mass spectrometry profiling. *PLoS On.* 2008; *3*: e2822.

[143] Stoeckli M, Staab D, Staufenbiel M, et al. Molecular imaging of amyloid beta peptides in mouse brain sections using mass spectrometry. *Anal. Biochem.* 2002;*311*:33-39.

[144] Palmer-Toy DE, Sarracino D A, Sgroi D, et al. Direct acquisition of matrix-assisted laser Desorption/Ionization time-of-flight mass spectra from laser capture microdissected tissues *Clin. Chem.* 2000;*46*:1513-1516.

[145] Dunn W B. Current trends and future requirements for the mass spectrometric investigation of microbial, mammalian and plant metabolomes. *Phys. Biol.* 2008; *5*: 011001.

[146] Sugiura Y, Konishi Y, Zaima N, et al. Visualization of the cell-selective distribution of PUFA-containing phosphatidylcholines in mouse brain by imaging mass spectrometry. *J. Lipid Res* . 2009;*50*:1776-1788.

[147] Nature Publishing Group and the LIPID MAPS consortium. Lipidomics Gateway. http://www.lipidmaps.org.

[148] Murphy RC, Hankin J A, Barkley R M. Imaging of lipid species by MALDI mass spectrometry *J. Lipid Res.* 2009;50:317-322.

[149] Kim Y, Shanta S R, Zhou L H, et al. Mass spectrometry based cellular phosphoinositides profilino and phospholipid analysis : a brief review. *Exp. Mol. Med.* 2010;*42*:1-11.

[150] Schiller J, Suss R, Arnhold J. et al. matrix-assisted laser desorption and ionization time-of-flight (MALDI-TOF) mass spectrometry in lipid and phospholipids research. *Prog. Lipid Res.* 2004;*43*: 449-488.

[151] Isaac G, Jeannotte R, Esch SW et al. New mass-spectrometry-based strategies for lipids. *Genet. Eng.* 2007; *28*:129- 157.

[152] Malmberg P, Borner K, Chen Y,et al. Localization of lipids in the aortic wall with imaging TOF-SIMS *Biochim. Biophys. Acta* 2007;*1771*:185-195.

[153] Debois D, Bralet M P, Le Naour F. et al. In situ lipidomic analysis of nonalcoholic fatty liver by cluster TOF-SIMS imaging. *Anal. Chem.* 2009;*81*:2823-2831.

[154] Patti G J, Woo H K, Yanes O et al. Detection of carbohydrates and steroids by cation-enhanced nanostructure-initiator mass spectrometry (NIMS) for biofluid analysis and tissue imaging. *Anal. Chem.* 2010; *82*:121-128.

[155] Rohner T C, Staab D, Stoeckli M. MALDI mass spectrometric imaging of biological tissue sections. *Mech. Ageing De*V. 2005;*126*:177-185.

[156] Cornett DS, Frappier S L, Caprioli R M. MALDI-FTICR imaging mass spectrometry of drugs and metabolites in tissue. *Anal. Chem.* 2008;*80*:5648-5653.

[157] Dekker L J, Van Kampen J J, Reedijk M L, et al. A mass spectrometry based imaging method developped for the intracellular detection of HV protease inhibitors. *Rapid Commun. Mass Spectrom.* 2009;*23*:1183-1188.

[158] Sinha T K, Khatib-Shahidi S, Yankeelov T E, et al. Integratine spatially resolved three-dimensional MALDI IMS with in vivo magnetic resonance imaging. J. C. *Nat. Methods.* 2008;*5*: 57-59.

[159] Andersson M, Groseclose M R, Deutch A Y et al. Imaging mass spectrometry of proteins and peptides: 3D volume reconstruction. *Nat. Methods.* 2008, *5*:101-108.

[160] Mccombie G, Staab D, Stoeckli M. Spatial and spectral correlations in MALDI mass spectrometry images by clustering and multivariate analysis. *Anal Chem*. 2005;77:6118-6124.

[161] Klerk LA, Dankers PY, Popa ER et al. Tof-secondary ion mass spectrometry imaging of polymeric scaffolds with surrounding tissue after in vivo implantation. *Anal Chem*. 2010**;**82:4337-43.

[162] Strott CA, Higashi Y. Cholesterol sulphate in human physiology: what's it all about? *J.Lipid Res*.2003;44:1268-1278.

[163] Byfield FJ, Aranda-Espinoza H, Romanenko VG. Cholesterol Depletion Increases Membrane Stiffness of Aortic Endothelial Cells. *J.Biophysic*.2004;87: 3336–3343.

[164] Fay E, Subramaniam S, Murphy R, et al. Update of the LIPID MAPS comprehendive classification system for lipids. *J. Lipids Res*. 2009;50:S9-S14.

[165] Goodpaster, B.H., He, J., Watkins, S. and Kelley, D.E. Skeletal muscle lipid content and insulin resistance: evidence for a paradox in endurance-trained athletes. *J Clin Endocrinol Metab.* 2001**;** 86:5755-5761.

[166] Lands WE, Hart P. Metabolism of glycerolipids VI specificities of acyl coenzyme A: phospholipids acyltransfererases. *J Biol Chem.*1965**;**240:1905-1911.

[167] Braunwald E. Biomarkers in Heart Failure. *N Engl J Med*. 2008;358:2148-2159.

[168] Unger, R H. The physiology of cellular liporegulation. *Annu. Rev. Physiol. 2003;* 65**:** 333 - 347.

[169] Sharma S, Adrogue J, Golfman L. Intramyocardial lipid accumulation in the failing human heart resembles the lipotoxic rat heart. *Faseb J*. 2004;18:1692–1700.

[170] Galton DJ, Wilson JP. A defect of glucose utilization in adipose tissue of adult diabetics and in some conditions which may predispose to diabetes. *Jun Clin Sci.* 1970;38: 649-60.

[171] Schmitz-Peiffer C, Browne CL, Oakes ND, et al. Alterations in the expression and cellular localization of protein kinase C isozyme epsilon and theta are associated with insulin resistance in skeletal muscle of the high-fat-fed rat. *Diabetes.* 1997; 46:169-78.

[172] Besterman JM, DuronioV, Cuatrecasas P. Diacylglycerol-induced translocation of diacylglycerol kinase: use of affinity-purified enzyme in a reconstitution system. *Proc Natl Acad Sci U S A.* 1986; 83: 6785-9.